

A MECHANISM TO IMPROVE DURABILITY OF ORIENTED STRAND COMPOSITE

By

SUDIP CHOWDHURY

A Thesis submitted in partial fulfillment of
the requirements for the degree of

MASTER OF SCIENCE IN CIVIL ENGINEERING

WASHINGTON STATE UNIVERSITY
College of Engineering and Architecture

August 2006

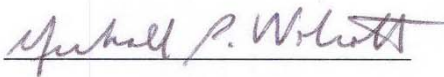
To the Faculty of Washington State University:

The members of the Committee appointed to examine the thesis of
SUDIP CHOWDHURY find it satisfactory and recommend that it be accepted.



Chair





A MECHANISM TO IMPROVE DURABILITY OF ORIENTED STRAND COMPOSITE

Abstract

by Sudip Chowdhury, MS
Washington State University
August 2006

Chair: Vikram Yadama

Recent research indicates that the first losses in properties of wood-based composites are more to do with wetting as a result of moisture infiltration than fungal attack. Thus, improving moisture resistance of the OSC panels is a means of improving the durability, as susceptibility to moisture leads to rapid degradation of wood composites. A mechanism to improve durability of oriented strand composites (OSC) while attempting not to significantly compromise the mechanical properties is presented in this thesis. Objectives of the study were two fold: investigate the effects of blending maleic anhydride polyolefins (MAPO) with phenol formaldehyde resin on its toughness; and, understand the influence of varying levels of phenol formaldehyde (PF) resin and proportions of co-polymer coupling agent on physical and mechanical properties of oriented strand composite. Anionic emulsion of MAPO was found to be most effective in achieving a resin blend with uniform distribution of additive in PF resin. Cure kinetics of the adhesive blends were evaluated using differential scanning calorimetry (DSC). Effects of MAPO addition on stiffness and toughness were studied using DMA and mode I fracture cleavage analysis to assist in choosing either MAPE or MAPP for use in the second objective of the study, evaluating influence of higher levels of PF with and without MAPO on OSC properties. MAPP anionic emulsion improved toughness of resin better than MAPE, even after 24-hr water soak; thus, MAPP anionic emulsion was chosen to apply along with PF resin to in fabricating OSC test

panels. Effects of different proportions of adhesive and MAPP on physical and mechanical properties of OSC were evaluated. Addition of MAPP did not significantly reduce MOE of test panels, however had significantly reduced MOR and IB especially at higher levels of MAPP. Use of higher levels of PF significantly improved the mechanical properties; however, addition of MAPP at high levels of PF was detrimental to board mechanical properties with improvements in moisture resistance. Moisture resistance of OSC test panels were investigated by measuring material permeance, diffusion constant and water absorption and thickness swelling. MAPP significantly improved moisture resistance properties of OSC panels. Based on the results of this study, it is believed that a better solution to improving moisture resistance without significantly reducing the mechanical properties is to increase the levels of PF resin in composite panels. MAPP, though improves moisture resistance, has a tendency to significantly reduce mechanical properties, especially MOR and IB.

Acknowledgement

I wish to express my deep sense of gratitude and respect to my advisor Dr. Vikram Yadama for giving me this opportunity to work in this project. I am indebted to him for his immense help, support and motivation at all times during my study and research.

I would like to express my sincere thanks to my committee members Dr. Marie-Pierre Laborie and Dr. Michael P. Wolcott for providing valuable guidance through out my study period.

I am thankful to the Office of Naval Research for funding this project.

I sincerely thank Dr. Armando McDonald for his help and support at the Department of Forest Products in The University of Idaho.

I am also grateful to Mr. Bob Duncan and Mr. Scott Lewis for providing all sorts of help during this work. My genuine gratitude extends to all personnel of WMEL for their constant help and warmth which created a comfortable work space for me.

I am grateful to all my fellow graduate students, without whose support, cooperation and timely help this work would not have been a success.

Last but not the least, my heartfelt thanks goes to my wife and my family whose presence and support has been a constant source of inspiration for me to overcome all obstacles and work better.

Table of Contents

ACKNOWLEDGEMENT	V
TABLE OF CONTENTS	VI
LIST OF FIGURES	IX
LIST OF TABLES	XVI
CHAPTER 1	1
PROJECT INTRODUCTION.....	1
OBJECTIVES	2
CHAPTER 2.....	4
EFFECT OF CO-POLYMER COUPLING AGENT ON PROPERTIES OF A COMMERCIAL OSB PHENOL FORMALDEHYDE RESIN	
ABSTRACT	4
KEYWORDS	5
INTRODUCTION	5
<i>Objectives</i>	6
<i>Literature Review</i>	7
MATERIALS AND METHODS	13
<i>Particle Size Analysis</i>	15
<i>Determination of Curing Parameters of Resin Blends</i>	17
<i>Effect of MAPO on Resin Properties</i>	19
<i>Dynamic Properties of Specimens during and after Cure</i>	19
<i>Fracture Cleavage Analysis</i>	21

RESULTS AND DISCUSSION	25
<i>Particle Size Analysis</i>	25
<i>Dynamic Properties of Resin Blends</i>	29
<i>Curing Parameters of Resin Blends</i>	30
<i>Effect of MAPO on Resin Properties (Dynamic Mechanical Properties and Fracture Toughness)</i>	33
<i>Fracture Cleavage Analysis</i>	39
CONCLUSION	47
REFERENCES	49
CHAPTER 3.....	53
EFFECT OF COUPLING AGENT AND HIGH RESIN CONTENT ON PHYSICAL AND MECHANICAL PROPERTIES OF ORIENTED STRAND COMPOSITE	
ABSTRACT	53
KEYWORDS	54
INTRODUCTION	54
<i>Objectives</i>	56
<i>Literature Review</i>	56
MATERIALS AND METHODS	60
<i>Materials</i>	60
<i>Experimental Design</i>	61
<i>Oriented Strand Composite (OSC) Fabrication</i>	62
<i>Testing of OSC Panels</i>	64
RESULTS AND DISCUSSION	71

<i>Mechanical Properties</i>	71
<i>Evaluation of Physical Properties</i>	86
CONCLUSIONS.....	114
REFERENCE.....	117
CHAPTER 4	120
PROJECT CONCLUSIONS	120
CHAPTER 5	125
APPENDIX	125
<i>Theory behind the fracture cleavage test</i>	125
<i>Derivation of shear corrected compliance method equation</i>	126
<i>Experimental Graph for DMA</i>	130
<i>Physical and Mechanical Properties of OSC Test panels</i>	131

List of Figures

FIGURE 2.1 FLOW CHART FOR THE STUDY METHODOLOGY.....	13
FIGURE 2.2 DIMENSION OF FRACTURE CLEAVAGE TEST SPECIMEN FOR MODE I FRACTURE.....	22
FIGURE 2.3 TYPICAL PLOT OF LOAD VERSUS EXTENSION FOR SINGLE FRACTURE SPECIMEN AT REPEATED LOAD CYCLES.....	24
FIGURE 2.4 ACTUAL PARTICLE SIZE DISTRIBUTION FOR 80-MESH MAPP BATCH OBTAINED USING LIGHT SCATTERING PARTICLE SIZE ANALYZER.	26
FIGURE 2.5 ACTUAL PARTICLE SIZE DISTRIBUTION FOR 100-MESH MAPP BATCH OBTAINED USING LIGHT SCATTERING PARTICLE SIZE ANALYZER.	26
FIGURE 2.6 ACTUAL PARTICLE SIZE DISTRIBUTION FOR 200- MESH MAPP BATCH OBTAINED USING LIGHT SCATTERING PARTICLE SIZE ANALYZER.	27
FIGURE 2.7 SEM PICTURES FOR CURED ADHESIVE FORMULATIONS WITH MAPP (A) PF+80 MESH MAPP, (B) PF + 100MESH MAPP, (C) PF + 200 MESH MAPP AND (D) PF + MAPP ANIONIC EMULSION	28
FIGURE 2.8 COMPARISON OF PERCENTAGE INCREASE IN E' USING DMA DURING CURE OF BLENDS WITH DIFFERENT FORMS OF MAPP PARTICLES IN PF RESIN.	29
FIGURE 2.9 DYNAMIC RAMPING OF NEAT PF AND PF+ 6% MAPP MIXTURE IN DSC.....	31
FIGURE 2.10 DYNAMIC TEMP RAMP WITH CURED PF+ 6% MAPP FORMULATIONS FOR VARYING TIME PERIODS IN DSC.	32
FIGURE 2.11 PERCENTAGE INCREASE IN STORAGE MODULUS (E') DURING CURING PROCESS WITH DMA.	34
FIGURE 2.12 AVERAGE PERCENTAGE INCREASE IN STORAGE MODULUS (E') OBTAINED USING DMA FOR DIFFERENT ADHESIVE FORMULATIONS.	35

FIGURE 2.13 TYPICAL TREND OF $TAN\Delta$ FOR ADHESIVE FORMULATIONS DURING CURING PROCESS. 36

FIGURE 2.14 TYPICAL TREND OF E' AND $TAN\Delta$ FOR THE CURED LAMINATES UNDER RAMPING. THE INCREASE IN THE E' IS DUE TO LOSS OF MOISTURE..... 37

FIGURE 2.15 COMPARISON OF NORMALIZED $TAN\Delta$ FOR CURED FORMULATIONS WITH DIFFERENT PROPORTIONS OF MAPO (MAPE /MAPP) AT 40 °C 38

FIGURE 2.16 FRACTURE ENERGIES FOR PF+MAPE FORMULATIONS AT 12% MC; BARS WITH SAME LETTERS INDICATE THAT FRACTURE ENERGIES OF THESE BLENDS WERE NOT STATISTICALLY SIGNIFICANT FROM EACH OTHER AT SIGNIFICANCE LEVEL OF 0.05..... 41

FIGURE 2.17 FRACTURE ENERGIES FOR PF+MAPP FORMULATIONS AT 12% MC; BARS WITH SAME LETTERS INDICATE NO SIGNIFICANT DIFFERENCES IN ENERGY VALUES. 42

FIGURE 2.18 AVERAGE FRACTURE ENERGIES FOR FORMULATION WITH MAPE EMULSION AFTER 24-HR WATER SOAK. COMPARISONS OF MEANS TEST RESULTS ARE INCLUDED ON THE TOP OF THE BARS. 45

FIGURE 2.19 AVERAGE FRACTURE ENERGIES FOR FORMULATION WITH MAPP EMULSION AFTER 24-HR WATER SOAK. COMPARISONS OF MEANS TEST RESULTS AT SIGNIFICANCE LEVEL OF 0.05 ARE INCLUDED ON TOP OF THE BARS; FORMULATIONS WITH SAME LETTERS INDICATE NO SIGNIFICANT DIFFERENCE..... 46

FIGURE 3.1 CUTTING PATTERN OF TEST SPECIMENS FROM OSC TEST PANELS. SIX FLEXURE (MOE/MOR), SIX INTERNAL BOND (IB), TWO WATER ABSORPTION AND THICKNESS SWELLING (WA & TS), TWO EQUILIBRIUM MOISTURE CONTENT (EMC) AND ONE WATER VAPOR TRANSMISSION AND PERMEANCE (WVT/P) SPECIMENS WERE PREPARED FROM EACH TEST PANEL. 65

FIGURE 3.2 TEST SETUP FOR WATER VAPOR TRANSMISSION AND PERMEANCE MEASUREMENT. 68

FIGURE 3.3 RESPONSE SURFACE FOR MOE WITH VARYING MAPP AND PF LEVELS FOR SPECIMENS AT 12%MC AND A FIXED TARGET DENSITY OF 641 KG/M ³ .	72
FIGURE 3.4 COMPARISON OF MOE OF PANELS WITH 6% MAPP AND VARYING PF LEVELS AND PMDI AT 12%MC. COMPARISON OF MEAN (DUNCAN) TEST RESULTS AT 0.05 SIGNIFICANCE LEVEL ARE SHOWN ON TOP OF THE BARS.	74
FIGURE 3.5. RESPONSE SURFACE FOR MOR WITH VARYING LEVELS OF PF AND MAPP FOR 12% MC FLEXURE SPECIMENS AT CONSTANT TARGET DENSITY OF 641 KG/M ³ .	75
FIGURE 3.6 COMPARISON OF MOR FOR BOARDS WITH VARYING MAPP LEVELS AT 6% AND 25% PF LEVELS AND PMDI AT 12% MC.	76
FIGURE 3.7 RESPONSE SURFACE FOR FRACTION OF MOE RETAINED AFTER 24 HOURS WATER SOAK OF STATIC BENDING SPECIMENS.	78
FIGURE 3.8 COMPARISONS OF FRACTION OF MOE RETAINED AFTER 24 HOUR WATER SOAK FOR PANELS WITH 6 AND 25% PF CONTENT AT VARYING MAPP LEVELS. FRACTION OF MOE RETENTION FOR PMDI PANELS IS ALSO INCLUDED.	79
FIGURE 3.9 RESPONSE SURFACE FOR FRACTION OF MOR RETAINED WITH VARYING LEVELS OF PF AND MAPP FOR STATIC BENDING SPECIMENS AFTER 24 HOURS WATER SOAK	80
FIGURE 3.10 COMPARISONS OF FRACTION OF MOR RETAINED AFTER 24 HOUR WATER SOAK FOR PANELS WITH 6 AND 25% PF CONTENT AT VARYING MAPP LEVELS. FRACTION OF MOR RETENTION FOR PMDI PANELS IS ALSO INCLUDED.	81
FIGURE 3.11 RESPONSE SURFACE PLOT FOR INTERNAL BOND STRENGTH AT VARYING LEVELS OF MAPP AND PF	83

FIGURE 3.12 COMPARISON OF INTERNAL BOND STRENGTH FOR SPECIMENS AT 6% AND 25% PF LEVELS WITH VARYING MAPP CONTENTS AND PMDI RESIN. COMPARISON OF MEANS TEST RESULTS ARE ALSO INDICATED.....	84
FIGURE 3.13 CHANGE IN IB STRENGTH OF TEST SPECIMENS WITH VARYING PF LEVELS AT 6% MAPP. AVERAGE IB OF SPECIMENS BONDED WITH PMDI RESIN IS ALSO SHOWN. COMPARISON MEAN TEST RESULTS ARE INDICATED AS WELL.....	85
FIGURE 3.14 RESPONSE SURFACE FOR WATER ABSORPTION FOR VARYING PF CONTENT AND MAPP CONTENT FOR 2-HOUR OF WATER SOAK TESTING.	86
FIGURE 3.15 COMPARISON OF 2-HOUR WATER ABSORPTION RESULTS FOR 6% AND 25% PF CONTENT AT VARYING MAPP CONTENT AND FOR PANELS BONDED WITH PMDI.	87
FIGURE 3.16 RESPONSE SURFACE FOR 2-HOUR THICKNESS SWELLING AS MAPP CONTENT AND PF CONTENT WERE CHANGED.....	88
FIGURE 3.17 COMPARISON OF 2 HOURS THICKNESS SWELLING VALUES FOR 6% AND 25% PF CONTENT AT VARYING MAPP CONTENT, COMPARED WITH PMDI PANELS.....	89
FIGURE 3.18 CHANGE IN WATER ABSORPTION AFTER 24-HOUR WATER SOAK AS MAPP AND PF LEVELS VARIED.	90
FIGURE 3.19 COMPARISON OF WATER ABSORPTION AFTER 24- HOUR WATER SOAK FOR PANELS WITH 6% AND 25% PF CONTENT AT VARYING MAPP CONTENT AND FOR PMDI PANELS.	91
FIGURE 3.20 CHANGES IN THICKNESS SWELLING AFTER 24-HOUR WATER SOAK WITH VARYING MAPP AND PF CONTENTS.	92
FIGURE 3.21 COMPARISON OF THICKNESS SWELLING AFTER 24-HOUR WATER SOAK FOR 6% AND 25% PF PANELS AT VARYING MAPP LEVELS AND FOR PMDI PANELS.....	93

FIGURE 3.22 COMPARISON OF THICKNESS SWELLING AFTER 24-HOUR WATER SOAK FOR PANELS WITH 6% MAPP AND VARYING PF CONTENT AND FOR PMDI PANELS.....	94
FIGURE 3.23 DISTRIBUTION OF (A) THICKNESS AND (B) WIDTH OF THE STRANDS USED TO MANUFACTURE OSC TEST PANELS IN THIS STUDY.	95
FIGURE 3.24 TYPICAL PLOTS OF MOISTURE GAIN VS. TIME ELAPSED DATA FOR DIFFUSION COEFFICIENT SPECIMENS. (A) SLOPE OF MOISTURE GAIN FOR SPECIMENS WITH 6% PF CONTENT AT VARYING MAPP LEVELS. (B) SLOPE OF MOISTURE GAIN FOR SPECIMENS WITH 3% MAPP AT DIFFERENT PF CONTENTS.	96
FIGURE 3.25 RESPONSE SURFACE PLOT OF PERMEANCE OF TEST SPECIMENS WITH VARYING MAPP AND PF CONTENT.....	97
FIGURE 3.26 COMPARISON OF PERMEANCE FOR 6% AND 25% PF CONTENT AT VARYING MAPP LEVELS. INCLUDED ALSO IS THE AVERAGE PERMEANCE OF PMDI PANELS.	98
FIGURE 3.27 MOISTURE CONTENT GAIN OF 6% PF CONTENT PANELS WITH VARYING MAPP CONTENT, COMPARED WITH MOISTURE CONTENT GAIN OF PMDI PANEL AT 50% RH.	100
FIGURE 3.28 MOISTURE WEIGHT GAIN AS A FUNCTION OF TIME FOR PANELS BONDED WITH 25% PF CONTENT WITH VARYING MAPP LEVELS AND PMDI RESIN PANEL AT 50% RH.....	101
FIGURE 3.29. MOISTURE WEIGHT GAIN OF TEST PANELS WITH 3% MAPP AT VARYING PF CONTENT. ALSO INCLUDED ARE RESULTS OF PMDI BONDED PANELS.....	102
FIGURE 3.30 TYPICAL PLOTS OF MOISTURE GAIN VS. \sqrt{t} FOR DETERMINATION OF DIFFUSION CONSTANT. (A) MOISTURE GAIN VS. \sqrt{t} FOR SPECIMENS WITH 6% PF CONTENT AT DIFFERENT MAPP LEVELS. (B) MOISTURE GAIN VS. \sqrt{t} FOR SPECIMENS WITH 3% MAPP AT VARYING PF LEVELS, ALSO COMPARED WITH PMDI SPECIMEN.	103

FIGURE 3.31 COMPARISON OF DIFFUSION CONSTANT FOR 6 AND 25% PF CONTENT PANELS AT VARYING MAPP LEVELS AFTER SUBJECTING TO 50% RH. DIFFUSION CONSTANT VALUES FOR PMDI PANELS ARE ALSO INCLUDED	105
FIGURE 3.32. MOISTURE WEIGHT GAIN OVER TIME FOR TEST PANELS BONDED WITH 6% PF RESIN AT VARYING MAPP LEVELS AT 80% RH. MOISTURE WEIGHT GAIN OF PMDI TEST PANELS IS ALSO SHOWN.....	106
FIGURE 3.33. MOISTURE CONTENT GAIN OF 3% MAPP CONTENT PANELS WITH VARYING PF CONTENT, COMPARED WITH MOISTURE CONTENT GAIN OF PMDI PANEL AT 80% RH.	107
FIGURE 3.34 TYPICAL PLOTS OF MOISTURE GAIN VS. \sqrt{t} FOR DETERMINATION OF DIFFUSION CONSTANT OF SPECIMENS SUBJECTED TO 80% RH. (A) MOISTURE GAIN VS. \sqrt{t} FOR SPECIMENS WITH 6% PF CONTENT AT DIFFERENT MAPP LEVELS. (B) MOISTURE GAIN VS. \sqrt{t} FOR SPECIMENS WITH 3% MAPP AT VARYING PF LEVELS, ALSO COMPARED WITH PMDI SPECIMEN.	108
FIGURE 3.35 COMPARISON OF DIFFUSION CONSTANT FOR 6 AND 25% PF CONTENT PANELS AT VARYING MAPP LEVELS AFTER SUBJECTING TO 80% RH. DIFFUSION CONSTANT VALUES FOR PMDI PANELS ARE ALSO INCLUDED	109
FIGURE 3.36 COMPARISON OF PROPERTIES OF TEST PANELS WITH 6% PF CONTENT AND VARYING LEVELS OF MAPP	111
FIGURE 3.37 COMPARISON OF PROPERTIES OF TEST PANELS AT 6% MAPP LEVEL WITH VARYING PF CONTENTS.....	112
FIGURE 3.38 COMPARISON OF PROPERTIES FOR OSC TEST PANELS WITH NEAT 6% AND 25% PF CONTENT AND OSC PANELS WITH SIMILAR PF CONTENT AT 6% MAPP LEVEL.	113
FIGURE 5.1 MODE I FRACTURE	125

FIGURE 5.2 MODE II FRACTURE.....	125
FIGURE 5.3 MODE III FRACTURE.....	126
FIGURE 5.4 TYPICAL PLOT FOR STORAGE MODULUS, LOSS MODULUS AND TAN Δ DURING CURE OF RESIN BLENDS IN DMA	130

List of Tables

TABLE 2.1 PROPERTIES OF MAPE AND MAPP ANIONIC EMULSION USED IN THIS STUDY.....	15
TABLE 2.2 COMPARISON FOR AVERAGE NORMALIZED HEAT OF CURE FOR NEAT PF AND PF WITH 6% MAPP EMULSION.	31
TABLE 2.3: AVERAGE G_{IC} AND G_{IA} VALUES FOR PF + MAPE ADHESIVE FORMULATIONS AT 12% MC.	40
TABLE 2.4 AVERAGE G_{IC} AND G_{IA} VALUE FOR PF + MAPP ADHESIVE FORMULATIONS AT 12% MC.	40
TABLE 2.5 AVERAGE FRACTURE TOUGHNESS ENERGIES FOR FORMULATIONS WITH MAPE AFTER 24-HR SOAK.	43
TABLE 2.6 AVERAGE FRACTURE TOUGHNESS ENERGIES FOR FORMULATIONS WITH MAPP AFTER 24-HR SOAK.	44
TABLE 3.1 FORMULATIONS AND NUMBER OF PANEL REPLICATES SUGGESTED BY D-OPTIMAL RESPONSE SURFACE DESIGN.	61
TABLE 3.2 LIST OF FRACTION OF MOE RETAINED AFTER ACCELERATED AGING OF STATIC BENDING SPECIMENS. VALUES IN THE PARENTHESIS REPRESENT COV.....	82
TABLE 3.3 LIST OF FRACTION OF MOR RETAINED AFTER ACCELERATED AGING OF STATIC BENDING SPECIMENS. VALUES IN THE PARENTHESIS REPRESENT COV.....	82
TABLE 3.4 LIST OF DIFFUSION CONSTANT FOR SPECIMENS SUBJECTED TO 50% RH.	104
TABLE 3.5 LIST OF DIFFUSION CONSTANT FOR SPECIMENS SUBJECTED AT 80% RH.	108
TABLE 5.1 FRACTURE CLEAVAGE TEST SPECIMENS AND SUBJECTED ENVIRONMENTAL CONDITIONS, SUGGESTED BY ONE FACTOR RESPONSE SURFACE MODEL.....	129

TABLE 5.2 SUMMARY TABLE OF FACTOR COEFFICIENTS AND P-VALUES FOR MECHANICAL AND
PHYSICAL PROPERTIES OF OSC TEST PANELS. 131

CHAPTER 1

Project Introduction

Oriented strand board (OSB) is one of the most utilized performance-rated structural panels. OSB is engineered for uniformity, versatility, strength and workability. Production and utilization of OSB panels have experienced huge growth since early 1980s and the production of OSB has now outreached the production of other wood composites (SBA 2003). In 2003 the production of OSB in North America was nearly 24 billion sq. ft. (3/8-inch basis). OSB is the most widely used panel product for floors (65% market share), walls (56% market share) and roofs (72% market share) (courtesy: SBA 2003). As a sheathing material OSB has the ability to absorb and dissipate moisture. However, poor construction practices and improper use of moisture barriers can trap moisture in wall, floor, or roof systems and lead to rapid degradation of OSB sheathing materials. Solutions to this problem include adopting better construction practices and developing a sheathing material that is more moisture resistance as moisture is which would reduce its susceptibility to decay in service.

Improving moisture resistance of wood and wood composites has been tried by many researchers for past few decades. Several methods were tried to reduce the inherent hygroscopicity of wood and wood composites through chemical modification (Chow et al. 1996, Youngquist et al. 1986 and Arora et al. 1981, Clemons et al. 1992, Mahlberg et al. 2001). Wood contains free hydroxyl (-OH) which are the main reason for the affinity of wood towards water. The central idea behind the chemical modification is conversion of the hydroxyl groups and substitution with a more hydrophobic group, consequently, reducing the affinity of wood for water. Treating wood with

organic acid anhydrides such as, acetic and maleic has been commonly explored to consume the free hydroxyl group of wood (Chow et al. 1996, Clemons et al.1992). Though these processes were found to improve the moisture resistance, mechanical properties are often reduced significantly (Mahlberg et al 2001). Thus, a need exists to explore alternate ways to improve the moisture resistance of OSC without significantly compromising its mechanical properties.

In this study, it is hypothesized that increased levels of PF resin would improve mechanical properties of wood composite panels and further more adding co-polymer coupling agents, such as maleic anhydride polyolefins (MAPO), to PF resin would impart toughness to brittle PF resin and improve panel moisture resistance. Addition of MAPO to resin could result in a phase separation leading to a reduction in resin brittleness and improvement in its toughness; this could lead to a production of OSC at a higher resin content level with improved toughness and moisture resistance. Furthermore, thermoplastic in MAPO could potentially act as a moisture barrier within the matrix by bulking the voids between the strands thus leaving less space for moisture penetration.

Objectives

The overall goal of this study was to produce an oriented strand composite (OSC) with enhanced moisture durability without significantly compromising mechanical properties. Specific objectives within this project are to:

1. Evaluate the effect of particle size and form (powder or emulsion) of MAPO on the phase distribution and dynamic mechanical properties of cured adhesive system.

2. Investigate the effect of blending MAPP with PF resin on its curing behavior and dynamic properties of PF resin blends.
3. Evaluate the effects of varying proportions of MAPO blended with PF resin on adhesive fracture toughness and moisture resistance.
4. Determine the effect of varying PF and MAPO (either MAPE or MAPP) levels on physical and mechanical properties of OSC.

Objectives 1, 2 and 3 will facilitate in determining whether to use MAPP or MAPE to blend with PF resin to improve its toughness when applied as a binder in manufacturing oriented strand composite panels and understand curing behavior of the blend. These objectives will also help in determining the required particle size and form of MAPO to achieve uniform distribution in PF resin that would result in a good phase separation in the resin. Good phase separation has been shown to absorb energy and improve toughness of a resin. Objective 4 will determine the effect of varying levels of PF resin and MAPO (either of MAPE or MAPP as decided from specific objectives 1, 2 and 3) on mechanical and physical properties of oriented strand composites (OSC).

CHAPTER 2

Effect of co-polymer coupling agent on properties of a commercial OSB Phenol Formaldehyde Resin

Abstract

A mechanism to improve toughness of a commercial oriented strand board (OSB) phenol formaldehyde (PF) resin is presented in this study. Effect of adding maleic anhydride polyolefins (MAPO), namely maleic anhydride polypropylene (MAPP) and maleic anhydride polyethylene (MAPE), on the toughness of phenol formaldehyde (PF) resin is investigated. Differential scanning calorimetry (DSC) was used to determine curing parameters. Dynamic properties of resin blends were analyzed using dynamic mechanical analysis (DMA) and toughness of adhesive blends was evaluated using fracture analysis. Particle size analysis using SEM indicated an emulsified form of MAPP resulted in a better distribution resin blend than blends with MAPP particles. DSC results indicated that 2.5 minutes at 145 °C was adequate for nearly 98% curing of the resin blends. With addition of MAPP, a dynamic temperature ramp test conducted with DMA showed an improvement in the storage modulus (E') or stiffness of the resin system during cure. Cured laminates were again dynamically ramped and damping property ($\tan\delta$) was examined at three discrete temperatures (35 °C, 40 °C and 45 °C). Examination of $\tan\delta$ at these temperatures with blends of MAPP or MAPE showed improvement in damping property. Fracture energies (G_{Ic} and G_{Ia}) at 12% MC were increased with the addition of MAPP at lower proportions (1.5% and 3%), whereas, addition of MAPE showed a

reduction in fracture energies. Furthermore, after 24-hour soak, specimens with MAPP showed significant improvements in G_{Ic} and G_{Ia} ; however, addition of MAPE resulted in a reduction of fracture energies. On the basis of these results MAPP anionic emulsion was chosen to blend with PF resin for fabrication of oriented strand composites (OSC) test boards discussed in Chapter 3.

Keywords

Cure kinetics, wood strands, phenol formaldehyde, coupling agents, thermomechanical analysis, fracture toughness.

Introduction

Phenol formaldehyde (PF) is a widely used resin to manufacture exterior grade oriented strand board (OSB), a commonly used sheathing material in low-rise building construction. OSB has the ability to absorb and dissipate moisture if allowed to breath, but often due to poor constructional practices and improper use of vapor barriers could be exposed to high humidity or repeated wet-dry cycles resulting in its rapid degradation. When exposed to high humidity, improving moisture resistance of OSB panels would make them less susceptible to absorbing moisture required for mold and fungal growth. Though panels made of polymeric methylene diphenyldiisocyanate (pMDI) have much better moisture resistance, but the associated high cost and hazardous production procedure make this process less desirable for making durable OSB.

Several methods have been used to reduce the inherent hygroscopicity of wood, including chemical modification (Chow et al. 1996, Clemons et al. 1992, Youngquist et al. 1986, Arora et al. 1981). Though these chemical treatments improved the moisture durability of the product, they significantly reduced their mechanical properties. Thus, there is a motivation to find an alternate method to produce a moisture resistant OSB panel without significantly compromising the mechanical properties, such as stiffness and strength. In this study, it is hypothesized that adding co-polymer coupling agents, such as maleic anhydride polyolefins (MAPO), to PF resin would impart toughness to brittle PF resin. Addition of MAPO to resin could result in a phase separation leading to a reduction in resin brittleness thus improving its toughness. Minimizing brittleness would require greater energy to propagate a crack and result in bond failure between the strands. This would result in a less void generation within the composite. Furthermore, thermoplastic in MAPO could potentially act as a moisture barrier within the matrix by bulking the voids.

Objectives

The goal of this study is to understand the behavior of PF resin in regards to its dynamic properties and toughness when blended with varying proportions of co-polymer coupling agents, namely MAPP and MAPE. Specific tasks formulated to achieve this objective are to:

1. Evaluate the effect of particle size of MAPO on its distribution in the cured adhesive blend and the dynamic properties of cured adhesive system.
2. Examine the effect of blending MAPP with PF resin on its curing parameters, namely curing temperature and curing time.

3. Investigate the effect of blending MAPP and MAPE with PF resin on dynamic properties of adhesive blends.
4. Evaluate the fracture toughness of the resin blends to study the effects of MAPP and MAPE mixed with PF resin.

These tasks will facilitate in determining whether to use MAPP or MAPE to blend with PF resin for improving its toughness when applied as a binder in manufacturing oriented strand composite panels and understand curing behavior of the blend. The study will also aid in deciding what form the co-polymer coupling agent (powder or emulsion) would be most effective to blend with PF resin.

Literature Review

Toughening of PF

Phenol formaldehyde, commonly used resin for OSB, has some excellent properties, but in glassy state it is brittle in nature (Chen and Lee 1995) thus exhibiting lower toughness. The low toughness of PF is inherent from rigid nature of phenolic structure. The toughness and flexibility can be increased with the addition of modifiers like acrylonitrile butadiene styrene (ABS), methacrylate butadiene styrene (MBS), polyaryl ethers, phenylene oxide and rubber particles (Gardziella et al 1999, Kim and Robertson 1992, Chen and Lee 1995, Pearson and Yee 1993, Romano et al. 1994 and Mezzenga and Manson 2001). The addition of polyaryl ether into the resin system nearly tripled the fracture toughness. The modification can be either a chemical modification or a physical one. The chemical modification can be achieved by introduction of a

flexible polymer segment into the rigid phenolic backbone during the preparation of resol resin (Gardziella et al. 1999).

In physical modification high molecular weight polymers, especially thermoplastics, are added to resin systems providing more flexibility to the polymer blend through phase separation, thus imparting toughness. This method of improving toughness is common in the epoxy systems, where a ductile thermoplastic phase is introduced in the tough epoxy phase (Gardziella et al. 1999). Fracture toughness of epoxy resin was shown to increase with addition of thermoplastic in the adhesive system (Kim and Robertson 1992). Chen et al. (1995) significantly improved fracture toughness energy of an epoxy system with the addition of carboxyl terminated butadiene rubber. Boogh et al. (1999) found that addition of hyperbranched polymers (HBP) in the brittle thermoset system causes improvement in the toughness of the cured system. Moreover, it increased the tensile strength up to 25% and reduced the internal stress generation during cure of the thermoset. Same class of additive was also used by Mezzenga and Manson (2001) as a thermoset resin toughener and obtained significant improvement in fracture toughness. Pearson and Yee (1993) used poly phenylene oxide to toughen epoxy; it improved fracture toughness linearly with volume fraction of the toughener in the epoxy system.

Romano et al. (1994) effectively used liquid rubber and phenoxy polymer together to toughen epoxy resin system. Their study showed that slow curing of the adhesive blend results in optimum morphology and phase separation, a key to effective toughening. Interfacial bonding and particle size of the modifier in the cured system depend on parameters such as curing rate and compatibility of epoxy and the modifier; these factors affect the fracture toughness.

Manziona and Gillham (1981) studied thermo-mechanical properties and extent of phase separation in rubber modified epoxies as a function of acrylonitrile content of the modifier and the temperature of cure. It was suggested that a finite time is required for rubber to separate into rubber rich domains; and the required time increases continually during cure as the viscosity of the system increases due to increasing molecular weight of the polymers. Qian et al. (1995) prepared poly (butadiene-co-styrene) core and poly(methyl methacrylate) shell using two-step emulsion polymerization to use as a toughening agent for epoxies. They found that fracture toughness was effectively doubled after modification. Dispersion of modifier particles in the epoxy system was suggested to play a significant role in toughening of epoxies, with greater degree of micro segregation of the particles in the epoxy matrix imparting greater fracture toughness to the modified epoxies.

More recently, Zheng et al. (2004) studied the rheological behavior, penetration characteristics, and fracture performance of liquid phenol-formaldehyde resole and polymeric diphenylmethane diisocyanate (pMDI) hybrid mixtures. They observed that hybrid properties are a function of simple emulsion effects. Improvement in toughness of PF matrix was significant at low pMDI levels due to dispersed urethane/urea/biuret phase; however, dispersed-PF phase resulting from addition of small quantities of PF to urethane/urea/biuret matrix did not result in a significant improvement in resin toughness.

Effect of maleated co-polymers

Maleic anhydride is extensively used in wood plastic composites (WPC) in the form of a grafted co-polymer with polypropylene or polyethylene (maleic anhydride polypropylene, MAPP;

maleic anhydride polyethylene, MAPE). Maleic anhydride is speculated to form a bond between wood flour and polymer matrix enhancing the performance of the composite (Felix and Gatenholm 1991, Maldas and Kokta 1991, Stark 1999, Simonsen et al. 1998, Lu et al. 2002). Simonsen et al. (1998) found that treating aspen fiber with styrene maleic anhydride (SMA) co-polymer enhances mechanical properties of the composite and reduces moisture absorption. In addition, it was suggested that the co-polymer (SMA) forms a strong moisture barrier, though it is not completely impermeable.

Reaction of the maleic anhydride moiety with the wood

Studies have been done to observe the effect of MAPP on moisture affinity and mechanical properties of wood (Marcovich et al. 1998, Patil et al. 2000 and Felix et al. 1991). Lu et al. (2002) treated wood flour with MAPP and found primary bond formation between wood and the maleated polymer. The work also suggested that the maleated polymer is grafted on the wood surface by a succinic half-ester bridge linkage.

Clemons et al. (1992) showed there was a primary bond formation between the hydroxyl group of wood and maleic anhydride. Fiberboards made out of the maleic anhydride treated fibers showed greatly reduced reversible and irreversible thickness swelling. Irreversible thickness swelling was shown to be completely removed when the wood was treated with maleic and succinic anhydride. Same work also revealed that esterification of wood also increases ductility of fiberboard. Hartley and Schneider (1993) studied the water vapor diffusion characteristics and adsorption isotherm of sugar maple wood flour and WPC made out of the same wood. They found a decrease in cell wall moisture uptake and reduction in water vapor diffusion for the

wood in WPC than in untreated wood. WPC made with maleic anhydride treated teak (*Tectona grandis*) sawdust showed a two to three fold improvement in hardness and reduced thickness swelling compared to untreated composite (Patil et al. 2000).

Snijder and Bos (2000) in their study on natural fiber thermoplastic composites found that the molecular weight of the MAPP was more of an important factor than maleic acid content for coupling efficiency. Addition of MAPP in Kudzu fiber PP composite increased the tensile strength and tensile modulus by 24% and 54% respectively due to better interfacial bonding between treated fiber and the matrix (Xiaoyu et al. 2002). However, excess of coupling agents at the interface was found to be detrimental to coupling action and may act as an inhibitor rather than a promoter of adhesion (Maldas and Kokta 1989, Snijder et al. 1997). Mechanical properties of composites increased with an increase in MAPP and reached a plateau at high MAPP levels. In a recent study Garcia et al. (2005) fabricated medium density fiberboard (MDF) from fibers treated with maleated polypropylene wax. They found a reduction in thickness swelling and water absorption with the treatment of MAPP. Same study also revealed that the modulus of elasticity, modulus of rupture and internal bond strength for the MDF increased with treatment with MAPP.

Fracture Cleavage Analysis

Fracture cleavage analysis method is widely used to investigate fracture toughness of an adhesive system. Dual cantilever beam (DCB) specimens are tested to investigate adhesive bond quality (Ebwele et al. 1986, River et al. 1989, Gagliano and Frazier 2001, Scoville 2001). Using linear elastic fracture mechanics, an energy balance is described when the DCB specimen is

loaded in opening or mode I cleavage (Figure 2-2). Displacement energy input from the test frame is balanced against the sum of two energies: potential energy stored in DCB and energy which is required to extend an interlaminar crack. The crack extension energy is often referred to as the mode I fracture energy, G_I (fracture energy at crack initiation, G_{Ic} , and at crack arrest, G_{Ia}), as shown in Equation 2.1 (Blackman et al. 1991, Scoville 2001).

$$G_I = \frac{P_c^2}{2B} \frac{dC}{da} \quad \text{Equation 2.1}$$

Where,

P_c = Critical load when crack extension is initiated or arrested (N)

B = Width of the DCB (mm)

$\left(\frac{dC}{da}\right)$ = Change in compliance (C) with the change in the crack length, a , $\left(\frac{N}{mm}\right)$

As the crack length increases along the bondline in a DCB specimen, the stiffness of the beam decreases and the compliance increases. Modifications are made to take into account the change in compliance as the crack length increases. This method is termed as shear corrected compliance method (Blackman et al. 1991, Schmidt 1998, Scoville 2001, Gagliano and Frazier 2001) as in equation 2.

$$G_I = \frac{P_c^2}{B} \frac{(a + \chi)^2}{EI_{eff}} \quad \text{Equation 2.2}$$

Where,

P_c = Critical load when crack extension is initiated or arrested (N)

B = Width of the DCB (mm)

a = Crack length (mm)

χ = Shear correction factor (see Appendix)

EI_{eff} = effective flexural rigidity of the Double Cantilever Beam specimen

This method of adhesive characterization has been used by many researchers. Ebewele et al. (1982) stated that fracture behavior, if carefully controlled using fracture mechanics principles in specimen design, could explain very complicated nature of wood bonding and be very useful for the evaluation of adhesive properties. River et al. (1989) also concluded that fracture cleavage test for crack initiation energy and crack growth rate stability provides more useful information about the behavior of adhesive than conventional shear tests.

Materials and Methods

A series of tests including, particle size analysis, resin cure kinetics and resin toughness were conducted to test the hypothesis and achieve the goal of this study. Figure 2.1 summarizes schematically the methodology implemented in this study to accomplish the objectives.

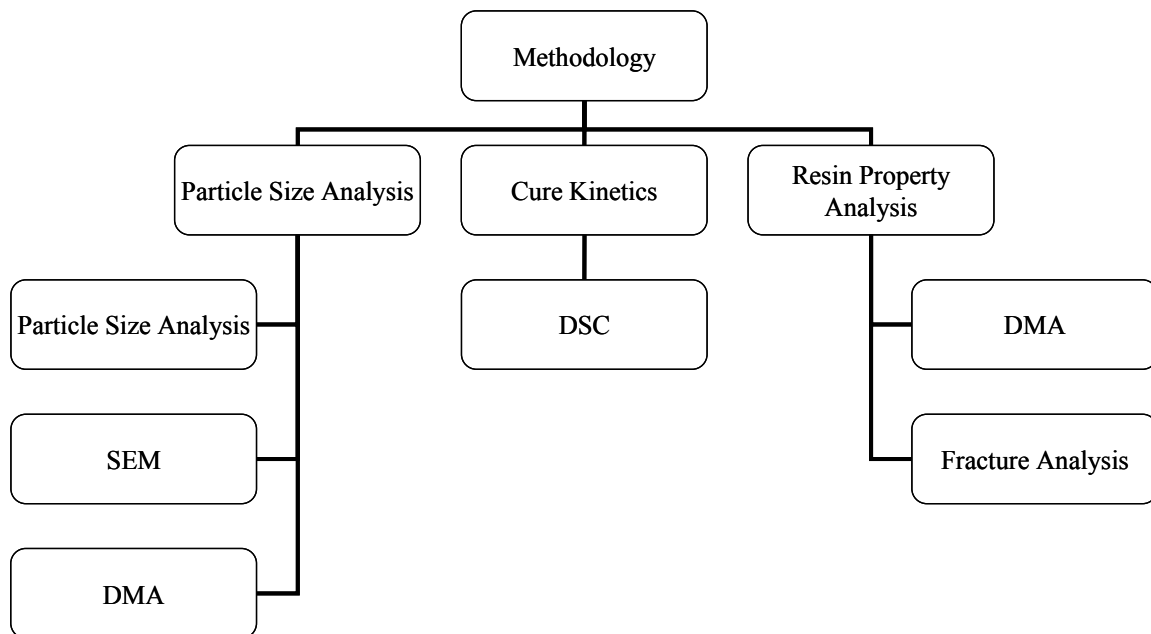


Figure 2.1 Flow chart for the study methodology.

Commercially available OSB phenol formaldehyde face resin (50% solid content), from Dynea chemicals, was used in this study. Maleic anhydride polyethylene (MAPE) and maleic anhydride polypropylene (MAPP) are commercially available in different forms. The most common forms are pellet, atomized particles (or powdered form) and emulsion form. Palette form was not considered in this study as it was necessary to have a thorough mixture of liquid phenol formaldehyde resin and MAPE or MAPP before application for a uniform distribution of additive in the resin and the composite panel. MAPE and MAPP were obtained in both solid form (20-mesh) and emulsion form (1 micron particles suspended in water). Two forms of MAPO emulsions were available, namely anionic and nonionic emulsions. The emulsifier present in anionic emulsion was diethylaminoethanol and that for nonionic emulsion was Tomadol 25-9®. A discussion with Honeywell experts revealed that when anionic emulsion is heated at higher temperatures ($> 120^{\circ}\text{C}$), the emulsion breaks down and the emulsifier diethylaminoethanol disintegrates and evaporates out of the system. Therefore, when the system is cooled MAPO can not go back into an emulsion form as the emulsifier will not be present. On the contrary, in case of non-ionic emulsion of MAPO, the emulsifier Tomadol 25-9® is stable at the range of temperatures applied during OSB pressing process; therefore, in the cured system MAPO can still go back to an emulsion form. In a cured adhesive system containing anionic MAPO emulsions, MAPO will not go back into an emulsion form and, thus, would not leach out when it will come in contact with moisture. MAPE and MAPP anionic emulsions, supplied by Honeywell Specialty Chemicals, were used in this study; their properties are summarized in Table 2.1 (Honeywell 2005).

Table 2.1 Properties of MAPE and MAPP anionic emulsion used in this study.

MAPO Type	Solid Content (%)	Maleic anhydride Content (%)	pH	Viscosity (cps)
MAPE	25%	3.059%	8.5	25.6
MAPP	30%	6.992%	8.5	14.5

Atomized particle or powdered form of MAPO was also supplied by Honeywell Specialty Chemicals. Powder form of MAPE and MAPP were further pulverized to finer particles (will be discussed in the later sections). Resin formulations were prepared by thoroughly mixing MAPE or MAPP (either in particle form or in emulsion form) with liquid phenol formaldehyde resin. All formulations were prepared starting with 100 g of liquid PF resin in a 250 ml beaker. Amounts of MAPE and MAPP were calculated on the basis of solid content of PF resin and added to the beaker. The beaker was then placed on a stirrer and mixed for 15 minutes to get uniformly blended resin formulations. Same procedure was followed to prepare resin formulations for all tests as needed just prior to application. Commercially available basswood strips (1.5 mm nominal thickness and 6 mm wide) were used for DMA three point bending tests. Fracture analysis was performed with yellow poplar wood. Procedures used for each of the tasks as outlined in the objectives section will be discussed next.

Particle Size Analysis

Effect of MAPE or MAPP in the cured resin system significantly depends on how well they are distributed in the system, thus particle size plays a significant role (Romano et al. 1994). Due to limited resources it was assumed that MAPE and MAPP would have similar particle size

effects, thus determination of particle size influence on the resin system, during and after cure, were investigated with only MAPP. The effects of different particle sizes of MAPP in atomized form (80-mesh, 100-mesh and 200-mesh) and in emulsion form were compared. Scanning electron microscopy (SEM) was used to observe the distribution of MAPP particles in the cured resin system. The effect of different particle size on the dynamic properties during cure was monitored using dynamic mechanical analysis (DMA).

Determination of Particle Size Distribution

Commercially available atomized MAPP averaged a particle size of 20-mesh (0.841 mm). As the goal was to achieve a good distribution of MAPO particles in the resin as it would facilitate better phase separation, thus imparting more toughness to the resin system. Particles were further ground in a Wiley mill grinder followed by a ball mill grinder to reduce particle size to less than 80-mesh (0.177 mm). Three different particle sizes were examined to study the influence on MAPO distribution in the resin: 80-mesh, 100-mesh (0.149 mm) and 200-mesh (0.074 mm). As for MAPP anionic emulsion, size of the particles was 1 micron. Particles were separated through standard wire meshes as per ASTM E11 (ASTM 2004). Light scattering particle size analysis was performed using AccuSizer®780 automatic particle size analyzer to determine the actual distribution of particle sizes in each mesh size batch.

Distribution of MAPO in the Resin

Scanning electron microscope (SEM) was used to observe cured specimens of resin blends. Specimens were prepared by thoroughly mixing liquid phenol formaldehyde resin with MAPP (particles or emulsion) to make an adhesive formulation of PF and 1.5% MAPP. The mixtures

were then poured in petri dishes and kept in ambient temperature for 48 hours to allow evaporation of water from the resin. The dishes were put into the oven at 145 °C for 30 minutes to get complete cure of the adhesive system. SEM specimens were prepared from these cured resin specimens and examined at varying magnifications ranging from 50x to 1000x.

Effect of Particle Size on Storage Modulus of Cured Resin Blend

Effect of MAPO particle size in resin blend on the storage modulus was investigated using DMA. Mixture of PF and 0.5% MAPP, both in emulsion form and particle forms (80 mesh, 100 mesh and 200 mesh) were tested in three point bending in DMA. Sample preparation and testing procedure followed are the same as described at later part of this chapter. Dynamic moduli (storage modulus, loss modulus and $\tan\delta$) were recorded during the curing process. Percentage increase in storage modulus (E') during cure of different formulations was observed and compared. Based on the results of specific objective 1, as will be discussed later, emulsion form of MAPO was found to be more effective than powder form in blending with the PF resin and yielding a uniform distribution of MAPO particles in the resin; therefore, in the next two tasks only MAPO emulsions were examined in investigating whether to blend MAPE or MAPP with PF resin in manufacturing OSC test specimens (Chapter3).

Determination of Curing Parameters of Resin Blends

Differential Scanning Calorimetry was used to determine the curing parameters, namely curing temperature and curing time, of the resin blends. The intent was to investigate any changes in curing parameters of the PF thermoset resin system due to addition of MAPO emulsions because application of proper curing parameters is very important to cure the adhesive systems

completely before comparing their properties. It was also assumed that MAPP and MAPE anionic emulsions had similar behavior in terms of curing temperature and curing time when mixed with PF resin. Based on discussions with Honeywell Specialty Chemicals, it was understood that these two emulsions had similar chemical composition except for the fact that MAPE and MAPP had different melting temperatures (melting point of MAPE around 110°C and melting point of MAPP is around 140°C). It is believed that in the emulsion form the melting of MAPP and MAPE would not change significantly; and, as MAPP has higher melting temperature, determination of curing temperature and time of PF and MAPO blends was assumed to be controlled by MAPP. Therefore, curing time and temperature were determined for PF + MAPP emulsions and same curing parameters were applied for curing of PF + MAPE emulsion.

Neat PF resin and blend of PF and anionic emulsion of MAPP at 6% level were dynamically ramped in Metlar-Toledo 822° DSC from 25 °C to 200 °C at a ramping rate of 5 °C/min. High pressure sealed gold plated 30µL pans were used for these tests. Results were compared to see if there was any change in the curing parameters due to addition of MAPP. The temperature at which the reaction rate became highest was monitored. It was observed that at 135°C the reaction rate becomes highest. Thus, 145°C was chosen as the curing temperature to ensure that complete curing of the resin blends was obtained.

Curing time was then determined in a two-step process. First, resin specimens were isothermally cured in the DSC cell at 145°C for varied periods of time, ranging from 0.5 min to 2.5 min with an increment of 0.5 min. After curing for the specified time, the resin samples were promptly

plunged into ice water to arrest the reaction. This step was then followed by dynamic ramping of the cured samples from 25 °C to 220 °C at a ramping rate of 5°C /min. The residual heat of curing (h) for all the specimens was recorded. The extent of cure (α) was then calculated as a percentage of the total heat of cure (H) using the following equation (Wang et al. 2005),

$$\alpha(\%) = \frac{H - h}{H} \times 100 \quad \text{Equation 2.3}$$

Effect of MAPO on Resin Properties

Effect of MAPO on resin blend properties, namely stiffness and toughness were evaluated using DMA and fracture analysis. Molecular level changes, interactions and energy dissipation were monitored using DMA whereas; fracture analysis investigated the effect of phase separation, due to addition of MAPO, on resin blend toughness. Three point bending specimens were tested in DMA to investigate the effects of MAPO on the dynamic properties of resin. Dynamic properties of laminates bonded with different resin blends were tested during and after curing. Mode I fracture cleavage tests were performed to evaluate and compare the effects of MAPO on the fracture toughness of the resin system.

Dynamic Properties of Specimens during and after Cure

Sample Preparation

.Test specimens were prepared from commercially available basswood strips. Strips were cut to a length of 52 mm. Nominal width and thickness of the strips were 6 mm and 1.5 mm,

respectively. The pieces obtained were then conditioned to 12% MC. After conditioning, resin blends were applied on one side of each strip to sufficiently form a uniform thin layer, and two strips were then used to form a laminate with the resin layer in the middle. The laminates were then gently pressed to squeeze out the excess resin and wiped off. It was found from the first few test runs that 11% resin content on the basis of wood weight was sufficient to form a uniform thin layer of resin. Therefore, for rest of the tests 11% resin content was used to form the laminates.

The resin blends tested were, neat PF and PF blended with 0.5%, 1.5% and 6% MAPE and MAPP anionic emulsion. Three replicates for each blend were tested. Laminates were put into a Rheometric II DMA chamber and subjected to three point bending. The frequency of testing was set to 1 Hz. Determining the strain level to conduct the tests at was vital to ensure that the test was always in the linear viscoelastic range of the specimen. The stiffness of laminates changed with temperature as at higher temperature resin curing took place. Therefore, dynamic strain sweep test was performed with the laminates at different temperatures to determine the linear viscoelastic region throughout the test. A strain of 2×10^{-5} was found to be suitable to keep the test within linear viscoelastic region for entire range of temperature. The temperature of the DMA chamber was ramped from 25 °C to 180 °C at a ramping rate of 2 °C/min. Dynamic moduli (E' and E'') and $\tan\delta$ were compared.

Laminates with different adhesive blends were tested in two steps. First, laminates with uncured resin blends were subjected to the testing schedule mentioned previously and the changes in dynamic moduli were observed during resin curing process. In the second step, cured laminates

were then conditioned to 12% MC, and then were subjected to the same testing schedule as previous step. Changes in the dynamic moduli and $\tan\delta$ were monitored during the test.

Fracture Cleavage Analysis

Specimen Preparation

Rectangular blocks of dimensions 300mm x 200mm x thickness of the lumber were cut from yellow poplar lumber. The blocks were then edged in a jointer to clearly determine the grain direction. Using a band saw the blocks were then sliced along the thickness to get 16-17 mm thick plates while maintaining approximately 5° grain angle with the longitudinal axis. The plates were then planed to a thickness of 12 mm and placed in the conditioning room to equilibrate to 12 % MC. Prior to resin application after conditioning, the plates were re-planed to a final thickness of 10 mm.

Resin blends were applied uniformly on the bonding surface. Plates were weighed before and after resin application to determine the amount of adhesive applied. A continuous layer of resin was applied on the surface. It was found that 4% liquid resin on the basis of weight of the wood plates resulted in a uniform layer of resin. All plates were bonded by applying 4% resin on the basis of weight of the wood plates. A 35mm wide Teflon® film was placed at the end of the bonding surface to refrain that portion from bonding. This portion that was not bonded would then act as the pre-crack in the fracture specimens. Thickness of the Teflon® film was less than 13 μ m as suggested by Kinloch (2000). Specimens were pressed in a hot press to bond the matched plates together with different resin blends. Pressing schedule was maintained such that

the adhesive layer between the two wood panels reached 145°C and was held for 5 minutes to ensure complete cure of the adhesive (these parameters were determined based on DSC results discussed previously). A uniform pressure of 550 Kpa (80 psi) was maintained to bond the plates together. After pressing, the laminates were cooled, cut and trimmed into 20 mm wide and 200 mm long DCB specimens (Figure 2.2).

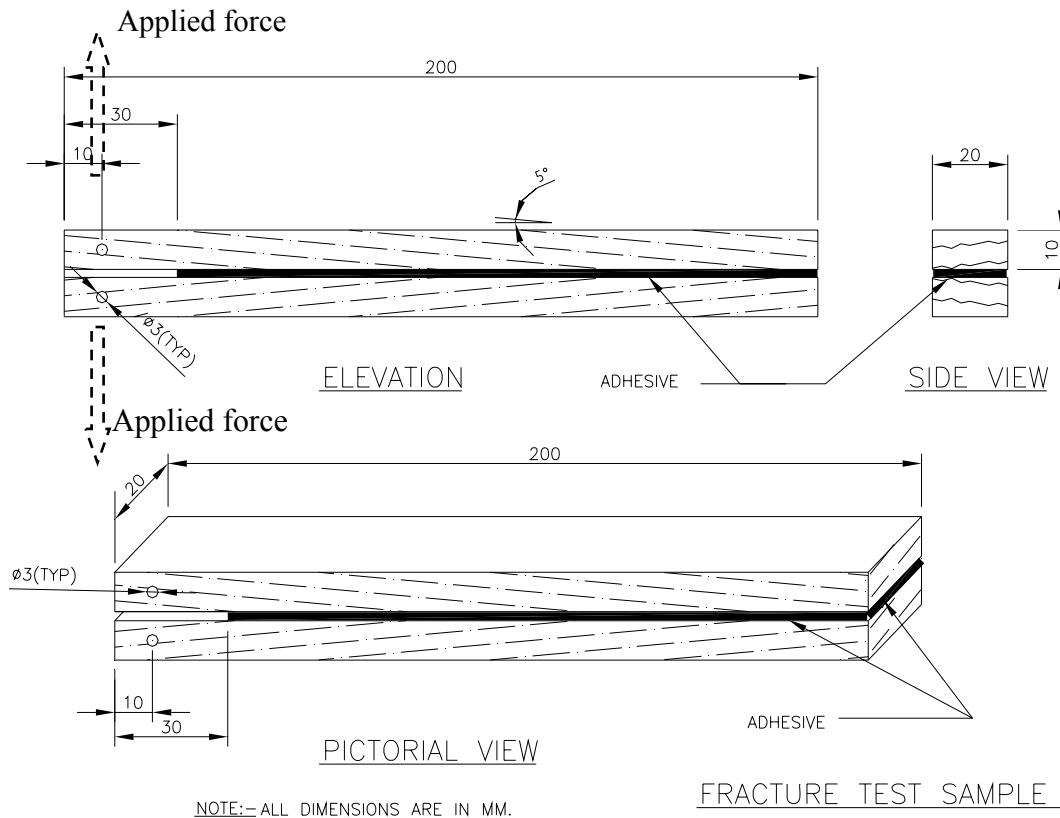


Figure 2.2 Dimension of fracture cleavage test specimen for Mode I fracture.

Two holes of 3 mm diameter were drilled 10 mm from the ends of each DCB specimens (Figure 2.2). A thin coat of white water based correction fluid was applied on the bond line at least 24 hrs before testing. A photocopy of millimeter ruler was glued onto the side of the test specimens to measure the crack length during the test.

Number of replicates for each resin blend was determined by one-factor response design, generated using Design-Expert® (Stat-ease 2006) software to limit the number of tests conducted to obtain statistically valid results. Neat PF and PF with anionic emulsion of MAPE and MAPP were tested. Proportion of MAPE and MAPP varied within lower and upper limits of 0 and 6 percent based on weight of the PF resin (100% solids). Prepared specimens were subjected to two environmental conditions: 12% MC and 24-hr water soak. In the one-factor design, MAPO content was considered as a numeric factor and the environmental conditions (12% MC and 24 hours water soak) and type of MAPO (MAPE and MAPP) were considered as categorical factors. Response variables were crack initiation (G_{Ic}) and crack arrest (G_{Ia}) energy values. Initial design suggested 36 runs. Additional replications were added to make the design more robust. Table 5.1 (Appendix) summarizes all the fracture cleavage test runs performed in this study

Fracture Testing Methodology

Fracture tests were conducted according to the protocol suggested by previous studies (Gagliano and Frazier 2001, Scoville 2001, Blackman and Kinloch 2000). Tests were conducted at a loading rate of 1 mm/min. With the drop in load upon crack initiation, the cross head was programmed to hold the position at 5% load drop for one minute. At the end of one-minute period, when a quasi-stable load state was reached, crack length, corresponding crack arrest load and displacement were recorded. Photographs were taken with a high-resolution digital camera to measure crack lengths. After recording the data, the cross head was returned to the starting point and the next cycle was started. These cycles were repeated until the crack tip exceeded 150 mm mark on the paper ruler or the specimen failed by propagation of the crack through the

length of the specimen. Figure 2.3 shows a typical load versus displacement plot for a fracture specimen. The test was carried out with a 5500 series Instron® universal testing machine controlled by Bluehill® software.

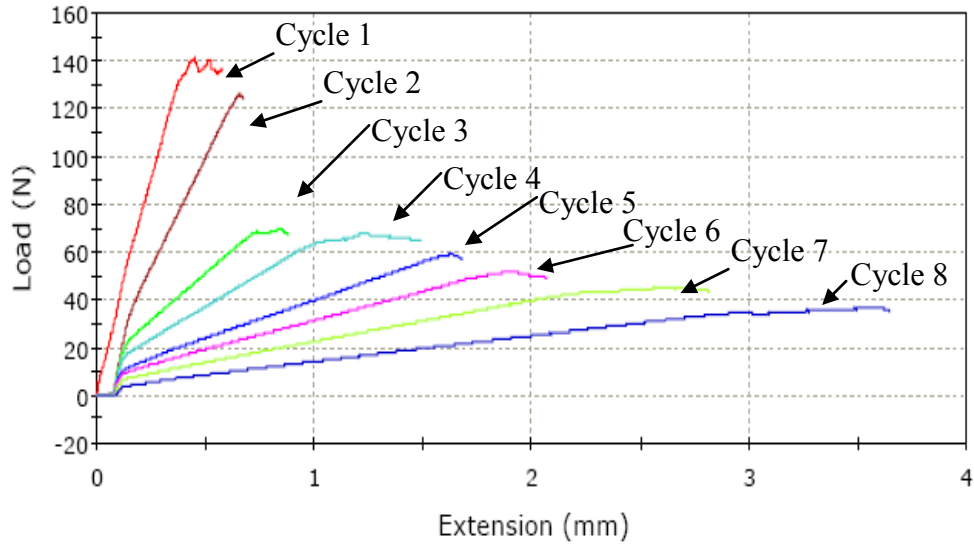


Figure 2.3 Typical plot of load versus extension for single fracture specimen at repeated load cycles.

Fracture energies were calculated using shear corrected compliance method as discussed previously (Blackman et al. 1991, Gagliano and Frazier 2001, Scoville 2001). A plot of crack length and the corresponding cube root of compliance was generated. Slope (m) and intercept (b) were determined from the plot. The shear correction factor (χ) is the ratio of intercept (b) to the slope (m). The crack initiation energy (G_{Ic}) and crack arrest energy (G_{Ia}) were calculated using Equations 2-4 and 2-5 respectively (Blackman et. al. 1991, Gagliano and Frazier. 2001, Scoville 2001).

$$G_{Ic} = \frac{P_c^2}{B} \frac{(a + \chi)^2}{EI_{eff}} \quad \text{Equation 2.4}$$

Where,

a = Crack length (m)

P_c = Critical load for crack initiation (N)

B = Width of the specimen (m)

χ = Shear correction factor, $\chi = \frac{b}{m}$, (m)

EI_{eff} = Effective flexural rigidity of the Double Cantilever Beam specimen, $EI_{eff} = \frac{2}{3m}$

$$G_{Ia} = \frac{P_a^2 (a + \chi)^2}{B EI_{eff}} \quad \text{Equation 2.5}$$

Where, P_a is the critical load at crack arrest.

Results and Discussion

Particle Size Analysis

Figures 2.4 to 2.6 show the volume percentage distribution of particle diameters for 80, 100 and 200-mesh batches of MAPP in dry particle form obtained by light scattering particle size analyzer (AccuSizer[®] 780), respectively.

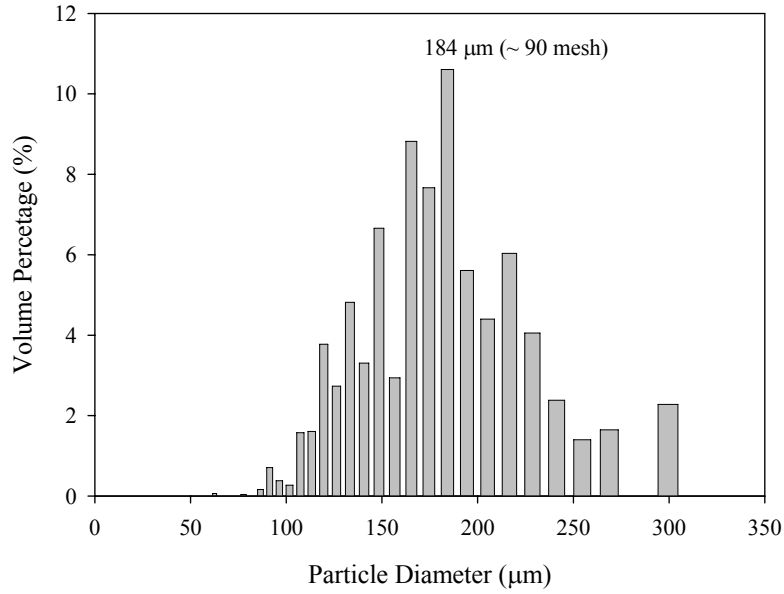


Figure 2.4 Actual particle size distribution for 80-mesh MAPP batch obtained using light scattering particle size analyzer.

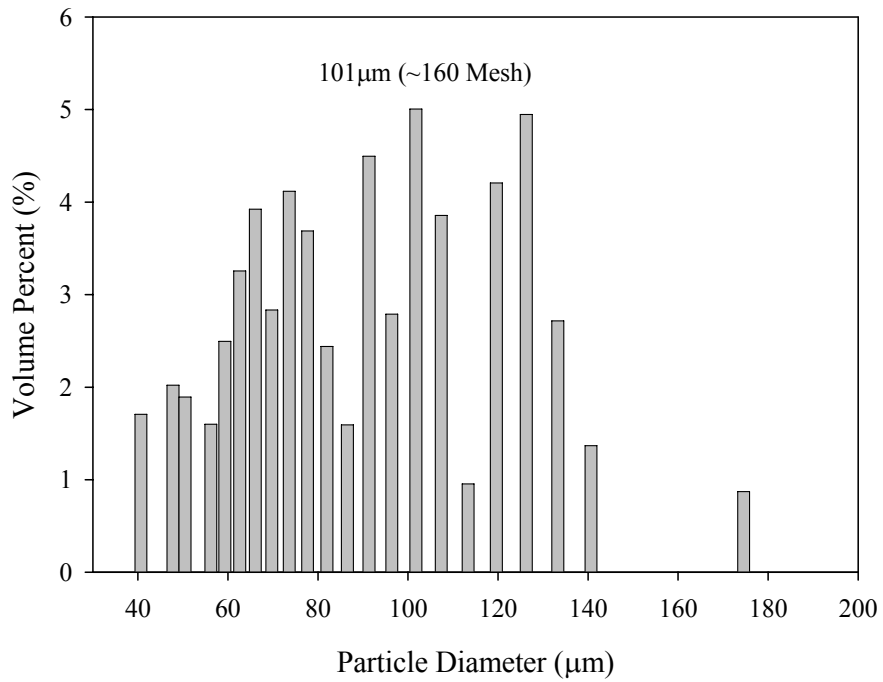


Figure 2.5 Actual particle size distribution for 100-mesh MAPP batch obtained using light scattering particle size analyzer.

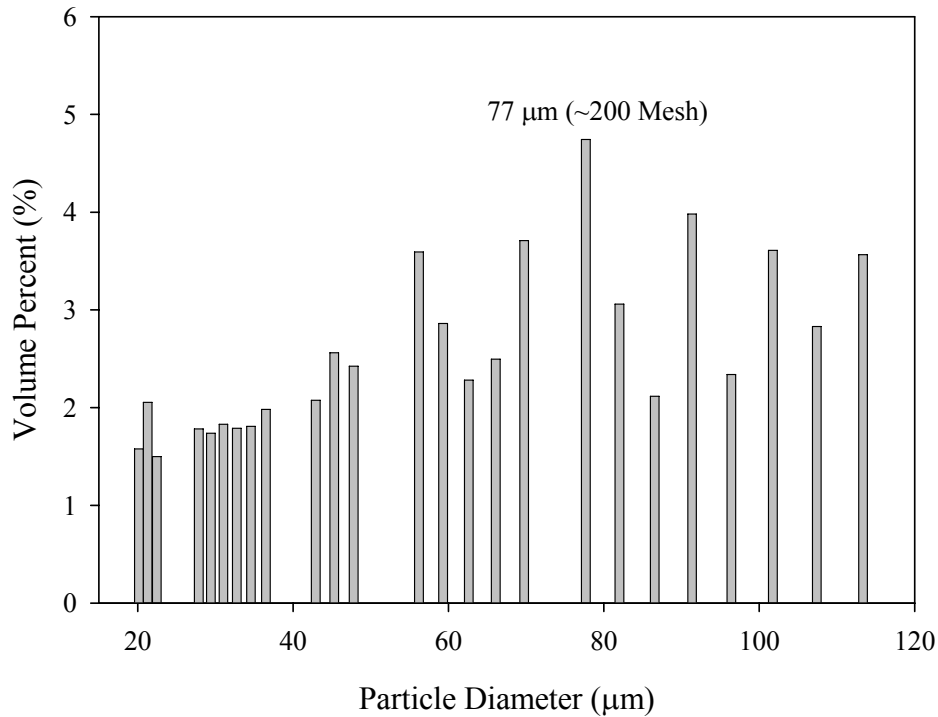


Figure 2.6 Actual particle size distribution for 200- mesh MAPP batch obtained using light scattering particle size analyzer.

Distributions indicate that every batch consisted of a wide range of particle diameters.

Considering the maximum volume percentage in each batch, 80-mesh (Figure 2.4) and 200-mesh batches (Figure 2.6) had comparable or slightly smaller size to the targeted values than 100-mesh batch (Figure 2.5) where greater number of particles was finer than targeted size. Significant proportions of finer particles were expected as particles were ground in a ball mill, where there is limited control on the process. It was especially difficult to reduce MAPP and MAPE particles as they were more malleable and did not break down into finer particles even after extended periods of processing in the ball mill. In the rest of the report, we will refer to the batches as 80-mesh, 100-mesh and 200-mesh.

Distribution of MAPP in Resin Blends

Scanning electron microscopy (SEM) of cured resin blends of PF and 1.5% MAPP (blended in the form of dry particles and emulsion) clearly showed distinct differences in distribution and surface topography as we vary the particle size. SEM pictures of cured resin formulation consisting 80-mesh, 100-mesh, 200-mesh particles and MAPP anionic emulsion are shown in Figure 2.7.

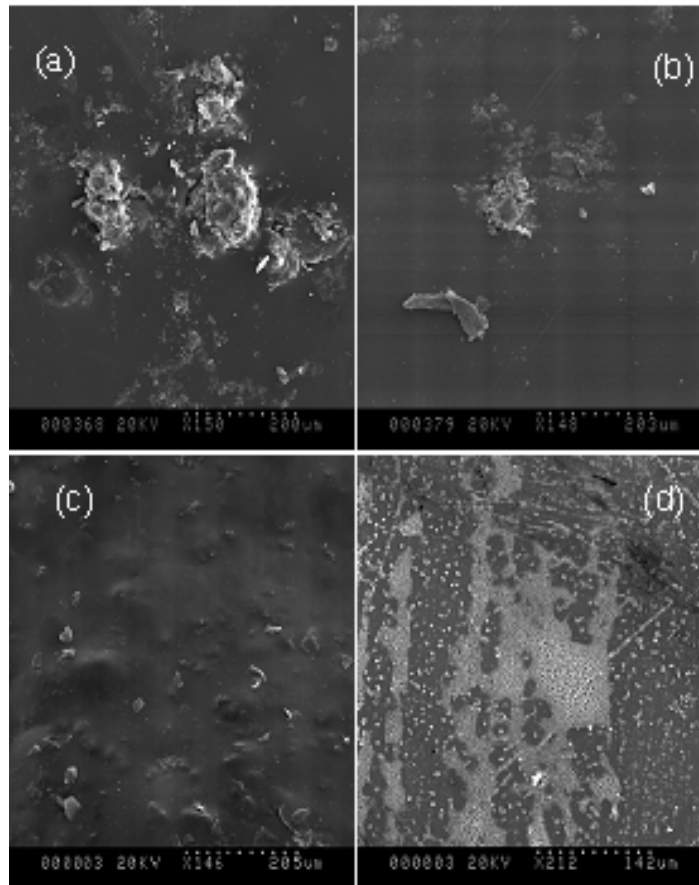


Figure 2.7 SEM pictures for cured adhesive formulations with MAPP (a) PF+80 mesh MAPP, (b) PF + 100mesh MAPP, (c) PF + 200 mesh MAPP and (d) PF + MAPP anionic emulsion

Emulsified MAPP clearly yielded the most uniform distribution in the PF resin. The surface qualities were found to get better as finer particles were used. Larger particles (80-mesh and 100-mesh) resulted in more agglomeration or clumping of particles and was harder to achieve a uniform distribution (Figure 2.7a and 2.7b). SEM pictures of formulation with PF and MAPP anionic emulsion (particle size of 1 micron) showed better distribution of MAPP in the resin, even at a higher magnification (Figure 2.7d). Even the surface topography was much better and uniform when MAPP anionic emulsion was used.

Dynamic Properties of Resin Blends

Storage modulus (E') during the cure process with MAPP solid particles as well as emulsion was compared as a measure of stiffness of the laminates. Figure 2.8 shows the comparison of percentage increment in E' for different formulations during cure.

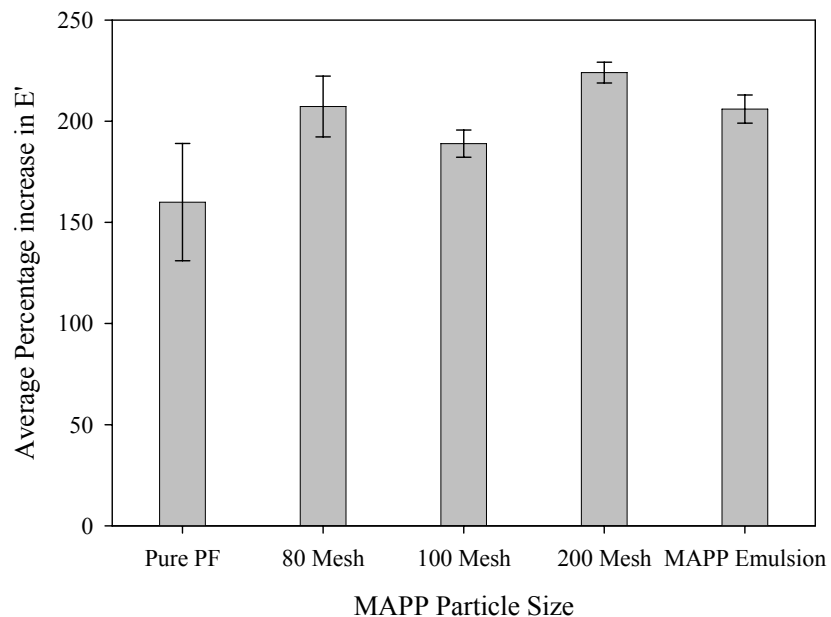


Figure 2.8 Comparison of percentage increase in E' using DMA during cure of blends with different forms of MAPP particles in PF resin.

Even though PF resin with MAPP in all forms yielded higher percentage increase in storage modulus, comparison of percentage increment in E' during cure did not show a significant difference between the formulations with different MAPP solid particle sizes and emulsion (p-value = 0.168). From this analysis, it could be inferred that though the storage modulus of the resin blends was not greatly influenced by different particle sizes (Figure 2.8), the distribution of MAPP in the blend was significantly improved with finer particles.

Considering the ease of application during manufacturing of oriented strand composite panels, liquid MAPP emulsion with particle size of one micron would be much easier to apply and would yield a better mixture than solid MAPP particles. Therefore, further analysis on cure kinetics of resin blends using DSC and efficacy of blending MAPP or MAPE in PF resin to improve its toughness and moisture resistance with DMA and fracture cleavage test were conducted only on blends with MAPO anionic emulsions.

Curing Parameters of Resin Blends

DSC analysis under temperature ramping of uncured PF resin and PF and MAPP anionic emulsion blend showed an exothermal peak at 135 °C (Figure 2.9).

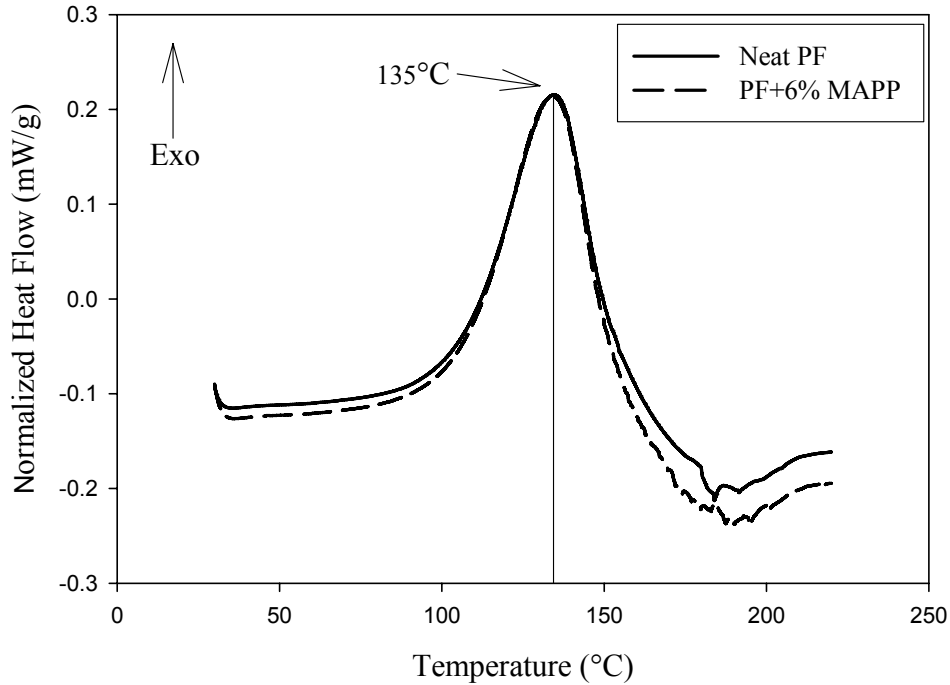


Figure 2.9 Dynamic ramping of neat PF and PF+ 6% MAPP mixture in DSC.

The peak temperature did not change between neat PF resin and formulation with PF and 6% MAPP anionic emulsion. To ensure complete cure, the curing temperature for all the formulations was fixed at 145°C. From this graph the total heat of cure was calculated. This was done by integrating the curve from the onset to end point of the exothermal peak. The total heat of cure was then normalized for heat of cure per gram of resin. The values of normalized heat of cure from different formulations were found to be quite close to each other (Table 2.2).

Table 2.2 Comparison for average normalized heat of cure for neat PF and PF with 6% MAPP emulsion.

Blend	Average Normalized Heat of	
	Cure (J/g)	CoV (%)
Neat PF	99.5	4%
PF + 6% MAPP	101.7	5%

Formulations cured at 145°C for different time periods were then dynamically ramped to determine residual heat of cure. Normalized heat flow vs. temperature plots for mixture of PF and 6% MAPP anionic emulsion cured at 145°C for different time periods are shown in Figure 2.10.

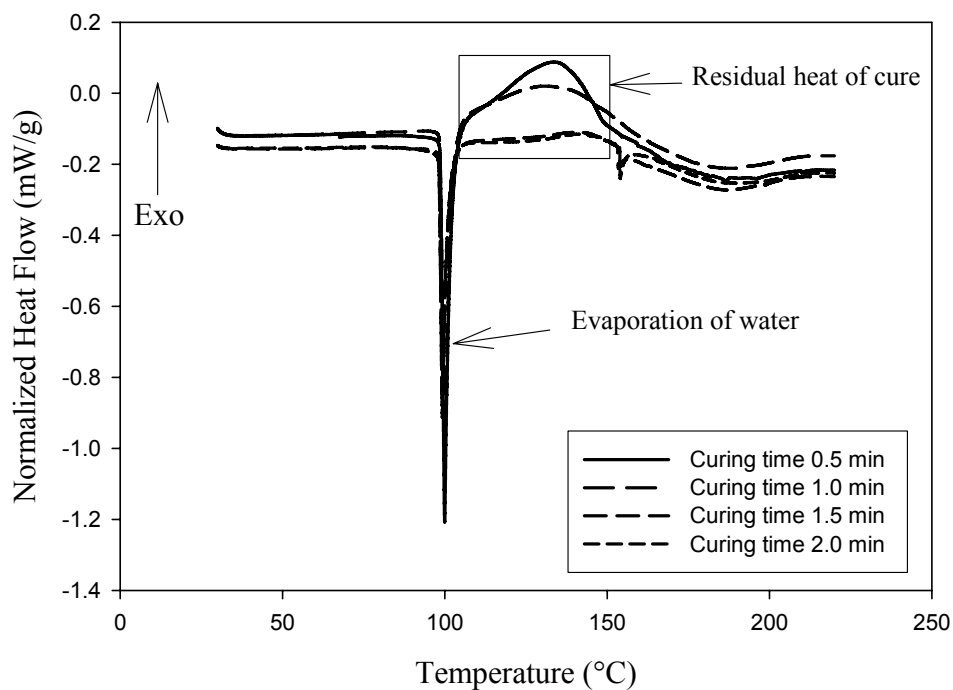


Figure 2.10 Dynamic temp ramp with cured PF+ 6% MAPP formulations for varying time periods in DSC.

The residual heat of cure (h) was calculated for each of the cured samples by integrating the residual exotherm curve. The extent of cure (α) was then calculated using Equation 1.3. It was found that 2.5 minutes at 145°C resulted in 98% cure of the resin formulation (PF + 6% MAPP). The endothermic peaks at 100°C represent evaporation of water. It was mentioned by earlier researchers (Vick and Christiansen 1993) that with the use of high pressure sealed pans it was not possible to observe the secondary processes like evaporation of water. However in this case lower magnitude of residual heat of cure for uncured resin was not much higher in magnitude

than the heat flow for evaporation of water. Therefore, both the processes were significant and were observed during temperature scan. This was validated by the temperature scan of cured specimens after drying; endothermic peaks were not present for dried specimens, justifying the fact that these endothermic peaks were indeed due to the evaporation of water.

Effect of MAPO on Resin Properties (Dynamic Mechanical Properties and Fracture Toughness)

Dynamic mechanical analysis was employed during and after curing to investigate the effect of MAPO on the adhesive blend properties. Influences of the addition of MAPO in PF resin were investigated at molecular level in this method. During the curing process, as the temperature was ramped, the stiffness changes in the sample were monitored. Typical graph obtained during this process is shown in Figure 5.4 (Appendix). Figure 2.11 shows a typical trend of percent increase in storage modulus (E') during the curing process.

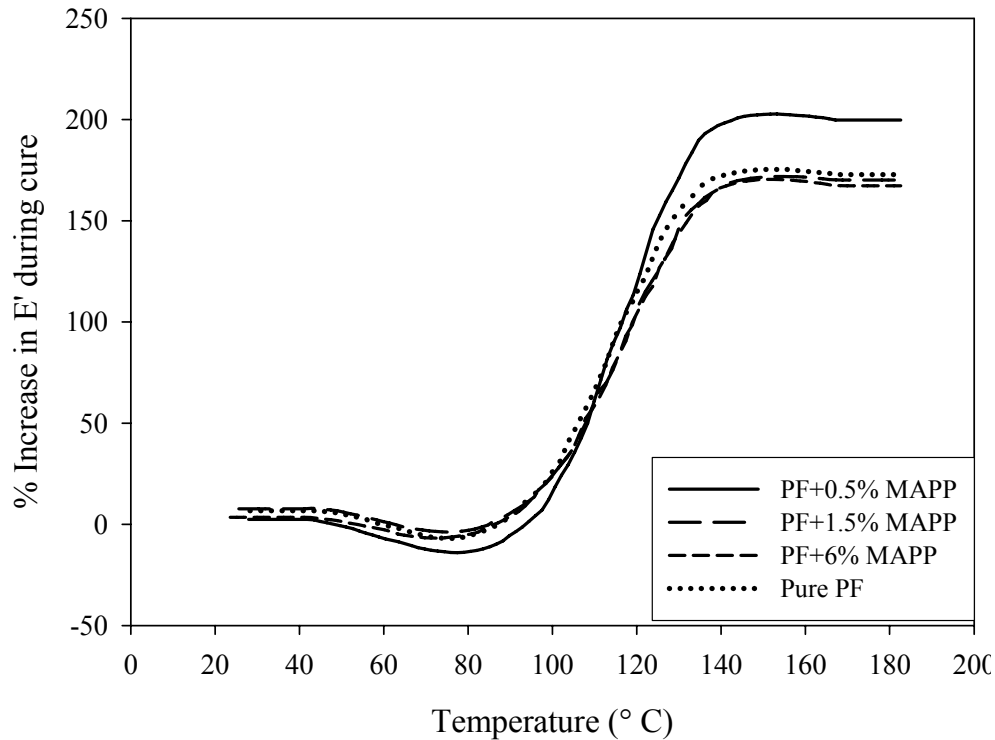


Figure 2.11 Percentage increase in storage modulus (E') during curing process with DMA.

Storage modulus (E') of the laminates remained fairly constant until the resin started curing at the temperature range of 80 °C to 100 °C, after which the stiffness modulus values increased, reached the maximum and leveled off. This is a typical curing trend for thermoset resin (Menard 1993, Lisperguer et al. 2005).

At the onset of curing, cross linking of resin starts and as it increases and ultimately becomes a cross-linked giant molecule of cure resin, the stiffness of the laminate also increases.

Percentage increases in the stiffness values during the curing process were then calculated from the initial storage modulus (E') and maximum storage modulus (E'). The maximum average percentage increase in the stiffness modulus (E') values for specimens with neat PF and

specimens with the mixture of PF and different MAPO anionic emulsions during the curing process were compared in Figure 2.12.

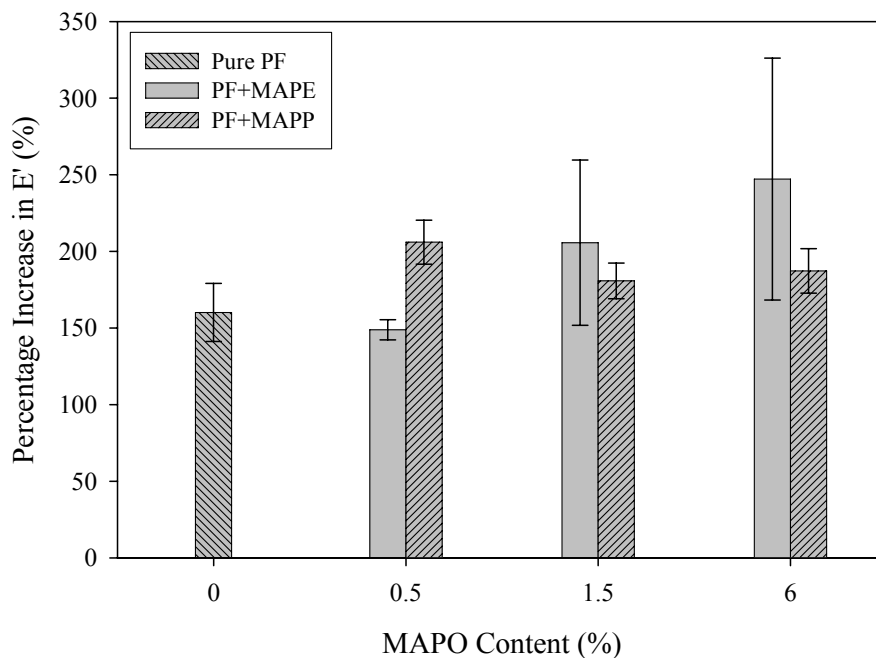


Figure 2.12 Average percentage increase in storage modulus (E') obtained using DMA for different adhesive formulations.

Addition of MAPP anionic emulsion was found to increase the laminate stiffness of the resin system during cure, though the increase was not significant. Addition of MAPE anionic emulsion into PF also showed an improvement in E' during the curing process, however there was much higher variations in the results. Analysis of variance indicated that the differences between the formulations were not statistically significant (p -value = 0.0764). However, it was evident from the results that the addition of MAPP or MAPE did not decrease the resin stiffness as it cured due to addition of thermoplastic co-polymer. This is a positive outcome as the investigators would like to improve the resin toughness without adversely effecting resin stiffness with addition of MAPO (MAPP or MAPE) anionic emulsions in the resin system.

Parameter $\tan\delta$ is a measure of energy dissipation or damping of a polymer. A typical trend of $\tan\delta$ for resin blends tested is shown in Figure 2.13.

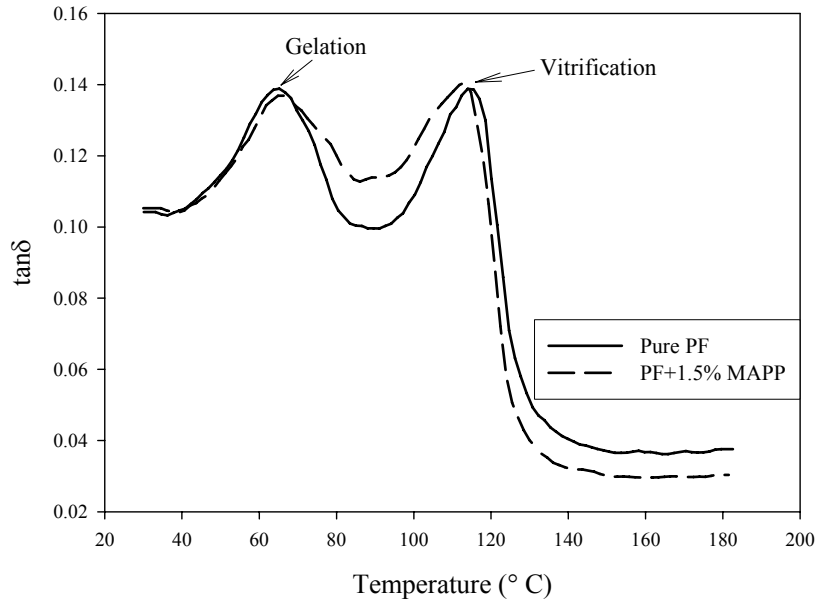


Figure 2.13 Typical trend of $\tan\delta$ for adhesive formulations during curing process.

Two distinct peaks can be noticed. The first peak was obtained at about 60 °C and the second one was found in the vicinity of 120°C. Previous studies also observed a similar trend (Geimer et.al. 1990, Lisperguer et.al. 2005). The peak at lower temperature is termed as the gelation point where the monomers rapidly start forming network structure and the viscosity of the system dramatically increases. At this point the system transforms from sol state to gel state (Turi 1981, Craver 1983). The second peak is the vitrification point, where the polymer reaches a rigid network of infinite molecular weight and transforms from rubbery to glassy state. This usually happens at the glass transition temperature of the polymer (Turi 1981, Craver1983). The trend of $\tan\delta$ showed that with the addition of MAPO into the mixture the transition of adhesive systems from sol to the gel state and from there to the vitrified state did not change significantly.

As indicated in the procedures, a follow-up analysis with DMA was performed with the cured laminates to determine the effects of MAPO on the damping property of the cured resin systems. A typical trend of storage modulus (E') and $\tan\delta$ when cured specimens were ramped from 25°C to 180°C at 2°C /minute rate, is shown in Figure 2.14.

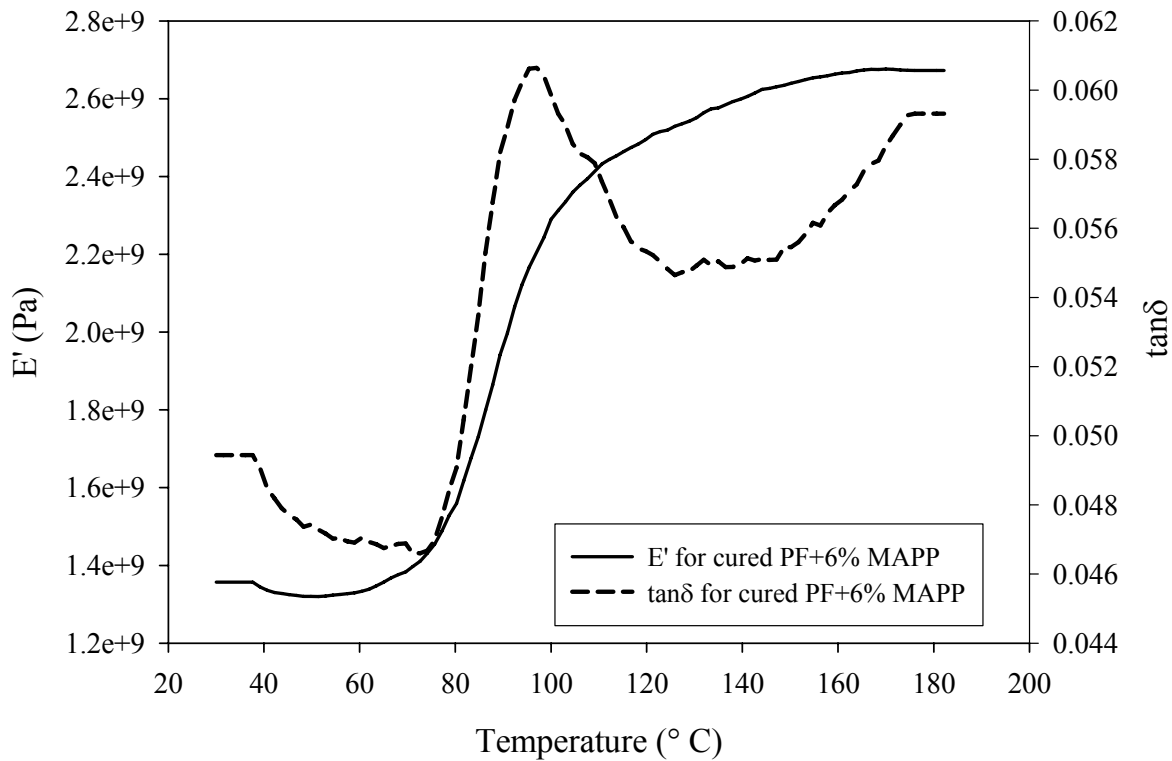


Figure 2.14 Typical trend of E' and $\tan\delta$ for the cured laminates under ramping. The increase in the E' is due to loss of moisture

Storage modulus of the sample starts to increase from about 80 °C and reaches a maximum at about 100 °C. It was assumed that this increase was due to the loss of moisture during the temperature ramp. Similar test with dry specimen was conducted to confirm this assumption. It was found that with dry specimen the storage modulus was constant throughout the temperature ramp, confirming that the increase in stiffness was due to loss of moisture.

The effect of different formulations on the damping property of the cured resin system was investigated by examining the normalized $\tan\delta$ of the specimens at three different temperatures, 35 °C, 40 °C and 45 °C. These values were obtained by normalizing storage (E') and loss moduli (E'') values on the basis of initial E' and E'' values of uncured laminates and calculating $\tan\delta$ based on them ($\tan\delta = E''/E'$). Because fitting a polynomial to $\tan\delta$ values at specified temperatures did not yield good predictive model, discrete values from the experimental data at specified temperatures (35 °C, 40 °C and 45 °C) were compared. Comparison of normalized (for uncured laminate moduli) $\tan\delta$ for cured formulations with PF and different proportions of MAPO (MAPE and MAPP) at 40°C is shown in Figure 2.15. Similar trends were observed at 35 °C and 45 °C.

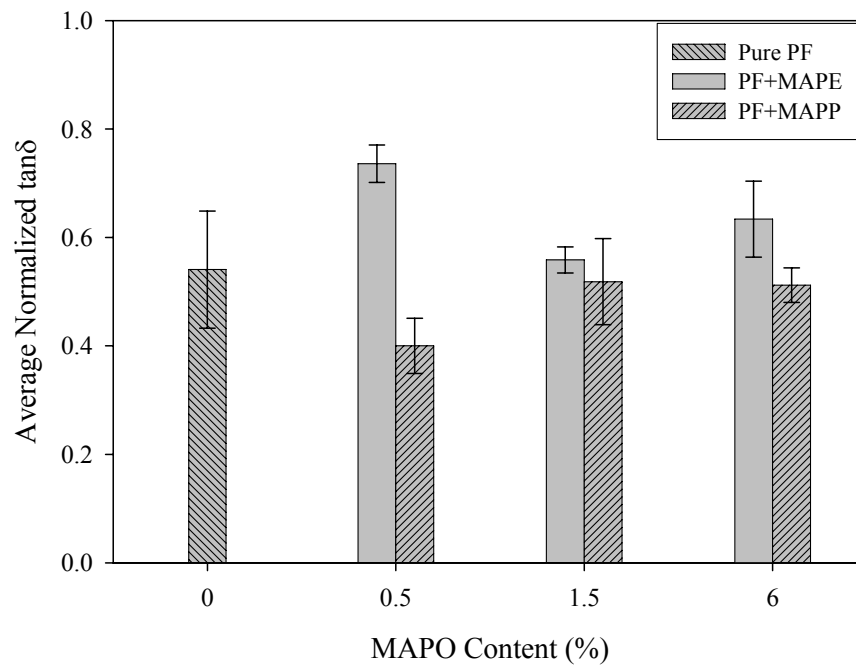


Figure 2.15 Comparison of normalized $\tan\delta$ for cured formulations with different proportions of MAPO (MAPE /MAPP) at 40 °C

Comparison of data indicates there is a distinct increase (~ 35% increase) in the $\tan\delta$ value with the addition of small amount (0.5%) of MAPE into the system. On the other hand addition of

MAPP showed no improvement. Comparison of mean test at 0.05-significance level indicated that formulation with 0.5% MAPE was statistically significant than other formulations; however, MAPP and PF values did not differ significantly at any other levels. As MAPP levels increased $\tan\delta$ of the specimens showed an increasing trend. One of the hypotheses of this study was with the addition of MAPO into resin blend the damping property should increase. Use of MAPE followed the hypothesis at lower proportion, but MAPP did not. This fact can be justified from the structural differences in MAPE and MAPP polymers. Addition of more flexible MAPE might have contributed in damping improvement, whereas addition of MAPP did not show significant difference in damping property. It should be kept in mind that DMA results are sensitive to specimen size and variations in wood from specimen to specimen. It is difficult to isolate the behavior of resin and examine the changes in resin damping property as blend compositions are changed. Thus, fracture cleavage analysis was also performed in an attempt to investigate differences in energy dissipation of fractured glue lines as resin blends were changed.

Fracture Cleavage Analysis

Fracture energies for dual cantilever beam (DCB) specimens were calculated. Tables 2.3 and 2.4 summarize average values and coefficient of variations (COV) of G_{Ic} and G_{Ia} for specimens with different formulations at 12% moisture content.

Table 2.3: Average G_{Ic} and G_{Ia} values for PF + MAPE adhesive formulations at 12% MC.

Blend	Number of Replicates	Avg. G_{Ic} (J/m²)	COV (%)	Avg. G_{Ia} (J/m²)	COV (%)
Pure PF	4	86	17	61	24
PF+ 1.5%MAPE	4	69	15	54	22
PF+ 3.0%MAPE	5	74	14	60	15
PF+ 4.5%MAPE	2	46	-	29	-
PF+ 6.0%MAPE	4	56	37	36	40

Table 2.4 Average G_{Ic} and G_{Ia} value for PF + MAPP adhesive formulations at 12% MC.

Blend	Number of Replicates	Avg. G_{Ic} (J/m²)	COV (%)	Avg. G_{Ia} (J/m²)	COV (%)
Pure PF	4	86	17	61	24
PF+ 1.5%MAPP	3	120	37	94	39
PF+ 3.0%MAPP	6	109	30	76	40
PF+ 4.5%MAPP	3	109	21	75	41
PF+ 6.0%MAPP	5	75	22	54	21

One factor response model indicate a decreasing trend in crack initiation energies with increasing proportion of MAPE anionic emulsion in the resin blend; however, with increasing MAPP content in the resin blend, crack initiation energy increases initially, reaching a maximum at 3% level and starts to decrease with further addition of MAPP.

Reduction of crack initiation and crack arrest energies were larger at higher proportions (4.5% and 6%) of MAPE in the resin system. Analysis of variance for the model showed that MAPE and MAPP significantly effected fracture energies at 12% moisture content ($p < 0.0001$). Figure 2.16 shows the comparison of fracture energies for varying levels of MAPE at 12% MC. Results of comparison of means at significance level of 0.05 are also shown in the figure; results with similar letters indicate no statistically significant difference.

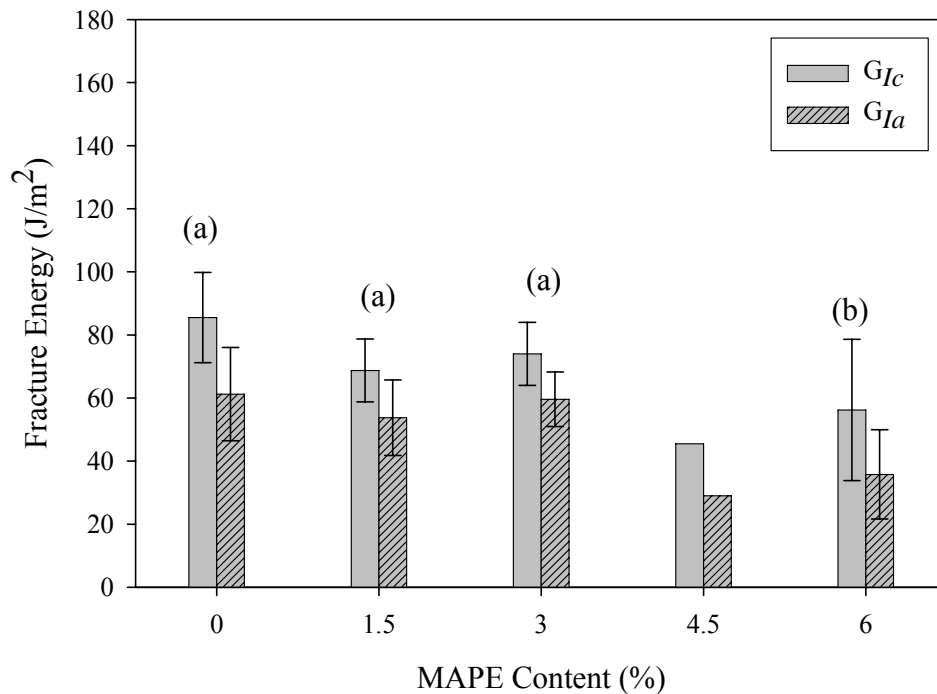


Figure 2.16 Fracture energies for PF+MAPE formulations at 12% MC; bars with same letters indicate that fracture energies of these blends were not statistically significant from each other at significance level of 0.05.

Addition of MAPP anionic emulsion improved the fracture energies of adhesive formulations at lower levels (1.5% and 3%); beyond this point the effect leveled off or reduced. Comparison of fracture energies at varying MAPP levels is shown in Figure 2.17 along with comparison of means test results at significance level of 0.05.

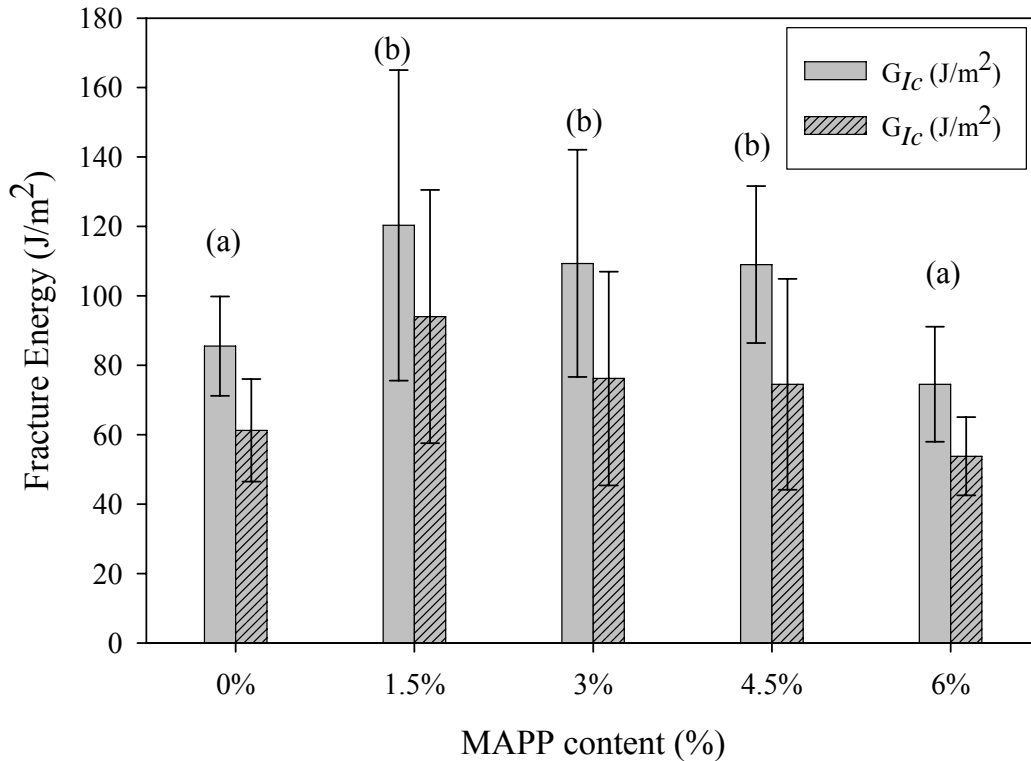


Figure 2.17 Fracture energies for PF+MAPP formulations at 12% MC; bars with same letters indicate no significant differences in energy values.

There was an increase of 41% in average G_{Ic} value for formulation with 1.5% MAPP compared to neat PF formulation; comparing same formulations, G_{Ia} increased by 53%. This trend could also be related with the previous works conducted on wood plastic composites, where with the addition of modifier the mechanical properties improved; however, addition of additive at higher proportions yielded no significant effect and even had a negative influence (Maldas et al. 1989 and Snijdar et.al. 1997). Similar trends were also found by previous researchers, where the addition of modifier at lower levels improved the mechanical properties of the adhesive system but the addition at higher proportions either did not have a significant effect or, in some cases, deteriorated the properties (Maldas et al. 1989 and Snijdar et.al. 1997). A comparison of means

test at 0.05 significance level showed that crack initiation energy at 1.5% and 3% MAPP levels were significantly better than other MAPP levels.

Fracture toughness tests of specimens after 24 hr water soaking indicated that specimens bonded with neat PF increased. This trend was also observed by previous researchers (Scoville 2001). DCB fracture specimens were fabricated with their grain orientations at 5° angle with their longitudinal axes (Figure 2.2). This specific grain orientation was preferred to keep the propagating crack within the bondline; however, this would also generate a lot of stress in the bonded specimens due to difference in shrinkage and swelling patterns of two adherents during 24-hr water soak. Under soaking, specimens release stress and fracture toughness increases (Scoville 2001). Difference in shrinkage and swelling pattern within bonded specimens also caused failure of some specimens after 24 hr soak. Tables 2.5 and 2.6 summarize the fracture toughness values for 24-hr soak specimens.

Table 2.5 Average fracture toughness energies for formulations with MAPE after 24-hr soak.

Blend	Number of Replicates	Avg. G_{Ic} (J/m²)	COV (%)	Avg. G_{Ia} (J/m²)	COV (%)
Neat PF	4	113	12	86	17
PF+ 1.5%MAPE	3	60	46	44	50
PF+ 3.0%MAPE	5	44	37	34	48
PF+ 4.5%MAPE	2	42	-	36	-
PF+ 6.0%MAPE	5	57	19	44	21

Table.2.6 Average fracture toughness energies for formulations with MAPP after 24-hr soak.

Blend	Number of Replicates	Avg. G_{Ic} (J/m²)	COV (%)	Avg. G_{Ia} (J/m²)	COV (%)
Neat PF	4	113	12	86	17
PF+ 1.5%MAPP	3	65	43	50	35
PF+ 3.0%MAPP	5	161	24	119	44
PF+ 4.5%MAPP	2	89	-	52	-
PF+ 6.0%MAPP	4	44	10	34	15

One factor response plot model demonstrates a decreasing trend in fracture energy with increasing MAPE anionic emulsion content for 24-hour water soak specimens; whereas, with addition of MAPP in the blend, fracture energy dropped initially but seem to increase again maximizing at around 3% level and then decrease again at higher levels. It should be noted that coefficient of variations are relatively high indicating the complexity involved in crack propagation through adhesive bond layer between wood substrates. Figure 2.18 represents the plot of fracture toughness of formulations with MAPE anionic emulsion after 24-hr water soak.

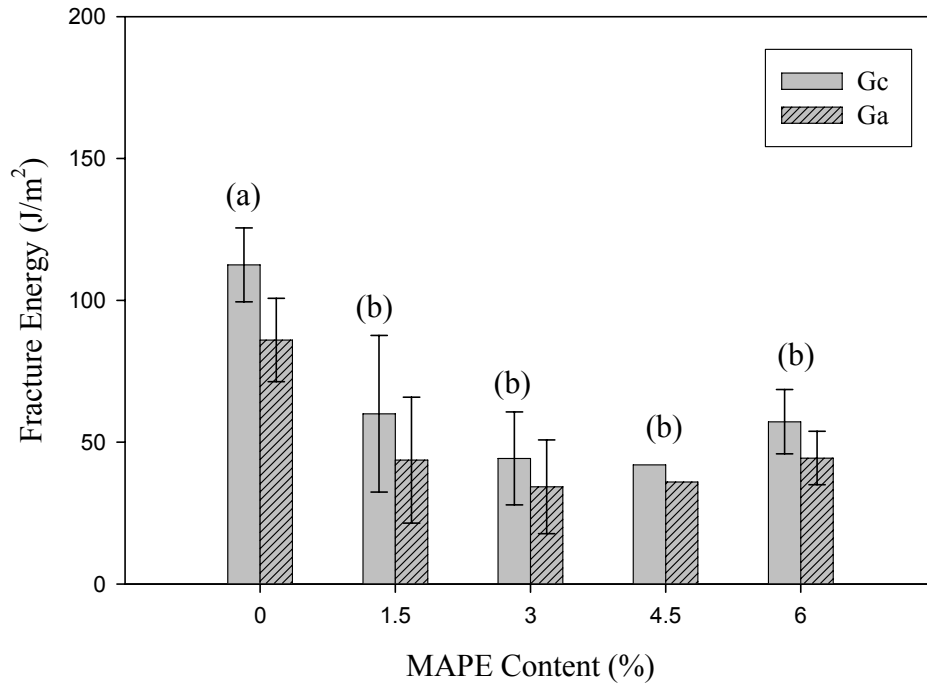


Figure 2.18 Average fracture energies for formulation with MAPE emulsion after 24-hr water soak. Comparisons of means test results are included on the top of the bars.

Fracture energies (both G_{Ic} and G_{Ia}) were considerably decreased with the addition of MAPE into the system. As MAPE content was increased from 0 to 1.5% a drop of 46% in the crack initiation energy and 49% in the crack arrest energy were observed. Comparison of means test at significance level of 0.05 indicated a significance difference between neat PF and other formulations with MAPE additive irrespective of the amount added; test indicated no significant differences among the PF formulations with MAPE blended in. Comparing G_{Ic} and G_{Ia} for the formulations with MAPP anionic emulsion, a 43% increase in the G_{Ic} and a 38% increase in G_{Ia} was observed for formulation with 3% MAPP (Figure 2.19). As for other formulations, the fracture cleavage energies were less than that of specimens with neat PF. Comparison of means test at significance level of 0.05 indicated differences in formulations; however, fracture

toughness of specimens bonded with neat PF were not significantly different than those of PF with 3% MAPP (Figure 2.19).

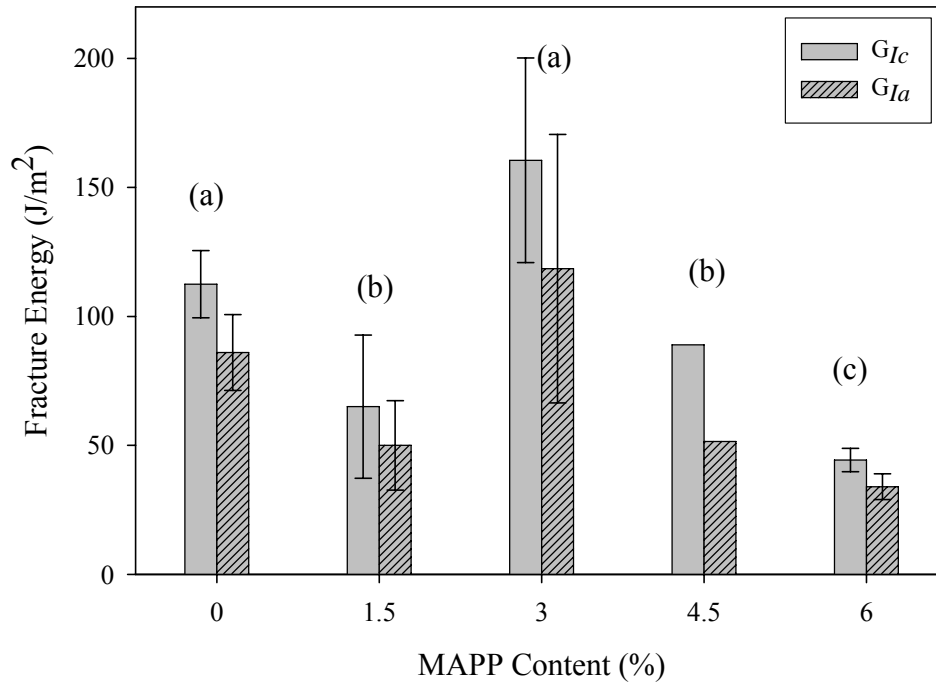


Figure 2.19 Average fracture energies for formulation with MAPP emulsion after 24-hr water soak. Comparisons of means test results at significance level of 0.05 are included on top of the bars; formulations with same letters indicate no significant difference.

Fracture toughness test results indicated different trends than DMA results. DMA showed addition of MAPE at lower proportion significantly improved the damping property, whereas, addition of MAPE decreased fracture toughness. This partially follows the hypothesis that addition of MAPO would improve the damping and toughness. At molecular level due to more flexible nature of MAPE polymer the energy dissipation was higher than blend with MAPP, but in fracture testing we characterized the wood-adhesive interphase. It could be possible that addition of MAPP resulted in a more uniform phase separation, which improved the fracture toughness of the adhesive blend more efficiently than addition of MAPE.

Trends in the results of one factor response models indicated that under both the environmental conditions (12% MC and 24-hr soak) MAPP adhesive formulations performed better than MAPE adhesive formulations. Fracture energy results indicate that effect of MAPP anionic emulsion in resin blend seems to maximize at 3% level yielding in improved fracture toughness under both 12%MC and 24-hr soak conditions. Addition of MAPE anionic emulsion seems to decrease fracture toughness of PF resin blends at even low levels and, eventually, leveling off at higher levels. One possible reason for better performance with MAPP could be because of differences in physical properties of the two co-polymer coupling agents (Table 2.1). MAPP anionic emulsion had higher solid content, percent of maleic anhydride content, and lower viscosity than MAPE, thus imparting better properties to the resin blends. High coefficient of variation was also observed with all fracture data. This trend was also observed by the previous researchers (Schmidt 1998, Scoville 2001, Gagliano and Frazier 2001). It was speculated that the inherent variation in the wood substrate made this process complex in nature and resulted in higher variations in the results.

Conclusion

Objectives of this study were to investigate the influence of MAPO (Maleic Anhydride Polyolefin) mixed in PF resin on the toughness of the adhesive system, to find the optimum particle size of MAPO to mix with PF and to determine the curing parameters of the adhesive blend. The findings of this study are:

- MAPP in emulsion form than in dry particle form results in a uniform distribution within a cured PF resin system leading to better phase separation.

- Particle size of MAPO did not have a significant effect on the dynamic stiffness property of cured resin blends.
- DSC analysis indicated that 2.5 minutes at 145°C resulted in 98% curing of PF and MAPP resin blend.
- DMA analysis indicated an improvement in dynamic stiffness moduli of resin blends with MAPP at lower proportions; whereas, addition of MAPE at lower proportions improved the damping property of cured resin blends.
- Fracture toughness tests showed an improvement in fracture energy of resin blends at lower proportions of MAPP (1.5 to 3% of the resin weight) in specimens conditioned to 12% MC; whereas, after 24-hr water soak treatment, resin blends with 3% MAPP showed an improvement in fracture energy.

Based on the results of this study, it can be concluded that emulsion form would perform better than particle form of MAPO if considered for application in producing oriented strand panels because of better distribution in the cured adhesive system and ease of application. MAPP was found to perform better in improving dynamic stiffness and did not have any adverse effect on the damping property of the cured resin systems. Fracture energies were also improved with the addition of MAPP than MAPE in the resin system, both at 12% moisture content and after subjecting to 24-hr water soak. Therefore, MAPP anionic emulsion will be chosen over MAPE anionic emulsion to blend with PF resin in manufacturing oriented strand composite (OSC) panels in the second part of the study where effect of adding MAPO to PF resin on physical and mechanical properties of OSC test panels will be evaluated.

References

1. American Society for Testing and Materials. (ASTM) 1999. Standard test methods for evaluating properties of wood-base fiber and particle panel materials. ASTM D 1037-99.
2. Arora, M.; Rajawat, M. and Gupta, R. 1981. Effect of acetylation on properties of particle boards prepared from acetylated and normal particles of wood. *Holzforschung und Holzverwertung*. 33(1): 8–10.
3. Blackman, B., Dear, J.P., Kinloch, A.J. and Osiyemi, S. 1991. The calculation of adhesive fracture energies from double-cantilever beam test specimens. *Journal of Material Science Letters*. v. 10, pp. 253-256
4. Blackman, B.R.K and Kinloch, A.J. 2000. Protocol for the determination of the Mode I adhesive fracture energy, G_{Ic} , of structural adhesives using the double cantilever beam (DCB) and tapered double cantilever beam (TDCB) specimens. Version 00-08. European Structural Integrity Society Polymers, Adhesives and Composites TC4 Committee.
5. Boogh, L., Jannerfeldt, G., Petterson, B., Bjornberg, H. and Manson, J.E. 1999. Dendritic-based additives for polymer matrix composites. Proc. Of the ICCM-12 conference, Paris, France. July 5-9.
6. Chen, J.P. and Lee, Y.D. 1995. A real time study of the phase-separation process during polymerization of rubber modified epoxy. *Polymer*. Vol. 36(1): 55-65
7. Chow, P.; Bao, Z. and Youngquist, J. 1996. Properties of hardboards made from acetylated aspen and southern pine. *Wood and Fiber Science*. 28(2): 252–258.
8. Clemons, C.; Young, R. and Rowell, R.M. 1992. Moisture sorption properties of composite boards from esterified aspen fiber. *Wood and Fiber Science*, 24(3), 1992, pp.353-363
9. Ebewele, R.O., River, B.H. and Koutsky, J.A. 1982. Relationship between phenolic adhesive chemistry, cure and joint performance. Part I. Effects of base resin constitution and hardener on fracture energy and thermal effects during cure. *Journal of Adhesion*. v. 14, pp. 189-217
10. Ebewele, R.O., River, B.H. and Koutsky, J.A. 1986. Relationship between phenolic adhesive chemistry, and adhesive joint performance: effect of filler type of fraction energy. *Journal of Applied Polymer Science*. v. 31, pp. 2275-2302
11. Felix, J.M. and Gatenholm, P. 1991. The nature of adhesion in composites of modified cellulose fibers and polypropylene. *Journal of Applied Polymer Science*, v. 42, 609-620
12. Gagliano, J.M. and Frazier, C.E. 2001. Improvement in the fracture cleavage testing of adhesively-bonded wood. *Wood and Fiber Science*. v. 33(3), pp. 377-385
13. Garcia, R.A., Cloutier, A. and Reidl, B. 2005. Dimensional stability of MDF panels produced from fibers treated with maleated polypropylene wax. *Wood Science and Technology*

14. Gardziella, A.; Pilato, L.A and Knop, A. Phenolic resins, chemistry, applications, standardization, safety and ecology. 2nd completely revised edition. pp. 75-81
15. Geimer, R.L., Follensbee, R.A., Christiansen, A.W., Koutsky, J.A. and Myers, G.E. 1990. Resin characterization. Proc. of 24th International Particle Board/ Composite Materials Symposium.
16. Hartley, I.D. and Schneider, M.H. 1993. Water vapor diffusion and adsorption characteristics of sugar maple (*Acer saccharum*, Marsh.) wood polymer composites. Wood Science and Technology, v. 27, pp. 421-427
17. Haygreen, G. and Gertjejasen, R.O. 1972. Influence of the amount and type of phenolic resin on the properties of a wafer-type particleboard. Forest Products Journal. v. 22(12), pp. 30-34
18. Hiziroglu, S. and Kamden, D.P. 1995. Physical and mechanical properties of hardboard made of black locust furnish. Forest Products Journal. 45(11/12): 66–70.
19. Kim, J.K. and Robertson, R.E. 1992. Possible phase transformation toughening of thermoset polymers by poly (butylenes terephthalate). Journal of Material Science, v. 27. pp. 3000-3009
20. Kim, J.K. and Robertson, R.E. 1992. Toughening of thermoset polymers by rigid crystalline particles. Journal of Material Science, 27. pp.161-174
21. Li, L. 2000. Dynamic mechanical analysis (DMA) basics and beyond. ParkinElmer Inc. <http://academic.sun.ac.za/unesco/PolymerED2000/Conf2000/LinLiDma-SF.pdf>
22. Lisperguer, J., Droguett, C., Ruf, B. and Nunez, M. 2005. Differential scanning calorimetry and dynamic mechanical analysis of phenol-resorcinol-formaldehyde resins. Journal of the Chilean Chemical Society. v.50 (n 2):451-453
23. Lu, J.Z., Wu, Q. and Negulescu, I.I. 2002. The influence of maleation on polymer adsorption and fixation, wood surface wettability and interfacial bonding strength in wood-PVC composites. Wood and Fiber Science. 34(3), pp. 434-459
24. Mahlberg, R., Paajanen, L., Nurmi, A., Kivisto.A., Koskela, K. and Rowell, R.M. 2001. Effect of chemical modification of wood on mechanical properties of wood fiber/ polypropylene fiber and polypropylene/ veneer composites. Holz als Roh – und Werkstoff. 59: 319-326
25. Maldas, D and Kokta, B.V. 1991. Surface modification of wood fibers using maleic anhydride and Isocyanate as coating components and their performance in polystyrene composites. J. Adhesion Sci. Technol. v. 5 (9), pp. 727-740
26. Maldas, D. and Kokta, B.V. 1989. Improving adhesion of wood fibers with polystyrene by the chemical treatment of fiber with a coupling agent and the influence on the mechanical properties of composites. Journal of Adhesion Science and Technology. v. 3(7), pp. 529-539
27. Manzione, L.T. and Gillham, J.K. 1981. Journal of Applied Polymer Science. Vol.26. 889-905
28. Marcinko, J.J., Devathala, S., Rinaldi, P.L. and Bao, S. 1998. Investigating the molecular and bulk dynamics of pMDI/wood and UF/wood composites. Forest Products Journal. 48(6):81-84.

29. Marcinko, J.J., Rinaldi, P.L. and Bao, S. 1999. Exploring the physicochemical nature of pMDI/wood structural composite adhesion. *Forest Products Journal*. 49(5):75-78
30. Marcovich, N.E., Reboredo, M.M. and Aranguren, M.I. 1998. Dependence of mechanical properties of woodflour-polymer composites on the moisture content. *Journal of Applied Polymer Science*, v. 68, pp. 2069-2076
31. Menard, K.P., 1999. *DMA: Introduction to the technique, its applications and theory*. CRC Press.
32. Mezzenga, R. and Manson, J.E. 2001. Novel modifier for thermoset resins: Dendritic hyperbranched polymers. *Polymer materials: science and engineering*. 84.
33. Patil, Y.P., Gajre, B., Dusane, D., Chavan, S. and Mishra, S. 2000. Effect of maleic anhydride treatment on steam and water absorption of wood polymer composites prepared from wheat straw, cane bagasse and Teak wood sawdust using Novolac as matrix. *Journal of Applied Polymer Science*, v. 77, pp. 2963-2967
34. Pearson, R.A. and Yee, A.F. 1993. Toughening mechanism in thermoplastic-modified epoxies: 1. Modification using poly(phenylene oxide). *Polymer*. Vol. 34(17): 3658-3670
35. Qian, J.Y., Pearson, R.A., Dimonie, V.L. and El-Aassar, M.S. 1995. Synthesis and application of core-shell particles as toughening agents for epoxies. *Journal of Applied Polymer Science*. Vol. 58. 439-448
36. River, B.H., 1995. Fracture of adhesive bonded wood joints. Chapter 9. *In: Pizzi, A., Mittal, K.L., eds. Handbook of adhesive technology*. New York: Marcel Dekker, Inc.
37. River, B.H., Scott, C.T. and Koutsky, J.A. 1989. Adhesive joint fracture behavior during setting and aging. *Forest Products Journal*. v. 39(11/12), pp. 23-28
38. Romano, A.M., Garbassi, F. and Braglia, R. 1994. Rubber- and thermoplastic-toughened epoxy adhesive films. *Journal of Applied Polymer Science*. Vol. 52. 1775-1783.
39. Schmidt, R.J. 1998. Aspects of wood adhesion: applications of ¹³C CP/MAS NMR and fracture testing. Ph.D. Dissertation, V.P.I. & S.U. Blacksburg, VA
40. Scoville, C.R. 2001. Characterizing the durability of PF and pMDI adhesive wood composites through fracture testing. MS thesis submitted to Virginia Polytechnic Institute and State University.
41. Simonsen, J., Jacobson, R. and Rowell, R. 1998. Wood fiber reinforcement of styrene maleic anhydride co-polymers. *Journal of Applied polymer Science*. 68 (10), pp. 1567-1573
42. Snijder, M.H.B. and Bos, H.L. 2000. Reinforcement of polypropylene by annual plant fibers: optimization of the coupling agent efficiency. *Composite Interfaces*, v. 7 (2), pp. 69-75
43. Snijder, M.H.B., Wissing, E. and Modder, J.F. 1997. Polyolefins and engineering plastics reinforced with annual plant fibers. *In Proc. 4th International conference on woodfiber-plastic composites*, Forest Products Society, Madison, WI. pp. 181-191

44. Stark, N.M., 1999. Wood fiber derived from scrap pallets used in polypropylene composites. *Forest Products Journal*. 49(6), pp. 39-46
45. Turi, E.A.. 1981. Thermosets. Pages 435-569 *in* Turi, E.A. eds. *Thermal characterization of polymeric materials*. Academic press. New York
46. Vick, C.B. and Christiansen, A.W. 1993. Cure of phenol-formaldehyde adhesive in the presence of CCA-treated wood by differential scanning calorimetry. *Wood and Fiber Science*. 25(1):77-86
47. Wang, J., Laborie, M.P. and Wolcott, M.P. 2005. Comparison of model free kinetic methods for modeling the cure kinetics of commercial phenol-formaldehyde resins. *Thermochimica Acta*. 439:68-73
48. Xiaoyu, L., Benson, R.S., Kit, K.M. and Dever, M. 2002. Kudzu Fiber-Reinforced Polypropylene Composite. *Journal of Applied Polymer Science*. v. 85, pp. 1961-1969
49. Youngquist, J.; Krzysik, A. and Rowell, R. 1986. Dimensional stability of acetylated aspen flakeboard. *Wood and Fiber Science*. 18(1): 90-98.
50. Zheng, J., S. C. Fox, and C. E. Frazier. 2004. Rheological, wood penetration, and fracture performance studies of PF/pMDI hybrid resins. *Forest Product Journal*. 54(10):74-81.

CHAPTER 3

Effect of Coupling Agent and High Resin Content on Physical and Mechanical Properties of Oriented Strand Composite

Abstract

Moisture intrusion into composite panels in service leads to eventual wetting and degradation of the panels. In this study, a mechanism to improve moisture durability of oriented strand composite (OSC) panels without significantly compromising their mechanical properties was investigated. OSC test panels were hot pressed with adhesive blends consisting varying proportions of phenol formaldehyde (PF) resin and maleic anhydride polypropylene (MAPP) anionic emulsion. Effect of increased levels of PF resin and addition of varying proportions of MAPP on physical and mechanical properties of OSC panels was investigated. To study the efficacy of increased levels of PF and addition of MAPP on moisture resistance and mechanical properties of panels, internal bond, static bending after conditioning to different environmental conditions, water absorption, thickness swell, material permeance, and equilibrium moisture content (EMC) properties were evaluated. MAPP did not significantly affect panel MOE but reduced MOR for 12% MC and 24-hour soak specimens. However, increase in PF content significantly improved MOE and MOR of specimens subjected to both environments. At higher PF levels, IB values were reduced with the addition of MAPP. Water absorption and thickness swelling were also significantly reduced with the addition of MAPP; increasing PF content also had similar effect on water absorption, but also reduced thickness swelling. However, inclusion of MAPP at higher levels in OSC panels significantly reduced water vapor transmission (WVT)

and permeance of the material. EMC at 50% and 80% RH indicated that with increasing MAPP content OSC panels equilibrate at lower moisture content. Results of this study indicate that increasing levels of PF is the most effective method of improving both moisture resistance and the mechanical properties of OSC panels; addition of MAPP improves the moisture resistance of the panels, but significantly reduces the mechanical properties, especially MOR and IB.

Keywords

Oriented strand composite, coupling agent, equilibrium moisture content, permeance, diffusion constant.

Introduction

Oriented strand board (OSB) is one of the most widely used panel products in construction industries with 65% of floor, 56% of wall and 72% of roof sheathing market shares in 2003 (SBA 2003). OSB is a structural panel product made of wood strands with exterior grade adhesives like phenol formaldehyde (PF) or polymeric methylene diphenyldiisocyanate (pMDI). As a sheathing material OSB has many positive qualities such as good mechanical properties and excellent insulating properties to heat, sound and electricity. In service, if the OSB sheathing is allowed to breathe properly and is not exposed to high humidity for extended periods, it will not degrade; however, if OSB panels are exposed to high humidity due to poor workmanship, it could lead to their rapid degradation. Decay of wood composites progresses quickly in the moist environments, therefore, any mechanism that can induce moisture resistance to composite panels would help to protect them in service and reduce their susceptibility to decay.

Many researchers have worked on improving the moisture resistance of solid wood and wood composites by reducing the inherent hygroscopicity of wood. Several methods have been used for this purpose including the chemical modification (Chow et al. 1996, Clemons et al. 1992, Youngquist et al. 1986, Arora et al. 1981) and the use of higher phenolic resin content (Beech et al. 1975, Hiziroglu and Kamden 1995, Haygreen and Gertjejasen 1972). Chemical modification process mainly aims at consuming hygroscopic hydroxyl (-OH) group from wood, thus reducing the moisture affinity (Marcovich et al. 1998). Though chemical modification was found to be effective in reducing the water absorption and thickness swelling of the composites, they often reduced mechanical properties of the finished composites (Marcovich et al. 1998). Higher resin content was another tried method for improving moisture resistance. This method also found to enhance moisture resistance. However, due to the brittle nature of phenolic resin the finished composite would become more brittle, an undesirable mechanical property for a structural material as sheathing. This provided the motivation for this study which aimed to improve the moisture resistance of oriented strand composite (OSC) without significantly compromising its mechanical properties.

It is hypothesized in this study that addition of higher amount of PF could improve mechanical properties and moisture resistance. It is also hypothesized that the addition of a thermoplastic co-polymer coupling agent, such as maleic anhydride polyolefins (MAPO), to the PF adhesive could potentially act as a moisture barrier within the matrix thus improving the moisture resistance of the finished OSC panels. In this study, we hope to understand the effects of interaction between PF resin and MAPP on OSC mechanical and physical properties. In the first phase of this study (Chapter 2), effects of two different MAPO were evaluated for their influence

on the energy dissipation and toughness of PF resin system using analytical techniques and fracture toughness tests. It was determined that maleic anhydride polypropylene (MAPP) had better influence than maleic anhydride polyethylene (MAPE). Therefore, MAPP was chosen in this study to mix with PF resin in manufacturing oriented strand composite panels for evaluating its efficacy on improving panel moisture resistance without compromising their mechanical properties.

Objectives

The goal of this study was to understand the effects of varying proportions of PF and MAPP on mechanical and physical properties of OSC panels, especially their moisture resistance properties. Specific tasks to achieve this overall goal include:

1. Determining the effects of increased levels of PF and varying proportions of MAPP on OSC mechanical properties.
2. Investigating the effect of varying PF and MAPP levels on moisture resistance that is reflected in changes to material permeance, equilibrium moisture content, and flexure properties after 24-hour water soak and accelerated aging.

Literature Review

Moisture susceptibility of wood composites has been one of the main concerns of researchers for many years. Techniques such as thermal (Suschland and Enlow 1968) and chemical (Chow et al. 1996, Youngquist et al. 1986 and Arora et al. 1981, Clemons et al. 1992, Mahlberg et al. 2001) modification have been used to reduce the moisture affinity of wood. In heat treatment, finished

wood composites are exposed to 165°C to 210°C in an oven (Carll 1997). Thickness swelling of flake boards was found to decrease with heat treatment and the reason was speculated as the further curing of the resin (Carll 1997). Wood has been treated with organic acid anhydrides such as acetic and maleic to consume the free hydroxyl groups (Chow et al. 1996, Youngquist et al. 1986 and Arora et al. 1981). These researchers found significant improvement in dimensional stability. Treatment of wood fibers (Clemons et al. 1992) and veneers (Mahlberg et al. 2001) with organic acid anhydrides resulted in better moisture resistance. Mahlberg et al. (2001) also found significant decrease in modulus of rupture with these treatments.

Application of higher levels of thermoset resin also found to improve mechanical and physical properties of wood composites (Maloney 1997, Beech 1975, Hiziroglu and Kamden 1995). Maloney (1997) suggested with the increase of resin content in a composite both mechanical and physical properties improved significantly. Beech (1975) found a consistent improvement in thickness swelling properties in particle and flake boards with higher resin content. Hiziroglu and Kamden (1995) found that increased adhesive content (in the range of 0% to 2%) reduced thickness swell of wet-process hardboard (as evaluated by water soak testing), but not significantly. The effects of higher resin content were found to be more evident in particleboard and flake board than in fiberboard (Carll, 1997).

Sun et al. (1994) studied the effect of higher levels of isocyanate and phenolic resin on the physical and mechanical properties of wood fiber composites. A PF resin level of approximately 20 percent was reported to be most efficient in minimizing water absorption and thickness swelling in wet condition while 30 percent resin content was most efficient to reduce the

accelerated aging test thickness swelling. Surprisingly, higher resin content did not have any effect on MOE and MOR in dry condition. In wet condition, however, both MOE and MOR were improved with higher resin content and reached a maximum at 30 percent resin level. Better bonding was observed as both dry and wet IB strengths improved with increase of PF resin and reached a maximum at 30 percent level. Wafer board made of PF resin impregnated wafers showed reduced thickness swelling by 35 to 55 percent (Haygreen and Gertjejasen 1972).

Maleic anhydride polypropylene (MAPP) is widely used in wood-plastic composites to enhance compatibility between wood and thermoplastic polymer matrix, consequently improving the mechanical properties of the composite (Felix and Gatenholm 1991, Maldas and Kokta 1991, Stark 1999, Simonsen et al. 1998, Lu et al. 2002). Several researchers investigated the effect of MAPP on the moisture resistance and mechanical properties of wood plastic composites (Marcovich et al. 1998, Patil et al. 2000, Felix et al. 1991). Improvement in dimensional stability was observed when wood was treated with MAPP. Maldas and Kokta (1989) and Snijder et al. (1997) observed that mechanical properties improved with increase of MAPP content up to a certain level beyond which properties either leveled off or decreased. Garcia et al. (2005) treated MDF fibers with MAPP wax and found significant improvement in moisture resistance and mechanical properties of the produced fiber boards. The binders used here were urea formaldehyde (UF) and melamine-urea-formaldehyde (MUF). Use of 3 to 5% MAPP wax resulted in a reduction of 2-hour thickness swelling of the UF boards by 46 to 41%. Decrease in water absorption and linear expansion after 2 and 24 hours of water soaking was also observed. It was also reported that treatment of fibers with MAPP wax improved bending properties and internal bond strength.

Wolcott (2003) prepared flat pressed wood panels with wood particles and high density polyethylene (HDPE). It was found that use of HDPE, water absorption and thickness swelling decreased: whereas, mechanical properties were adversely affected with the increasing proportion of thermoplastic. More recently, Zheng et al. (2004) studied the rheological behavior, penetration characteristics, and fracture performance of liquid phenol-formaldehyde resole and polymeric diphenylmethane diisocyanate (pMDI) hybrid mixtures. They observed that hybrid properties are a function of simple emulsion effects. Improvement in toughness of PF matrix was significant at low pMDI levels due to dispersed urethane/urea/biuret phase; however, dispersed-PF phase resulting from addition of small quantities of PF to urethane/urea/biuret matrix did not result in a significant improvement of resin toughness.

The premise of this study is that use of thermoplastic co-polymer coupling agent will impart moisture resistance to OSC through creating a barrier to moisture movement while not compromising the mechanical properties of the composite significantly. Another hypothesis is that use of higher amount of PF will improve the properties of panel. This study should also investigate how the interaction of PF and MAPP influence mechanical properties of OSC. Previous phase of this study (Chapter 2) indicated that the addition of MAPP emulsion improved the fracture toughness of PF blend. Higher toughness of adhesive can improve moisture resistance of composites by lowering the crack propagation within a panel, thus allowing fewer pathways for moisture to infiltrate.

Measurement of equilibrium moisture content, diffusion constant and permeance have been used by many researchers as a tool of measuring the moisture resistance of wood and wood

composites (Wu and Suchsland 1996, Clemons et al. 1992, Marcovich et al. 1999, Hukka 1999, Hartley and Schneider 1993, Wu and Lee 2002, Rangaraj and Smith 2000). They have found these methods of testing to be useful in understanding the moisture resistance of wood and wood composites.

Materials and Methods

Materials

Commercially available wood strands consisting of 60% aspen and 40% mixed hardwoods were obtained from Weyerhaeuser and used for fabricating oriented strand composites in the laboratory. Average nominal dimensions of strands were 71 mm by 13 mm by 1 mm. Typical OSB grade phenol formaldehyde resin (57% solid content) from Dynea Chemical was used. Maleic anhydride polypropylene (MAPP) anionic emulsion from Honeywell Chemicals was used as results of the first phase of the overall study (Chapter 2) revealed that maleic anhydride polypropylene (MAPP) anionic emulsion had performed better than maleic anhydride polyethylene (MAPE) anionic emulsion in improving toughness and moisture resistance of PF resin system. The emulsion had a solid content of 30%. Polymethylene diphenyl diisocyanate (pMDI) panels were prepared to serve as control specimens. pMDI bonded panels are accepted in the industry to yield board that have improved moisture resistance properties and better mechanical properties. pMDI adhesive was obtained from Bayer (Monodur® 541).

Experimental Design

Experimental design was established based on D-optimal response surface design using a design of experiment software (Design-Expert[®], Stat-Ease 2006). PF resin and MAPP emulsion were considered as factors affecting the response variables (such as flexure properties, internal bond, percent water absorption, etc.). Both PF and MAPP were calculated on the basis of dry weight of wood. The low and high levels for these factors were as follows: PF content ranged from 6 to 25% and MAPP content varied from 0 to 6%. The D-optimal design, which minimizes the error of the model coefficients, suggested that 20 runs were necessary. Better representation of design space was obtained by adding 6 more runs. Therefore a total of 26 runs were performed to evaluate the effect of variables. Experimental design points or runs, indicating the proportions of PF and MAPP for different runs, as suggested by response surface design are tabulated in Table 3.1.

Table 3.1 Formulations and number of panel replicates suggested by D-optimal response surface design.

MAPP Content (%)	PF Content (%)	Number of Replicates
0	6	2
0	12	1
0	25	2
0.5	18	2
1.5	10	1
1.5	22	1
2	6	2
3	6	1

3	15.5	2
3	25	2
4	6	1
4	10	1
4.5	20	1
6	6	2
6	15	2
6	25	3

Oriented Strand Composite (OSC) Fabrication

Wood strands were dried to 3% moisture content in a rotary drum drier. Dried strands were then screened with a 38 mm (1.5 inch) square screen to separate fines. Amount of strand, PF and MAPP emulsion required for OSC preparation were calculated to obtain a final board density of 640 kg/m³ (40 lb/ft³). It should be noted that amount of PF and MAPP were calculated based on dry weight of wood. Dimensions of the hot-pressed panels were 860 mm by 860 mm by 15.9 mm (34 inches by 34 inches by 0.625 inches). After fabrication the edges of the panels were trimmed (76.2 mm from each side) to get constant density. Therefore, the final dimensions of the test panels were 711.2 mm by 711.2 mm by 1.59 cm (30 inches by 30 inches by 0.625 inches).

Blending

Strands were then blended with PF resin and MAPP emulsion in a rotary blender. Initially, PF and MAPP emulsion were mixed thoroughly in a liquid blender and the mixture was sprayed. This method ensured proper distribution of MAPP into PF before spraying. However, spraying this mixture proved to be difficult as the mixing process generated lot of foam which clogged the spraying nozzles and slowed down the blending process significantly. Therefore, an alternate process was adopted where PF resin and MAPP emulsion were sprayed simultaneously from two sets of nozzles. This method was found to be convenient resulting in a uniform distribution of PF and MAPP emulsion throughout the spraying process without clogging up the nozzles. To ensure a good blend and even distribution of resin and emulsion, MAPP was added in small batches as the resin was being blended (this was especially critical at higher resin levels as emulsion, due to smaller quantities, would otherwise be atomized completely before resin). It was assumed that PF and MAPP blend together as they are deposited on strands in an atomized form and would behave similar to being mixed together prior to atomizing. This method was preferred over the earlier one because of its ease of application.

Blended strands (furnish) were then hand formed in a forming box of size 860 by 860 mm (34 by 34 inches). The forming box had metal vanes spaced 76.2 mm (3 inches) apart for proper alignment of the strands. After forming, the mats were pressed in a hot press to form an oriented strand composite.

Hot-Pressing

Pressing temperature and time were determined based on the studies done on cure kinetics of resin blends (Chapter 2). It was found through DSC study that 2.5 minutes at 145°C temperature resulted in approximately 98% cure of adhesive blends. Test runs were performed with temperature and gas probe to determine the pressing schedule which ensured that the core of the mat reached 145°C and stayed at that temperature for at least three minutes. Single layer, unidirectional strand mats were hot pressed at 182°C (360°F) using required amounts of resin and emulsion to a target density of 640 kg/m³ (40 lb/ft³). A 30-minute pressing schedule included 8 minutes of close time, 20 minutes hold and 2 minutes of vent time (1 minute after 10 minute of holding and 1 minute at the end of holding time). Pressed panels were then trimmed to final dimension. Three OSC panels were hot-pressed with 3% pMDI resin. Similar platen temperature (182°C) was maintained as for PF panels. Pressing time was reduced as the required curing temperature for pMDI resin was 100°C. A 24 minutes pressing cycle included 8 minute of close time, 15 minutes hold time and 1 minute vent time at the end.

Testing of OSC Panels

Specimens for mechanical and physical testing of finished panels were cut as shown in 3.1.

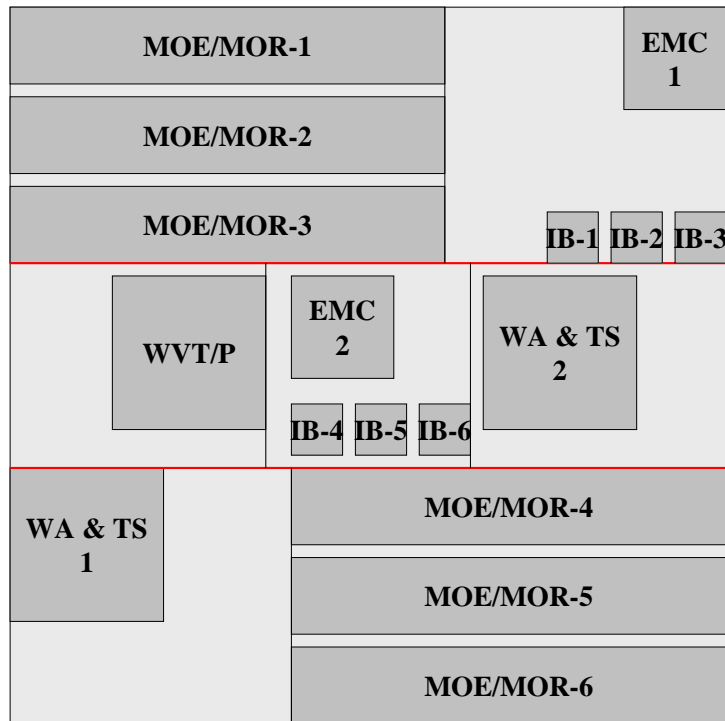


Figure 3.1 Cutting pattern of test specimens from OSC test panels. Six flexure (MOE/MOR), six internal bond (IB), two water absorption and thickness swelling (WA & TS), two equilibrium moisture content (EMC) and one water vapor transmission and permeance (WVT/P) specimens were prepared from each test panel.

Flexure, internal bond, and water absorption and thickness swell tests were performed according to ASTM D1037 (ASTM 1999a). Water vapor transmission and permeance were determined following the guidelines outlined in ASTM E96 (ASTM 1994). Equilibrium moisture content was also determined for test panels as a measure of moisture affinity. Diffusion constants for specimens were calculated to examine moisture diffusion property of panels with different formulations.

Evaluation of Mechanical Properties

Flexure Properties

Static bending test specimens were divided into three groups and each group was subjected to different environmental conditions prior to testing. From each panel six flexure specimens were obtained. Two specimens were randomly assigned to each of the environmental conditions. A set of specimens were placed in a controlled environment chamber with 20°C temperature and 68% relative humidity for two weeks to equilibrate to 12% MC. Second set of specimens were soaked in water for 24 hrs and were tested immediately after that. The third set of specimens was subjected to accelerated aging cycles as instructed in ASTM D1037. Six cycles were performed after which the specimens were placed in 12% equilibrium moisture content room for 48 hrs before testing for their flexure properties. Specimens were 431 mm in length by 76 mm in width by 15.9 mm in depth (17 by 3 by 0.625 inches). Speed of the testing was calculated on the basis of specimen dimension according to the formula suggested by the ASTM D1037; it was determined to be 7.62 mm per minute (0.3 inches/min).

Internal Bond Test (IB)

Standard internal bond tests were performed after conditioning the samples at 12% moisture content. Six specimens were obtained from each board. Dimension for the internal bond test specimens were 50.8 mm square (2" by 2") by the thickness of the panel. Standard procedure mentioned in ASTM D1037 was followed for sample preparation and calculating the testing speed (1.27 mm per minute (0.05 inch/min)). Maximum load at failure was recorded from which stress at failure was calculated using specimen cross section dimensions.

Evaluation of Physical Properties

Water Absorption and Thickness Swelling Test

Water absorption and thickness swelling tests were performed for short term soaking (2 hrs) and long term soaking (24 hrs). Specimens of dimensions 152.4 mm by 152.4 mm (6" by 6") by thickness of the panel were soaked in water following standard procedure. Two specimens for each run were tested. Water absorption was calculated as a percentage from initial weight and final weight. Similarly, thickness swelling also was calculated as a percent change from the initial thickness.

Permeance Measurement

Moisture resistance of test panels was investigated by measuring water vapor transmission (WVT) and permeance according to ASTM E 96 (ASTM 1994). Water vapor permeance can be defined as the time rate of water vapor transmission through unit area of flat material or construction induced by unit vapor pressure difference between two specific surfaces, under specified temperature and humidity conditions (ASTM 1994). Desiccant method was chosen for this test (Figure 3.2).



Figure 3.2 Test setup for water vapor transmission and permeance measurement.

One specimen from each board was tested. Specimens of dimensions 152.4 mm by 152.4 mm (6 inches by 6 inches) were first wax coated on the edges and then placed over the open mouth of a plastic container of dimensions 146 mm square (5.75 inch square) by 63.5 mm (2.5 inch) in depth. Before placing the specimens, the containers were partially filled with 350 g of anhydrous calcium chloride (CaCl_2). Anhydrous calcium chloride is a desiccant and would act as moisture sink. CaCl_2 absorbs moisture from the surrounding causing 0% relative humidity in the air between specimen and itself resulting in a moisture gradient between the two sides of the specimen. This would be the driving force for the moisture to flow through the OSC specimen. Specimens were sealed on the edges of plastic container using a silicone gel sealant. The whole system was placed in a controlled environment of 50% relative humidity and 22°C temperature. They were then weighed periodically to determine the moisture gain. Initially measurements were recorded every 6 hours and after steady state was reached, weights were recorded once a day. A straight line was fitted to the linear region of the plot. The slope of the steady state per

unit area represents the rate of water vapor transmission (ASTM 1994). From that value permeance was calculated according to ASTM E96 (1994).

EMC and Diffusion Constant Measurement

Equilibrium moisture content of the panels was determined by subjecting specimens of dimensions 101.6 mm by 101.6 mm (4 inches by 4 inches) by the thickness of the panel to two different environmental conditions: 80% relative humidity at 30°C temperature and 50% relative humidity at 22°C temperature. Procedures followed by previous researchers were used as guidelines for this test (Wu and Suchsland 1995, Lee and Biblis 1976). In the first step specimens were dried in an oven at 100°C until constant weights were reached. Specimens were then put into the test chambers at specified temperature and relative humidity as stated above. Weight gains of the specimens were measured periodically. Final moisture gain and the rate of moisture gain of test panels with different adhesive formulations were graphically compared from the percent moisture gain vs. time plot. In the next step, moisture weight gain is plotted against the square root of time for all specimens subjected to both environmental conditions. Evidence of a linear initial region of moisture-related weight gain indicates that water movement into material followed Fick's law of diffusion at initial stage (Rangaraj and Smith 2000, Pierron et al. 2002, Chateauminois et al. 1994). The percent weight gain, M , initially varies linearly with the square root of time, t , according to Fick's law (Rangaraj and Smith 2000).

$$M = \frac{4M_m \sqrt{D_A}}{h\sqrt{\pi}} \sqrt{t} \quad \text{Equation 3.1}$$

Where,

M_m = Percent weight gain at saturation (%)

D_A = Apparent diffusion constant (mm^2/s)

t = Time (s)

h = Thickness of the specimen

Apparent diffusion coefficient (D_A) was determined from slope of the linear region of the moisture gain vs. square root of time plot as,

$$D_A = \pi \frac{h^2}{16M_m^2} \left[\frac{M_2 - M_1}{\sqrt{t_2} - \sqrt{t_1}} \right]^2 \quad \text{Equation 3.2}$$

Here, M_2 and M_1 are percent moisture gain at corresponding time t_2 and t_1 . This apparent diffusion constant is calculated for one dimensional moisture flow, i.e., through thickness of the specimens. Correction for moisture flow through the edges are done by calculating the geometric edge correction factor, ECF (Rangaraj and Smith 2000) as,

$$ECF = \left(1 + \frac{h}{L} + \frac{h}{w} \right)^2 \quad \text{Equation 3.3}$$

In this equation L, w and h are length (mm), width (mm) and thickness (mm) respectively.

Now the corrected diffusion constant (D) was calculated using equation 3.4 as,

$$D = \frac{D_A}{ECF} \quad \text{Equation 3.4}$$

Diffusion constant values were then compared and statistically analyzed to evaluate the effect of different formulations on moisture diffusion through the test specimens.

Results and Discussion

Experimental results were analyzed using Design-Expert[®] version 7 software (Stat-Ease Inc. 2006). Results obtained from tests were fed into the response surface model discussed earlier and analyzed to examine the effects of PF and MAPP levels on the properties (response variables) of the test panels. It has been well established that properties of composite panels is directly correlated with their density. Therefore, statistical analyses were conducted taking specimen density as a covariate where significant. SAS (SAS Version 9, 2002) was used to perform covariance analysis considering PF and MAPP levels as independent variables and density as a covariate. If density effects were significant, significance of PF and MAPP levels was evaluated for each test after adjusting for the density factor.

Mechanical Properties

Flexure Properties at 12% Moisture Content

Response surface for MOE as the two independent variables, MAPP and PF levels, are varied within their low and high values is shown in Figure 3.3.

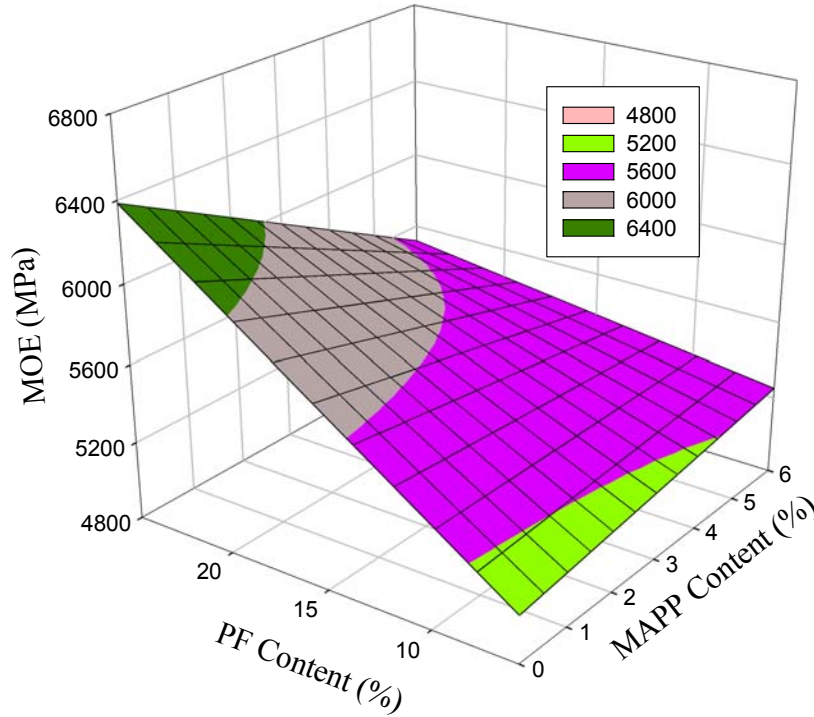


Figure 3.3 Response surface for MOE with varying MAPP and PF levels for specimens at 12%MC and a fixed target density of 641 kg/m³.

Analysis of variance (ANOVA) indicated that level of MAPP content did not have a significant effect on MOE at 0.05-alpha level (Model $R^2=0.6$). However, PF content and density of the specimens had a significant effect on MOE. Analysis of covariance (ANCOVA) was then performed to adjust MOE values for density to examine the effects of PF and MAPP levels without the interference of density factor. Analysis indicated that PF effect was still significant only for 3% MAPP content level (p-value = 0.0056), whereas for other MAPP content levels there was no significant effect of PF content (p-value range 0.3497 to 0.7592). MAPP effect was not significant (p-value = 0.8085) considering density as a covariate. This finding was contrary to what was reported by Mahlberg et al. (2001) where they found an increase of 20% in MOE when fiber boards were treated with maleic anhydride. This difference could be explained due to the presence of thermoplastic (polypropylene) in addition to maleic anhydride in this study. As

the response surface indicates, however, MAPP had a positive influence on specimen MOE at lower levels of PF (<15%) and a negative effect above this level. Influence of PF on MOE values of panels with 6% MAPP and varying PF contents are plotted in Figure 3.4. It is evident from the plot that with an increase in PF content the MOE increase significantly; an increase of 19% in MOE with an increase of PF content from 6% to 25%.

Results also indicate that panels with PF and MAPP blends performed significantly better than the pMDI panels. Specimens with 6% PF and MAPP each were found to have 20% higher MOE than pMDI panels. Specimens with 6% MAPP and 25% PF had 44% more average MOE than pMDI specimens. Whereas, panels made with 6% neat PF had 10% more average MOE than pMDI specimens. Comparison of means at 0.05 significance level indicated that specimens with 6% PF content were significantly different than 15% and 25% PF content specimens, whereas, 15% and 25% PF content panels were not found to be significantly different.

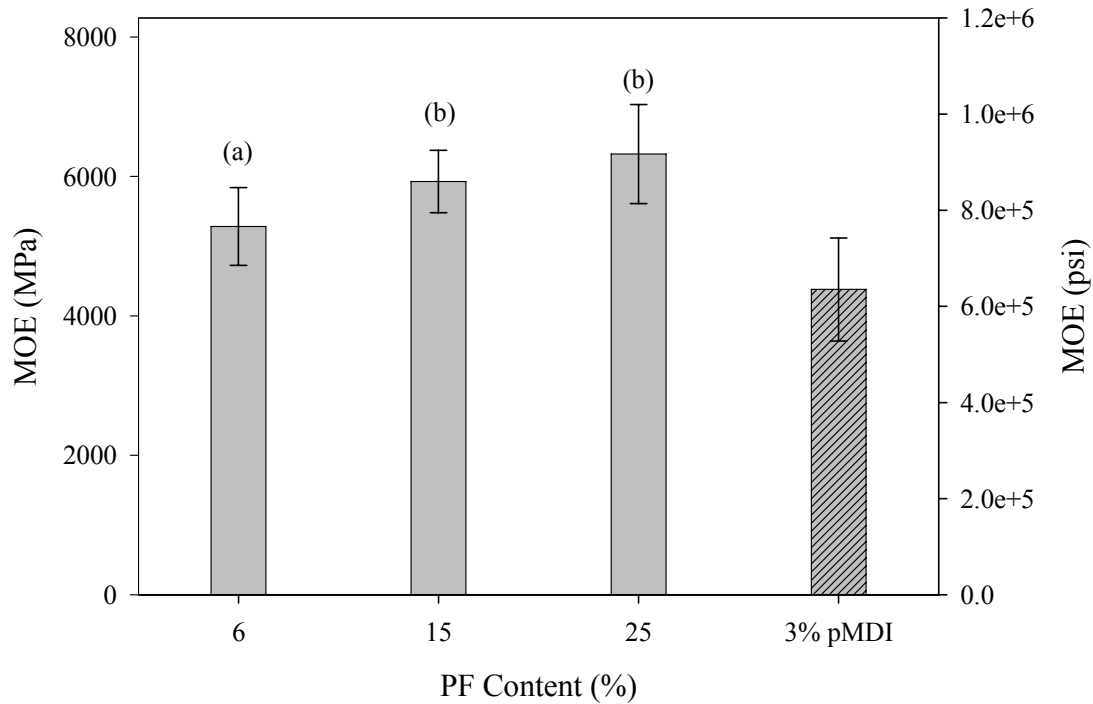


Figure 3.4 Comparison of MOE of panels with 6% MAPP and varying PF levels and pMDI at 12%MC. Comparison of mean (Duncan) test results at 0.05 significance level are shown on top of the bars.

Effect of varying levels of MAPP and PF on MOR of test panels is presented in Figure 3.5. The model indicates that MOR significantly increases with increasing PF content, whereas significantly decreases with increasing levels of MAPP (Model $R^2=0.4$)

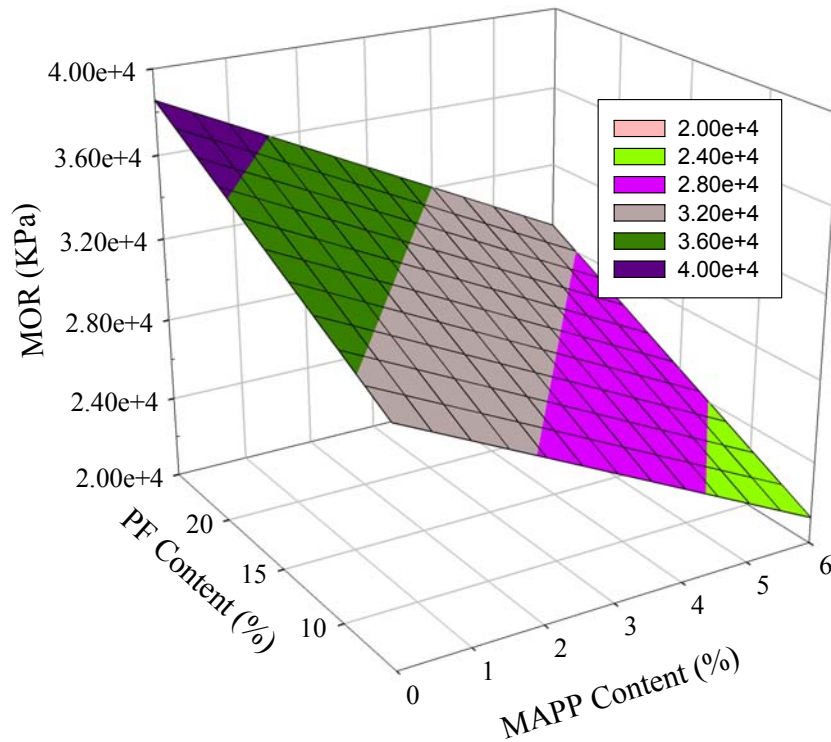


Figure 3.5. Response surface for MOR with varying levels of PF and MAPP for 12% MC flexure specimens at constant target density of 641 kg/m³.

Analysis of variance indicated that density effects were significant (p-value = 0.0009). Thus, model was adjusted by taking density as a covariate. ANCOVA indicated that density did not have significant effect on MOR of panels (p-value range = 0.0699 to 0.5726). Analysis also showed MAPP content had significant effect on MOR (p-value = 0.0187) especially at lower PF level (6%), whereas at higher PF level this effect was not significant (p-value = 0.1869).

Trend of MOR of OSC specimens at varying MAPP content at 6% and 25% PF levels are shown in Figure 3.6. These values were also compared with MOR of panels bonded with pMDI resin.

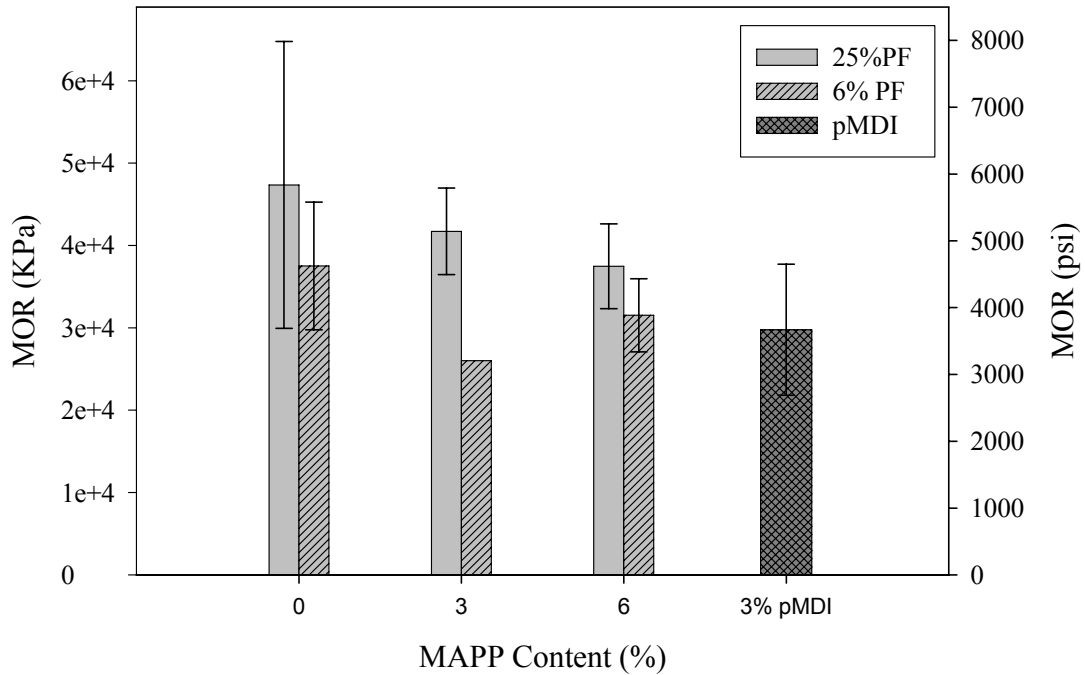


Figure 3.6 Comparison of MOR for boards with varying MAPP levels at 6% and 25% PF levels and pMDI at 12% MC.

Decrease in MOR as MAPP content was increased from 0 to 6% remained constant at all levels of PF resin (approximately 20%). Similar trend was also noticed by Mahlberg et al. (2001), where a 20% drop in MOR value was reported when fiber boards were treated with maleic anhydride. Average MOR value for pMDI boards was less than neat PF boards and was comparable with boards bonded with PF and 6% MAPP. This trend also held true with increasing levels of resin content.

Static Bending Test after 24- hr Water Soak

Static bending tests were performed after soaking the specimens in water for 24-hour. MOE and MOR values for specimens after 24 hours water soak were compared with MOE and MOR of 12% MC specimens. Proportion of MOE and MOR retained after 24 hours water soak were calculated by dividing MOE/MOR values of 24-hour water soak specimens by MOE/MOR values obtained from 12% MC specimen from the same test panel. Obtained values were then statistically analyzed as before.

Analysis of variance showed that MAPP content had a significant effect on retention of MOE values after 24 hours water soak of the specimens (p-value = 0.0048) whereas, PF content (p-value = 0.4322) and density (p-value = 0.0516) did not have significant effect on MOE retention. Figure 3.7 shows the response surface of proportion of MOE retained with the variation of PF and MAPP levels (Model $R^2 = 0.3$).

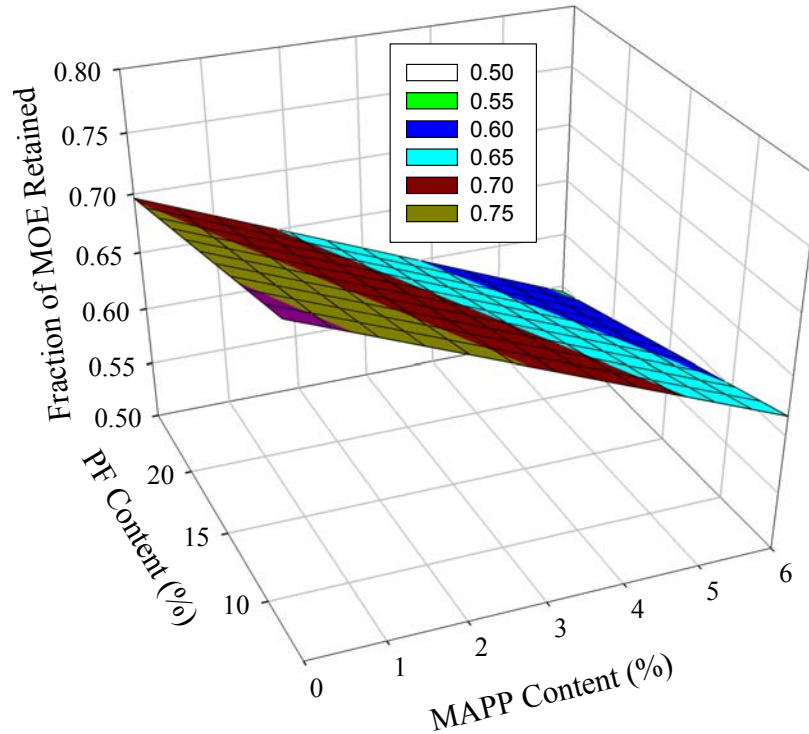


Figure 3.7 Response surface for fraction of MOE retained after 24 hours water soak of static bending specimens.

It was observed that with the increase in the MAPP content the proportion of MOE retention decreased. For panels with 6 and 25% PF content when MAPP levels were varied from 0 to 6% decrease in retention of MOE were observed (~25% for 6% PF content and 11% for 25% PF content panels). Figure 3.8 shows the comparison of fraction of MOE retention for 6 and 25% PF content panels at varying MAPP levels. When compared with fraction of MOE retained by pMDI panels it was found that pMDI panels had lower retention of MOE than panels with neat PF (34% lower than 25% PF panels and 23% lower than 6% PF panels). Though bar graphs (Figure 3.8) shows there is an increase in retention of MOE with increase in PF content, the response surface model did not show any significant effect of PF content on MOE retention.

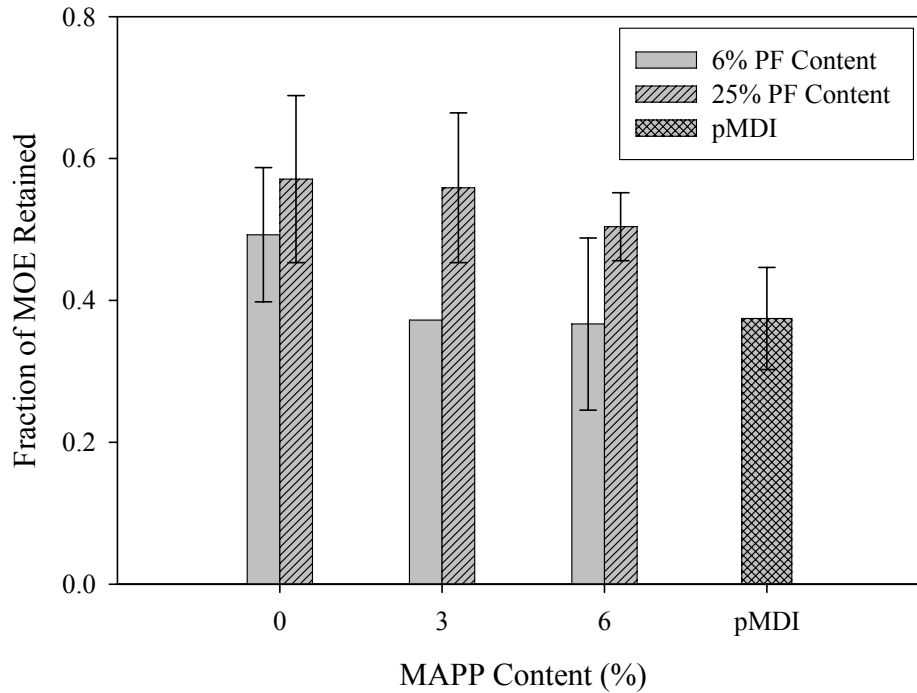


Figure 3.8 Comparisons of fraction of MOE retained after 24 hour water soak for panels with 6 and 25% PF content at varying MAPP levels. Fraction of MOE retention for pMDI panels is also included.

The response surface for fraction of MOR retained after 24 hour water soak is shown in Figure 3.9. The model (Model $R^2 = 0.4$) suggested that MAPP content (p-value = 0.0001) and density had significant effect on fraction retention of MOR of the specimens (p-value = 0.0169). However, PF content (p-value = 0.5258) did not have a significant effect.

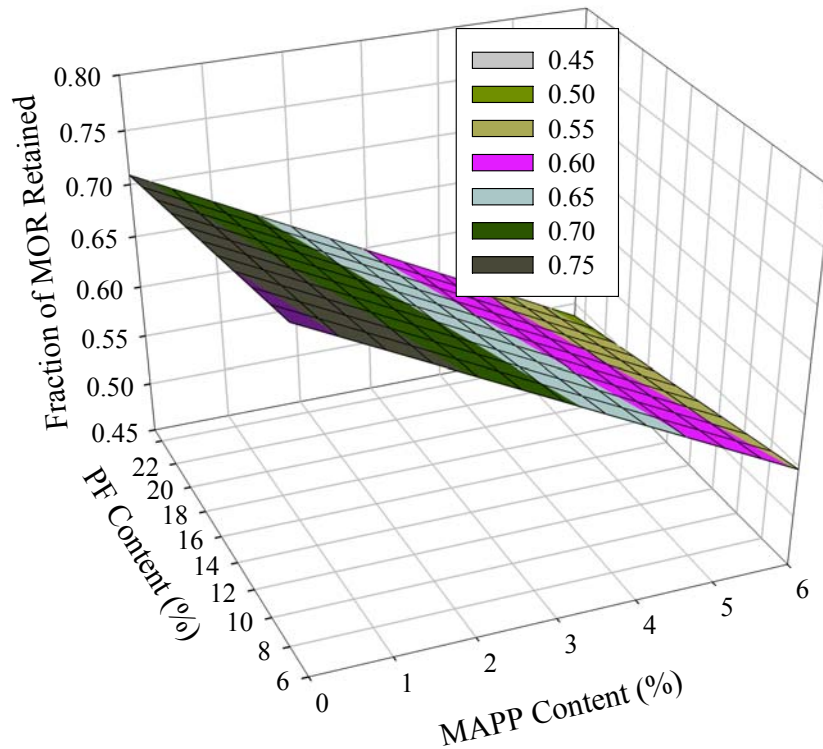


Figure 3.9 Response surface for fraction of MOR retained with varying levels of PF and MAPP for static bending specimens after 24 hours water soak

Analysis of covariance was performed with density as a covariate. Results suggested MAPP content at lower PF level (6%) significantly reduced MOR retention (p-value = 0.0270). Whereas, at higher PF levels this effect was not significant (p-value = 0.3726). Fraction of MOR retained was decreased with the increase in MAPP content in the panels. However with the increase in density the MOR retention was increased. MOR retention was compared for 6 and 25% PF content panels at varying MAPP levels (Figure 3.10). It was found that for 6% PF content specimens with the increase in MAPP content the fraction of MOR retention decreased. Increase in MAPP content from 0 to 6% resulted in a drop in MOR retention by 45%. For 25% PF content panels increase in MAPP from 0 to 3% initially enhanced the MOR retention by nearly 20% but further increase in MAPP content did not have much effect.

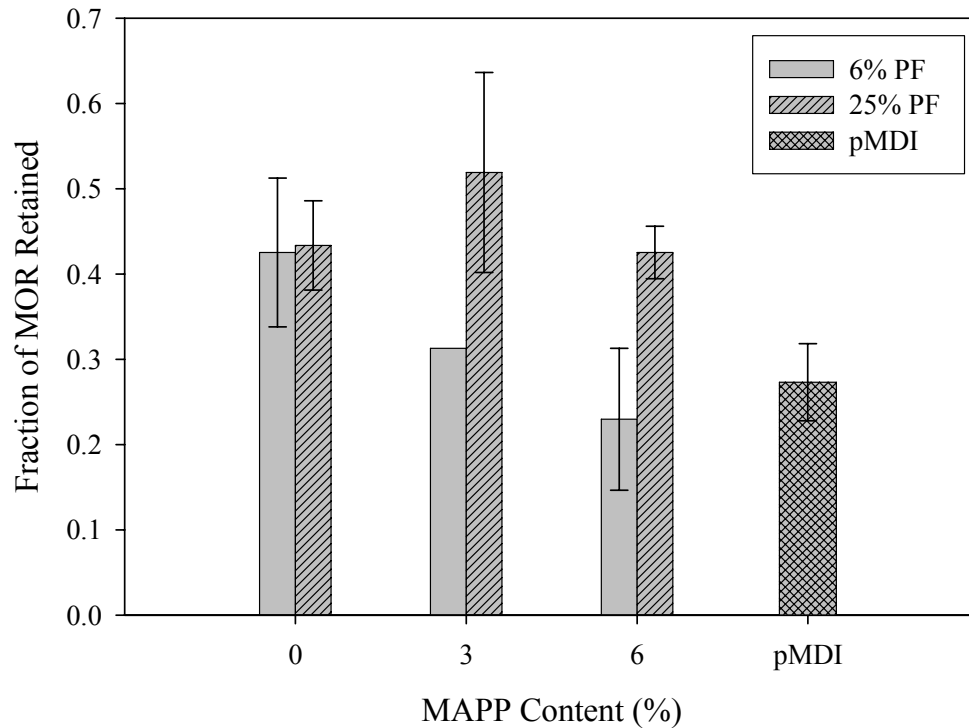


Figure 3.10 Comparisons of fraction of MOR retained after 24 hour water soak for panels with 6 and 25% PF content at varying MAPP levels. Fraction of MOR retention for pMDI panels is also included.

Static bending test after accelerated aging cycles

Flexure properties of the specimens were tested after subjecting them to accelerated aging cycles. Six cycles of accelerated aging (ASTM 1999a) were found to be too severe for the OSC test specimens. Sixty two percent of the specimens fell apart after the completion of 2 cycles; and, fifty percent of pMDI bonded specimens fell apart or failed after 2 cycles. It was observed that specimens with higher amount of PF resin content performed better under these severe conditions. This trend was also observed by previous researchers, where higher resin content (30%) panels performed better under accelerated aging (Sun et al. 1994). Table 3.2 and 3.3 summarizes fraction of MOE/MOR retained after accelerated aging.

Table 3.2 List of fraction of MOE retained after accelerated aging of static bending specimens. Values in the parenthesis represent COV.

PF MAPP	6	10	12	15	15.5	18	20	22	25	pMDI
0	Failed		0.793	*	*	*	*	*	0.764 (23%)	0.338 (12%)
0.5	*	*	*	*	*	0.882 (36%)	*	*	*	
1.5	*	0.266	*	*	*	*	*	0.489	*	
2	Failed	*	*	*	*	*	*	*	*	
3	Failed	*	*	*	0.132	*	*	*	0.247 (20%)	
4	Failed	Failed	*	*	*	*	*	*	*	
4.5	*	*	*	*	*	*	Failed	*	*	
6	Failed	*	*	Failed	*	*	*	*	0.194	

* Blend with this composition was not tested

Table 3.3 List of fraction of MOR retained after accelerated aging of static bending specimens. Values in the parenthesis represent COV.

PF MAPP	6	10	12	15	15.5	18	20	22	25	pMDI
0	Failed		0.676	*	*	*	*	*	0.635 (45%)	0.338 (12%)
0.5	*	*	*	*	*	0.935 (36%)	*	*	*	
1.5	*	0.289	*	*	*	*	*	0.410	*	
2	Failed	*	*	*	*	*	*	*	*	
3	Failed	*	*	*	0.207	*	*	*	0.264 (19%)	
4	Failed	Failed	*	*	*	*	*	*	*	
4.5	*	*	*	*	*	*	Failed	*	*	
6	Failed	*	*	Failed	*	*	*	*	0.203	

* Blend with this composition was not tested

Internal Bond Test

Internal bond (IB) tests were performed after conditioning the samples at 12% moisture content. This test reflects the tensile strength of the test panel perpendicular to the surface and is an indirect measure of fastener holding properties. Stress at failure was calculated for each specimen.

Analysis of data using D-optimal response surface model yielded a response surface for IB values as MAPP content and PF content varied (Figure 3.11).

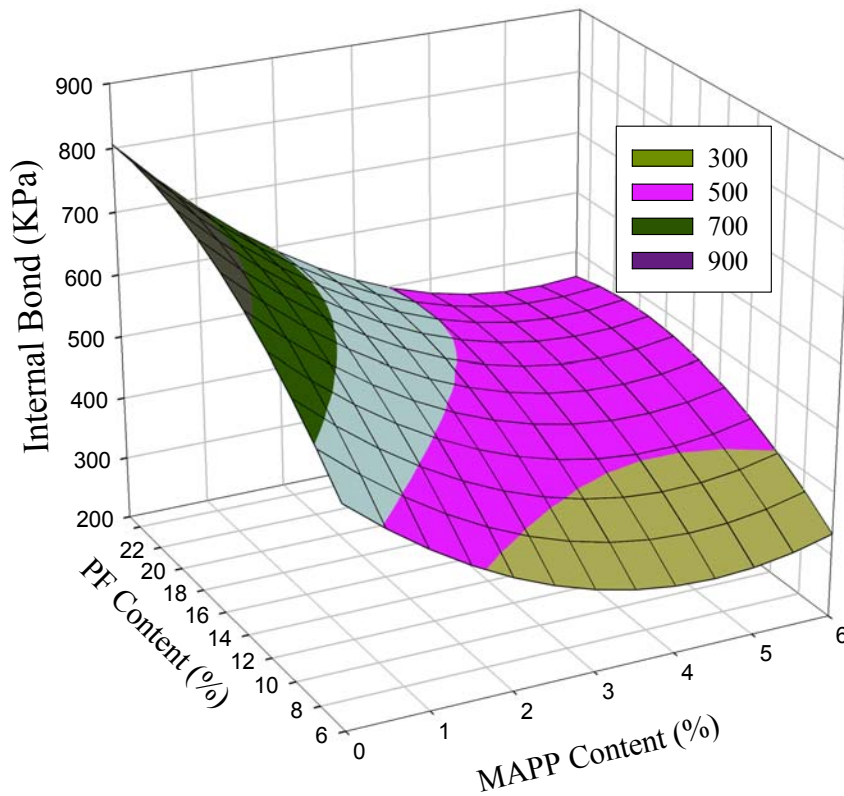


Figure 3.11 Response surface plot for internal bond strength at varying levels of MAPP and PF.

The analyzed model, with an R-square of 0.5, suggests that all three factors, namely PF content (p-value = <0.0001), MAPP content (p-value = <0.0001) and density (p-value = <0.0001), had

significant effect on internal bond strength. As MAPP content increased, the internal bond strength significantly decreased; however, PF content and density had positive effect on IB strengths as expected. Analysis of covariance with density as a covariate further indicated that increasing PF content had significant effect on increasing IB (p-value range = 0.0057 to 0.0351); however, at higher MAPP levels (higher than 3%) increasing PF did not show significant effects (p-value range = 0.0550 to 0.7285). Analysis also suggested that MAPP levels reduced IB strength significantly (p-value range = 0.0005 to 0.0044). Figure 3.12 compares IB values for specimens at 6% and 25% PF levels for different MAPP levels.

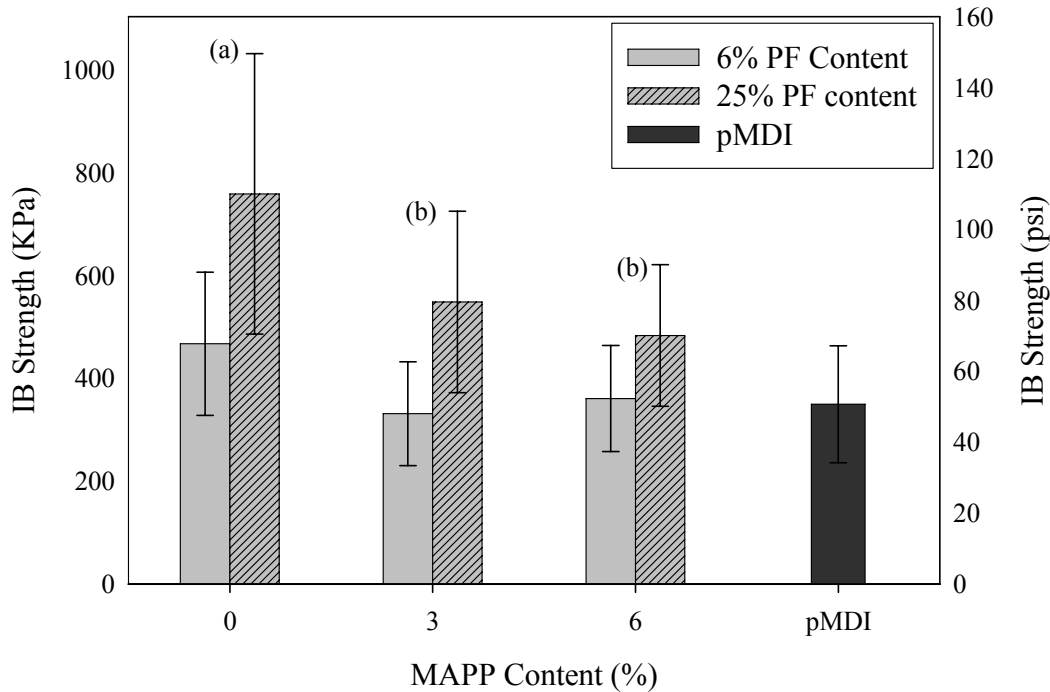


Figure 3.12 Comparison of internal bond strength for specimens at 6% and 25% PF levels with varying MAPP contents and pMDI resin. Comparison of means test results are also indicated.

For 25% PF content panels a decrease of 56% in IB strength was observed as MAPP content was increased from 0% to 6%. Comparison of means test at 0.05 significance level showed that 3% and 6% MAPP content specimens were significantly lower than specimens without MAPP.

Figure 3.13 compares IB at 6% MAPP content with varying PF levels. As the PF content was increased from 6% to 25%, a 34% increase in IB strength was observed at MAPP level of 3%.

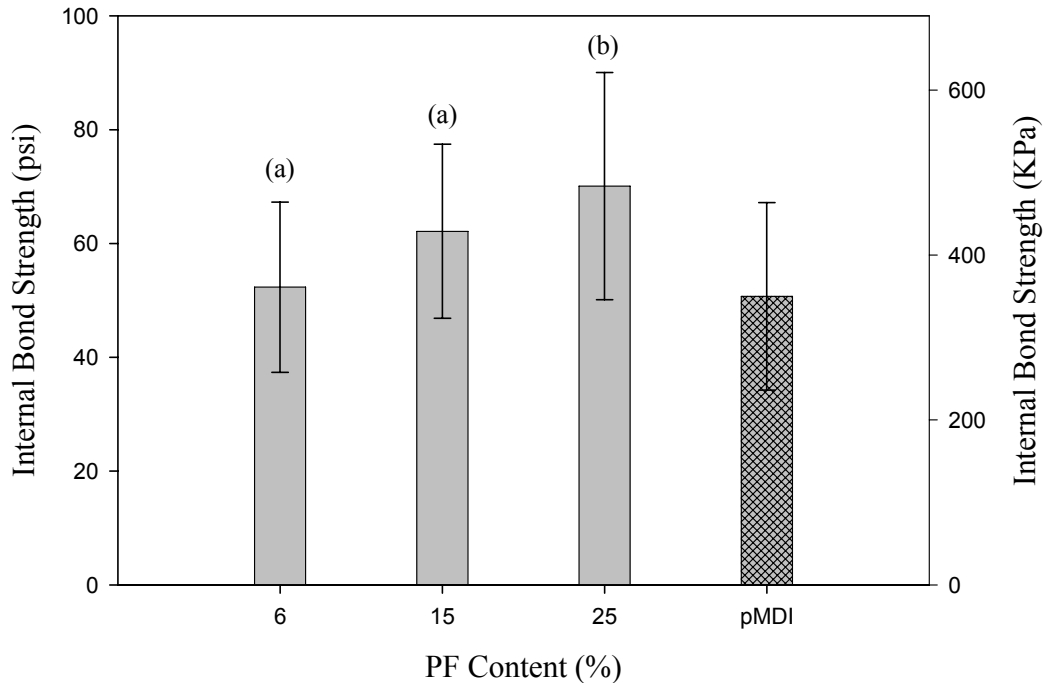


Figure 3.13 Change in IB strength of test specimens with varying PF levels at 6% MAPP. Average IB of specimens bonded with pMDI resin is also shown. Comparison mean test results are indicated as well.

On the basis of static bending and IB test results it could be seen that higher amount of PF resin significantly improve the mechanical properties. This finding supports the hypothesis that higher PF content improved mechanical properties. However addition of MAPP reduced mechanical properties especially at higher levels. This was against our study hypothesis that addition of MAPP would improve panel’s mechanical properties. It was however observed that addition of lower amount of MAPP did not severely affect the properties.

Evaluation of Physical Properties

Water Absorption and Thickness Swelling

Effect of MAPP and PF contents on moisture properties after short term (2hour) and long term (24-hour) water soak tests were evaluated as per ASTM D 1037 (ASTM 1999a). Response surface analyses were performed on water absorption and thickness swelling results using Design-Expert[®] software.

Short term (2 hours) water absorption and thickness swelling

Water absorption after 2 hours was calculated as a percentage of initial weight.

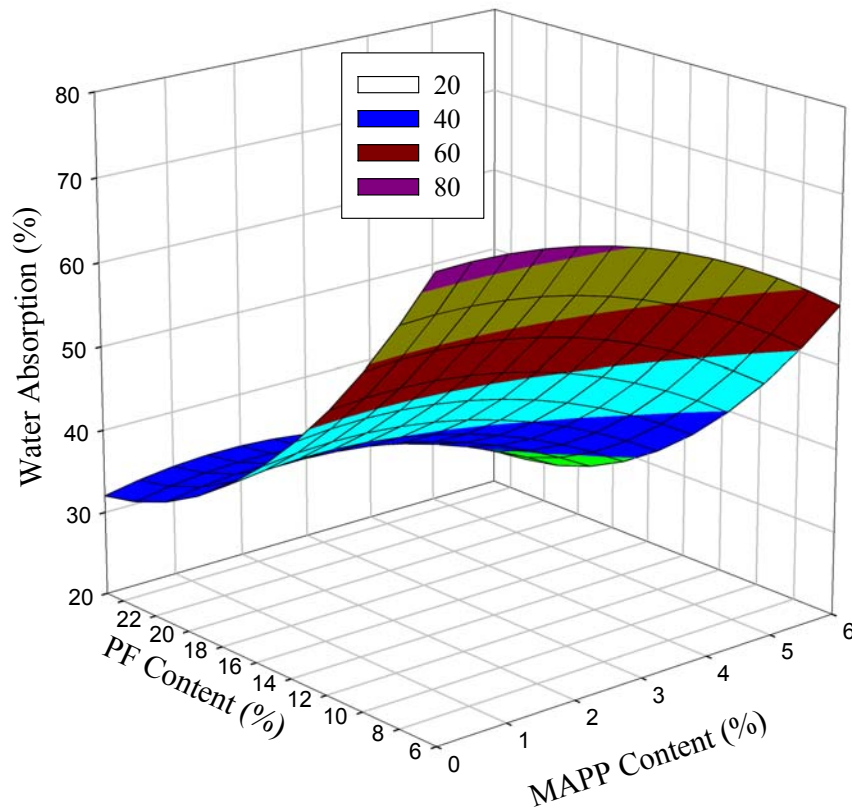


Figure 3.14 Response surface for water absorption for varying PF content and MAPP content for 2-hour of water soak testing.

Response surface model ($R^2 = 0.84$) suggested that varying MAPP and PF contents had significant impact (p-values less than 0.0003) on 2-hour water absorption values, whereas density effects were not significant. Increase in MAPP and PF contents decreased water absorption of test specimens (Figure 3.14). Effect of increasing MAPP content at 6% and 25% PF levels after 2-hr water absorption test is shown in Figure 3.15. An average drop of over 28% in water absorption was observed at both 6% and 25% PF levels as MAPP content was increased from 0% to 6%.

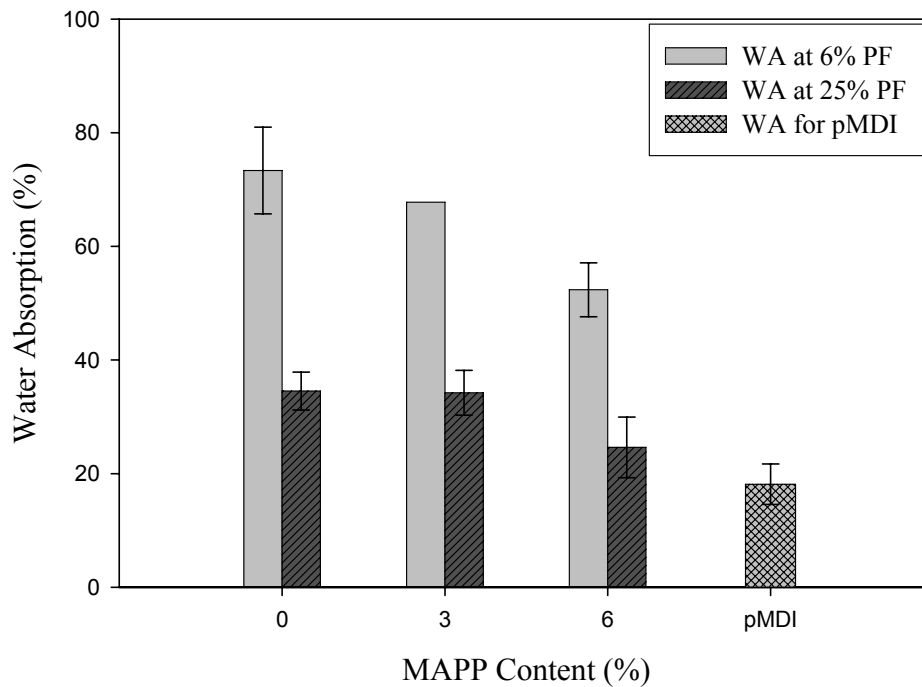


Figure 3.15 Comparison of 2-hour water absorption results for 6% and 25% PF content at varying MAPP content and for panels bonded with pMDI.

Response surface for thickness swelling after 2-hour water soak is shown in Figure 3.16 (model $R^2 = 0.92$). Analysis showed that PF factor was significant (p-value < 0.0001), whereas MAPP did not influence thickness swelling significantly.

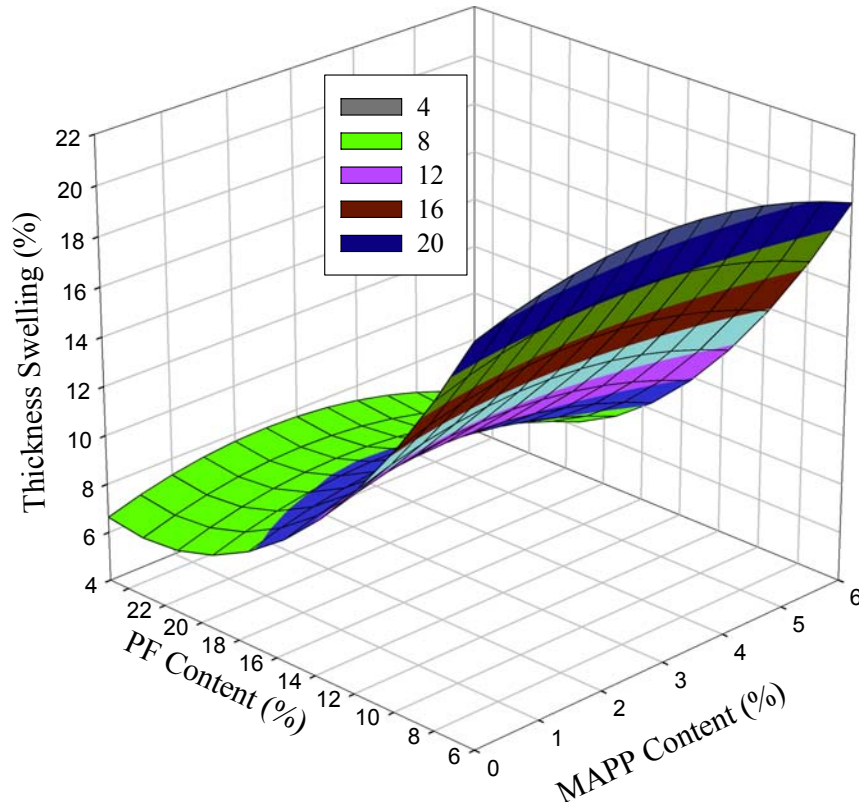


Figure 3.16 Response surface for 2-hour thickness swelling as MAPP content and PF content were changed.

Figure 3.17 presents changes in thickness swelling after 2-hr water soak for two different PF contents (6% and 25%) at varying MAPP levels. As PF content was increased from 6% to 25%, at 3% MAPP level, a 65% decrease in thickness swelling was observed. Increase in MAPP content showed a significant change in thickness swelling only at higher PF level (a decrease of 27%).

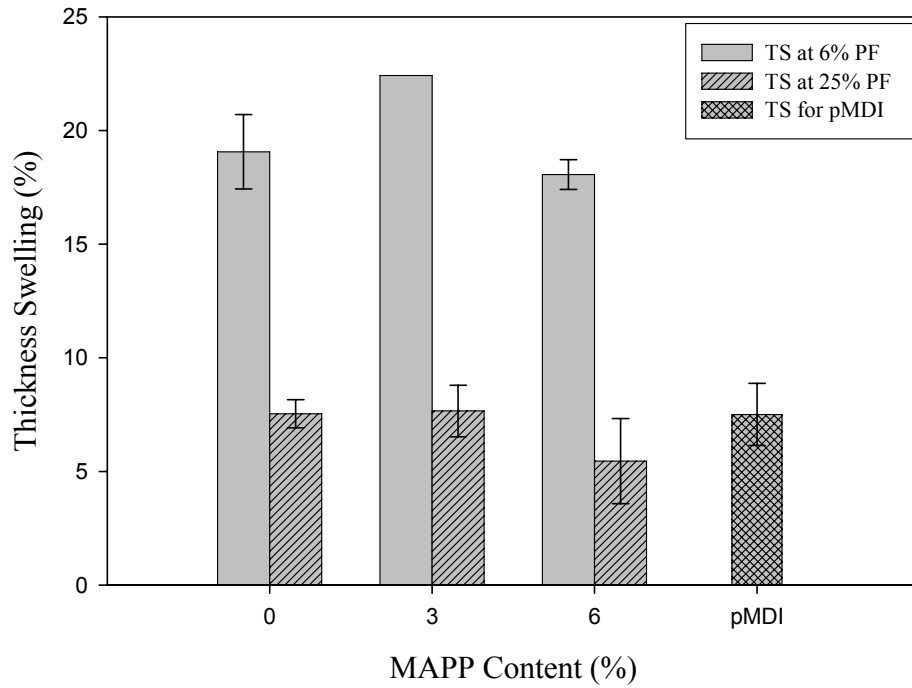


Figure 3.17 Comparison of 2 hours thickness swelling values for 6% and 25% PF content at varying MAPP content, compared with pMDI panels.

Long term (24- hour) water absorption and thickness swelling

Figure 3.18 shows response surface (model $R^2 = 0.83$) for long term water absorption (24 hours) with varying MAPP content and PF contents.

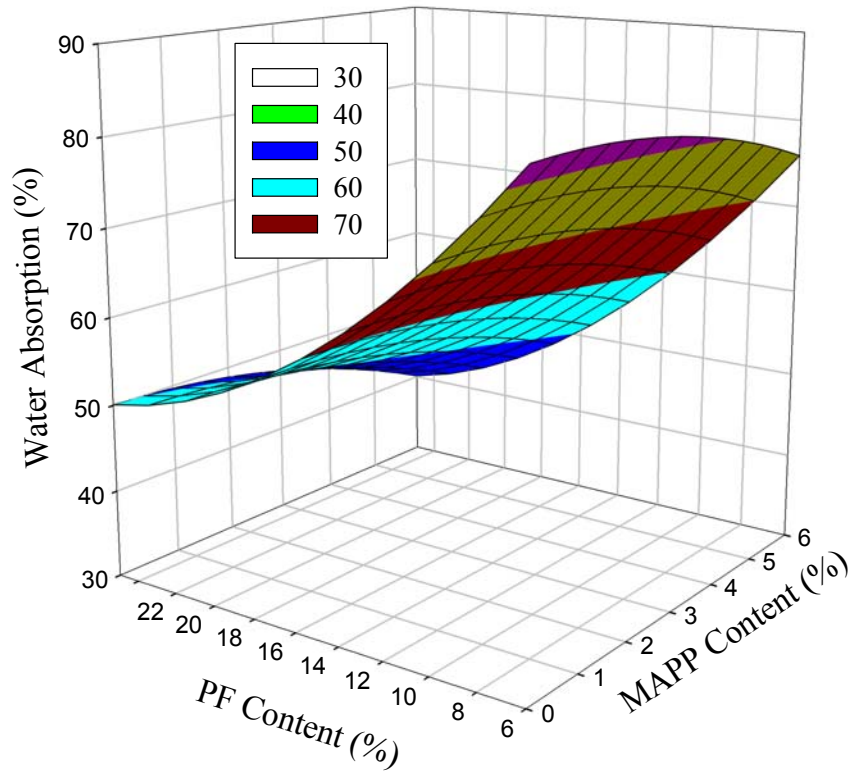


Figure 3.18 Change in water absorption after 24-hour water soak as MAPP and PF levels varied.

Analysis of variance indicated that both MAPP and PF content had significant effects on long term water absorption (p-values < 0.0049). Once again, density effects were not significant.

Figure 3.19 compares long term water absorption results for 6% and 25% PF contents at varying MAPP levels.

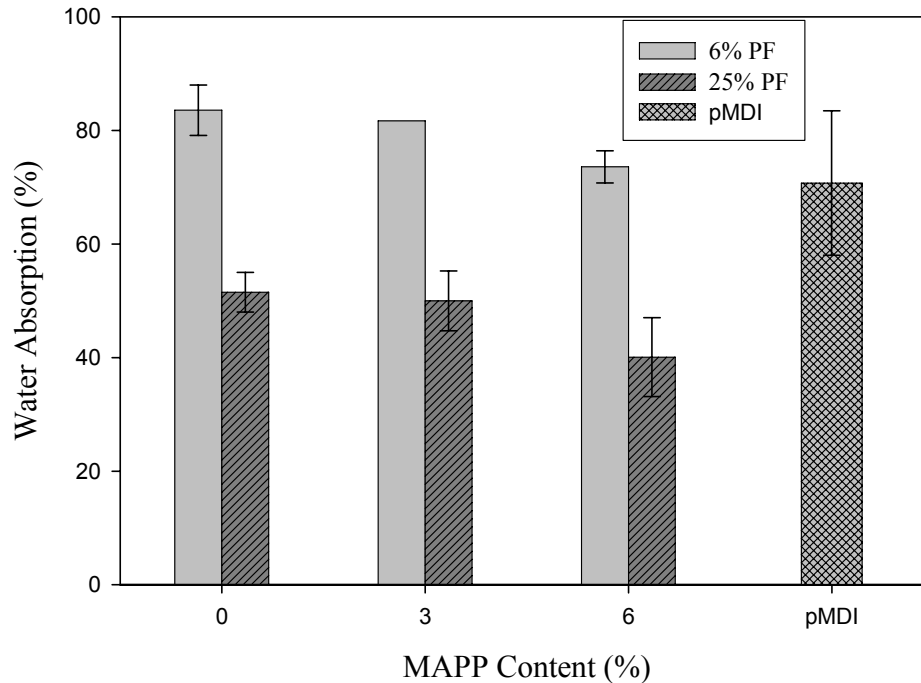


Figure 3.19 Comparison of water absorption after 24- hour water soak for panels with 6% and 25% PF content at varying MAPP content and for pMDI panels.

There is a sharp decrease in water absorption as PF content was increased from 6 to 25% percent (a reduction of 38% at 3% MAPP level). MAPP content also decreased water absorption values, but not so significantly. At 6% PF level, increase in MAPP content from 0% to 6% decreased water absorption by 12%; whereas, at 25% PF content, the water absorption reduced by 29%. Panels manufactured with higher PF content (25%) performed better than pMDI panels after 24-hour soak tests.

Changes in long term thickness swelling as MAPP and PF contents were varied are shown in Figure 3.20. Response model (model $R^2 = 0.92$) suggests that both MAPP and PF effects were significant for long term thickness swelling (p-value < 0.0001). Increase in PF content decreased thickness swell, similar to water absorption tests; but, contrary to waster absorption results

thickness swell increased as MAPP content was increased, especially at lower PF levels. This may be justified by the fact that longer soaking time allowed water to diffuse into the cell wall causing increase in the thickness swelling. Figure 3.21 shows a comparison of thickness swelling for 6% and 25% PF content panels at varying MAPP levels.

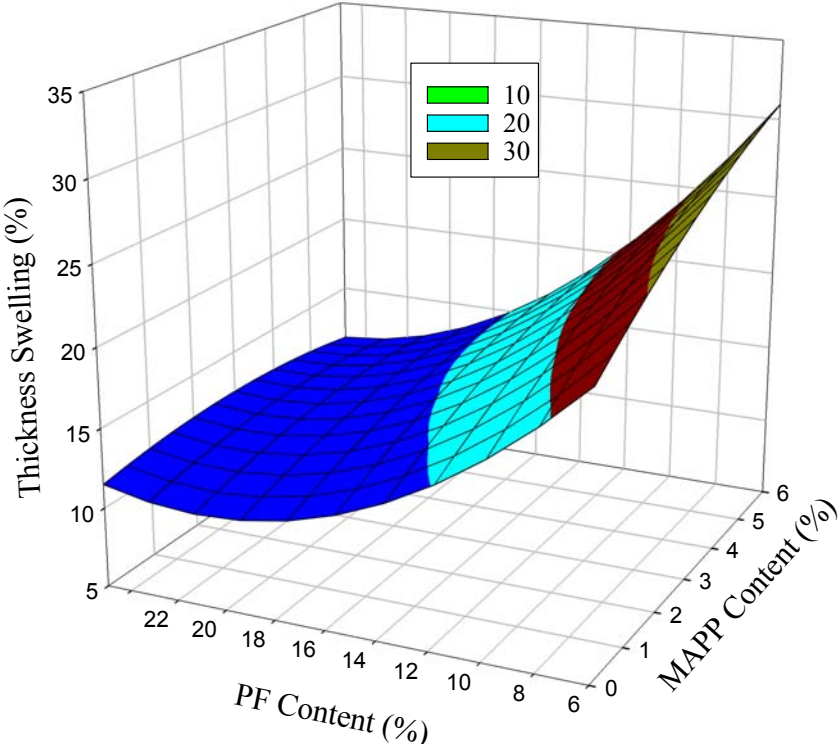


Figure 3.20 Changes in thickness swelling after 24-hour water soak with varying MAPP and PF contents.

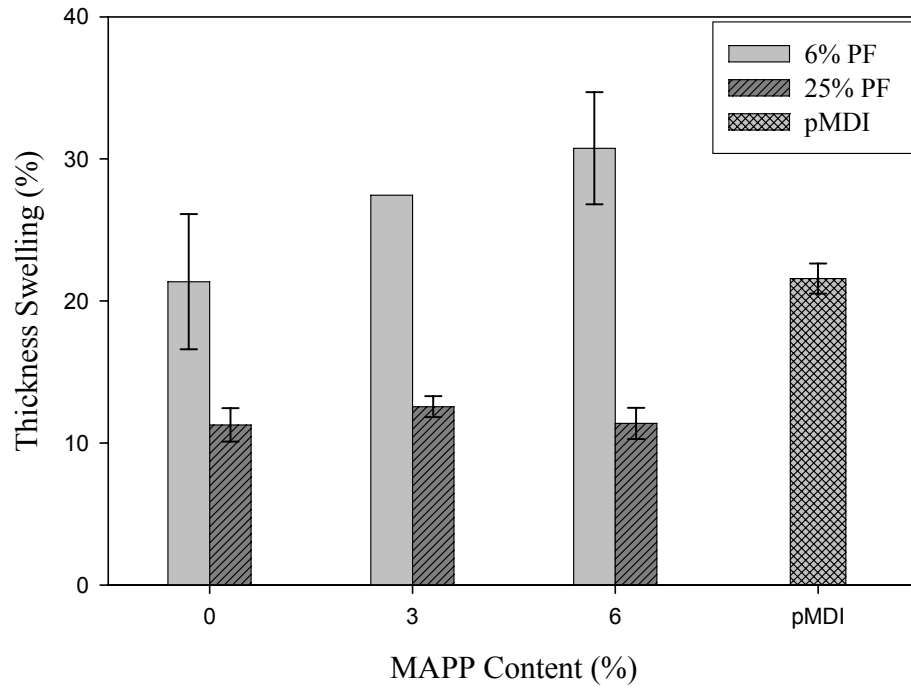


Figure 3.21 Comparison of thickness swelling after 24-hour water soak for 6% and 25% PF panels at varying MAPP levels and for pMDI panels

At 25% PF level, increase in MAPP content did not have much impact on thickness swelling. PF content though had a considerable effect on thickness swelling as MAPP level was kept constant.

Figure 3.22 compares the effect of varying PF content at 6% MAPP level on thickness swelling.

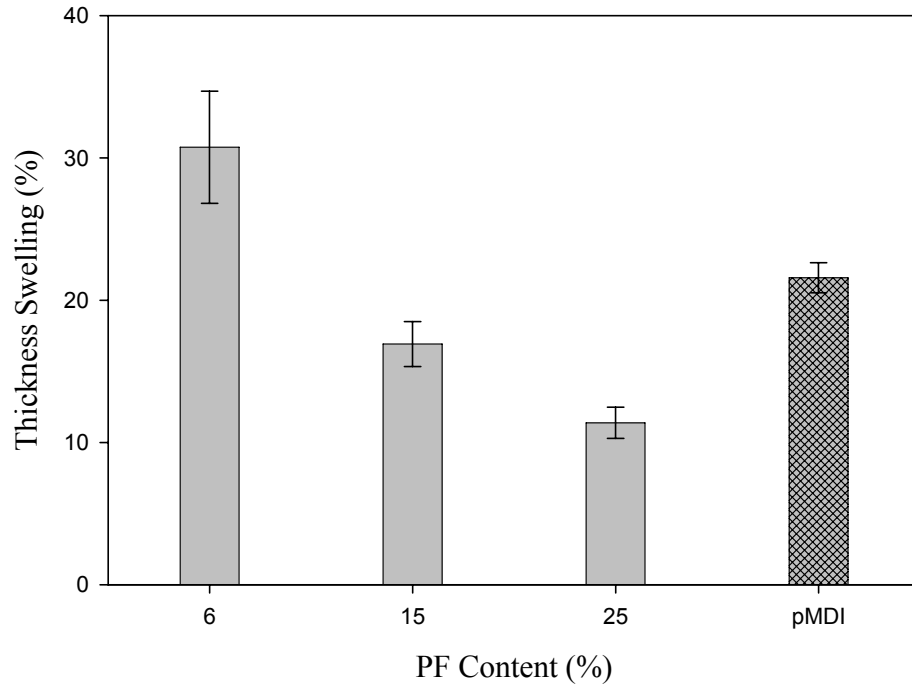


Figure 3.22 Comparison of thickness swelling after 24-hour water soak for panels with 6% MAPP and varying PF content and for pMDI panels.

A 63% decrease in thickness swelling was observed as the PF content was increased from 6% to 25%. Higher PF content panels were also found to have better resistance to thickness swelling than pMDI panels. Thickness swell could have increased with increasing MAPP level at lower PF content as a result of cell walls absorbing more water. However, due to bulking of cell lumens and between-strand voids with MAPP, water absorption did not necessarily increase with increasing MAPP levels, but instead decreased.

Water absorption and thickness swelling values for test panels were found to be much higher than commonly expected in commercially produced oriented strand composites, such as OSB. These values were also found to be higher than what was observed by other researchers (Gu et al.2005). It is believed that a reason for this is the quality of furnish used in this study. It was observed that there are wide variations in strand dimensions used in producing test panels. Dai

and Steiner (1997) suggested that flake dimensions have great impact on the horizontal density of finished panels; as length, width and thickness change, the variance in panel density increases. This effect is reflected in specimen density variations within each of the groups. Distributions of strand dimensions were characterized to confirm this hypothesis. Dimensions of 150 randomly chosen strands were measured and distributions were plotted (Figure 3.23). As distributions indicate, thickness and width of the strands used in this study had wide variations.

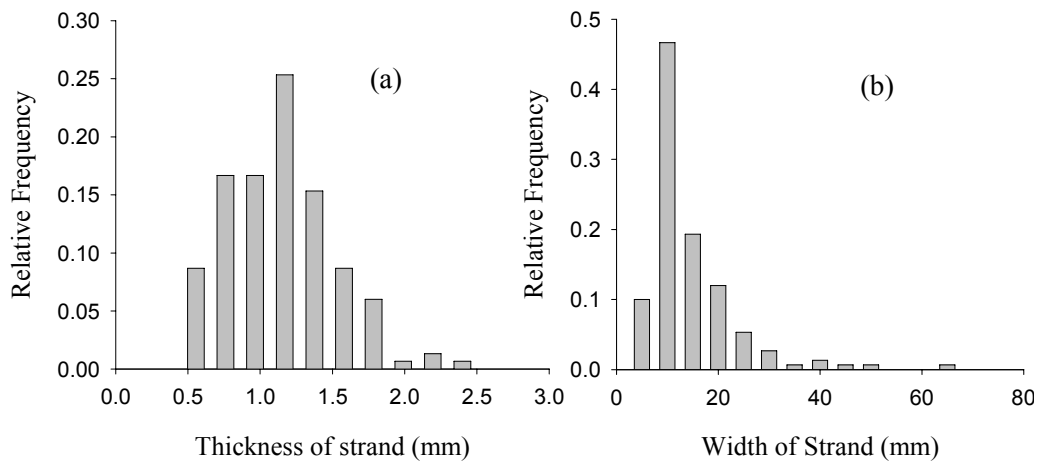


Figure 3.23 Distribution of (a) thickness and (b) width of the strands used to manufacture OSC test panels in this study.

Between width and thickness, the later has a more pronounced effect on density variation of the test panels (Dai and Steiner 1997). Variation in horizontal density results in higher between-strand void volume. Voids in the panel results in more absorption of water as found by Wolcott (2003). Therefore, in this study, it is speculated that wide variations in strand dimensions resulted in values of water absorption and thickness swelling values.

Water Vapor Transmission (WVT) and Permeance

Water vapor transmission and permeance were measured according to guidelines specified in ASTM E 96 (ASTM 1994) to evaluate the effect of varying amounts of MAPP and PF on moisture resistance characteristics of OSC panels. Typical examples of moisture gain vs. time plots are shown in Figure 3.24.

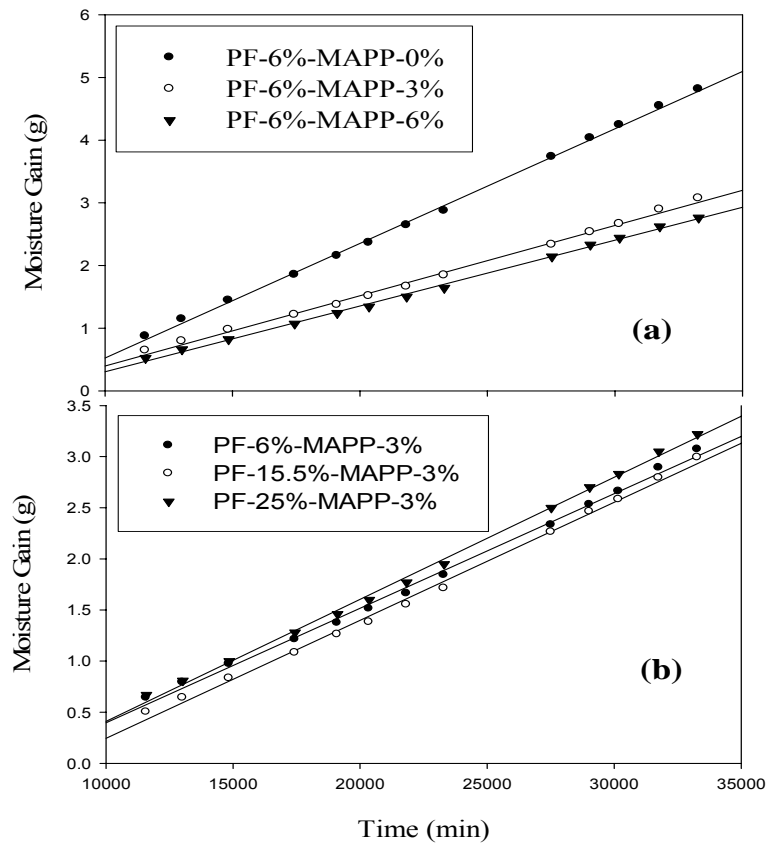


Figure 3.24 Typical plots of moisture gain vs. time elapsed data for diffusion coefficient specimens. (a) Slope of moisture gain for specimens with 6% PF content at varying MAPP levels. (b) Slope of moisture gain for specimens with 3% MAPP at different PF contents.

From the slope of the moisture gain vs. elapsed time graph, rate of water vapor transmission (WVT) for each specimen was calculated, and using WVT values, permeance for each specimen was calculated. These permeance values were then fed into the previously used D-optimal response surface model to see the effects of PF and MAPP content on the permeance of the

oriented strand composite. Figure 3.25 shows the response surface for permeance as the MAPP content and PF content were varied.

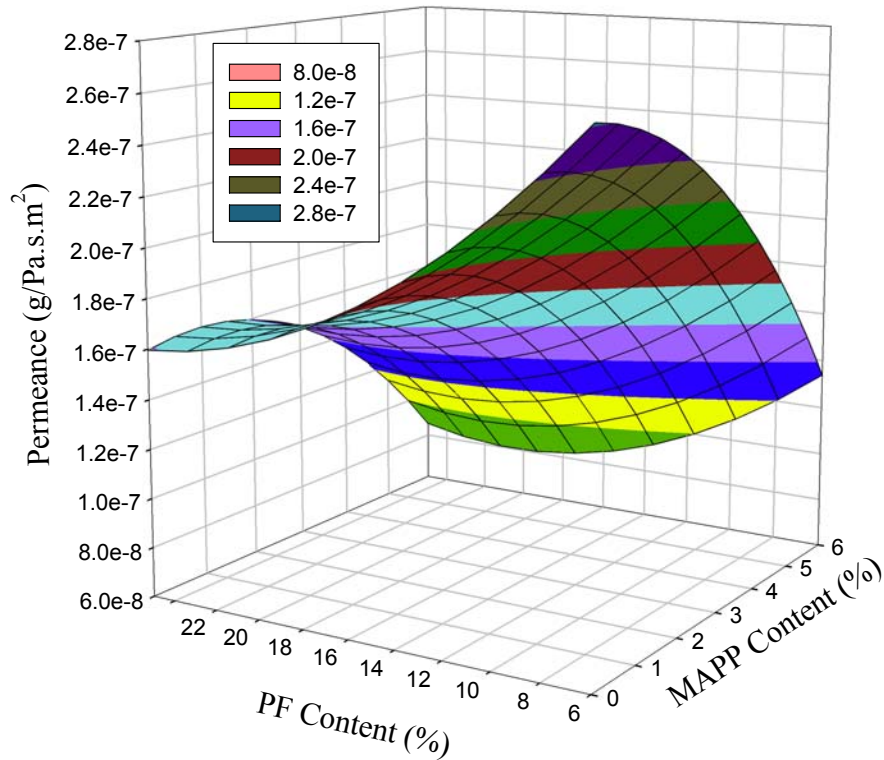


Figure 3.25 Response surface plot of permeance of test specimens with varying MAPP and PF content.

The response surface model ($R^2 = 0.83$) suggested that both MAPP and PF content had significant effect on permeance of the specimens (p -values < 0.0006). Density of test specimens was also observed to have a significant effect (p -value = 0.0011). An analysis of covariance (ANCOVA) was performed taking density as a covariate. Results indicated that MAPP effect was still significant (p -value = 0.0010) as for permeance; however, in the adjusted model PF was found to have no significant effect (p -value = 0.3624) on the permeance property of the specimens. Thus, results indicate that MAPP does play a significant role in reducing the

permeance of the panels supporting the hypothesis that it aids in improving the moisture resistance.

It could be seen from the response surface plot of permeance (Figure 3.25) that with an increase in MAPP content permeance of the specimens decreased significantly especially at lower levels of PF. Change in permeance with varying MAPP content is plotted in Figure 3.26 for two extreme levels of PF.

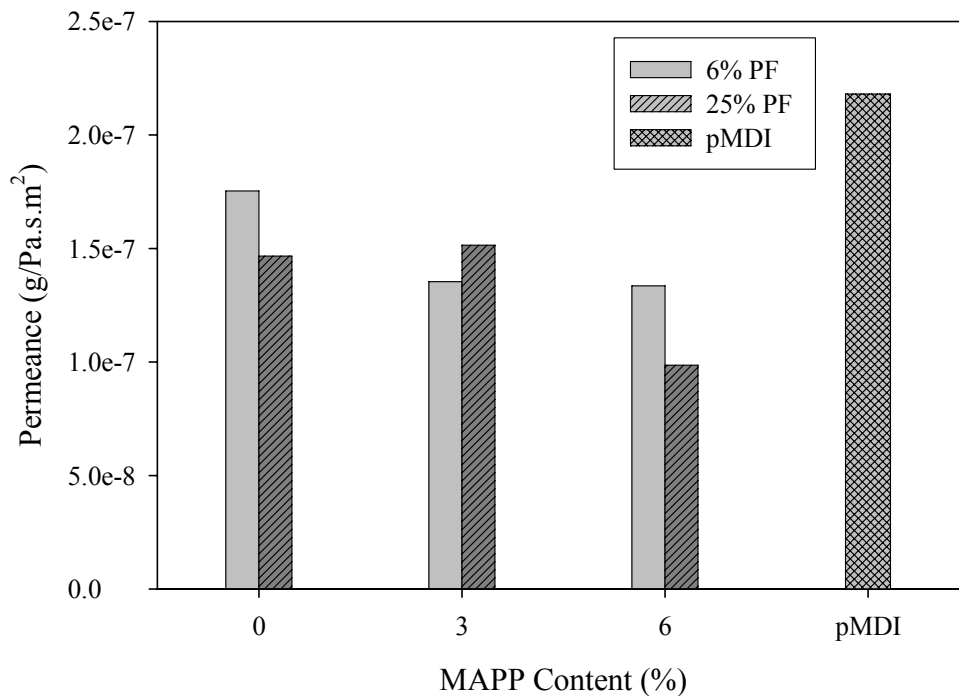


Figure 3.26 Comparison of permeance for 6% and 25% PF content at varying MAPP levels. Included also is the average permeance of pMDI panels.

For 6% PF content panels, increment in MAPP content from 0% to 6% resulted in a decrease of permeance of test panels by 23%. The permeance of 6% PF panel with 3% MAPP content was 37% lower than that of pMDI panels.

Comparison of EMC and Diffusion Constant

Equilibrium moisture content of test panels was evaluated after subjecting the specimens to two different environmental conditions. First set of specimens were subjected to 50% relative humidity (RH) and 22°C and the second set of specimens were subjected to 80% RH and 30°C. Moisture weight gain was plotted as a function of time for all formulations and examined to compare equilibrium moisture contents and relative rates of moisture sorption. Diffusion constants of test panels were compared to investigate differences in relative rates of moisture sorption as a result of varying proportions of PF and MAPP.

Specimens subjected to 50% RH and 22°C

Initially, when oven dried specimens were placed in the test chamber, they absorbed moisture rapidly and over time gradually equilibrated as expected. Figure 3.27 compares the trend in moisture weight gain for 6% PF content panels with varying MAPP content. The values were graphically compared with moisture weight gain of pMDI test specimens.

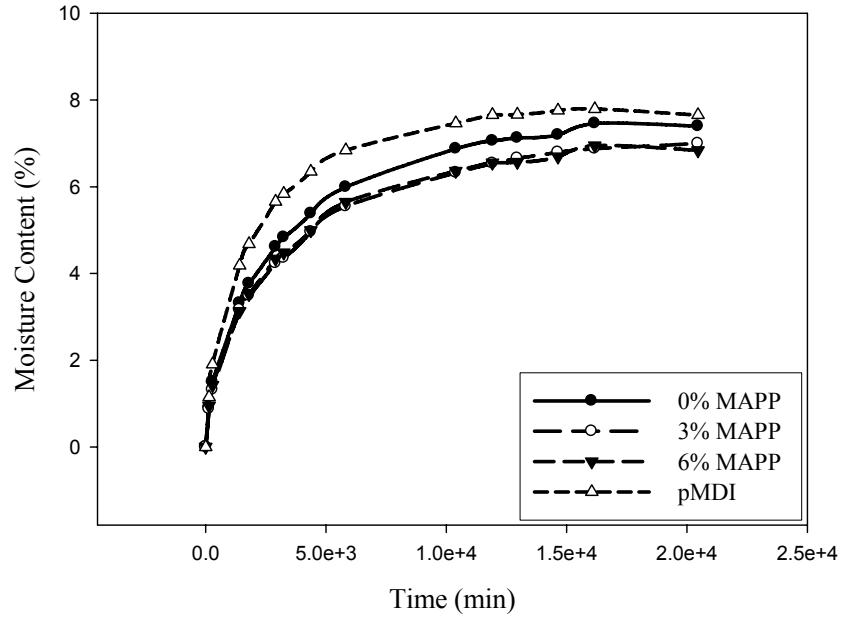


Figure 3.27 Moisture content gain of 6% PF content panels with varying MAPP content, compared with moisture content gain of pMDI panel at 50% RH.

As MAPP content was increased from 0% to 6%, the equilibrium moisture content of panels decreased from 7.39% to 6.99%. Panels bonded with pMDI resin equilibrated to higher moisture content when compared with 6% PF content panels with varying MAPP levels. Similar trend was also observed for higher PF content panels; at 25% PF level, EMC decreased from 7.08% to 5.79% as MAPP content was increased from 0 to 6%. Figure 3.28 shows the moisture weight gain as a function of time for panels with 25% PF and varying MAPP content.

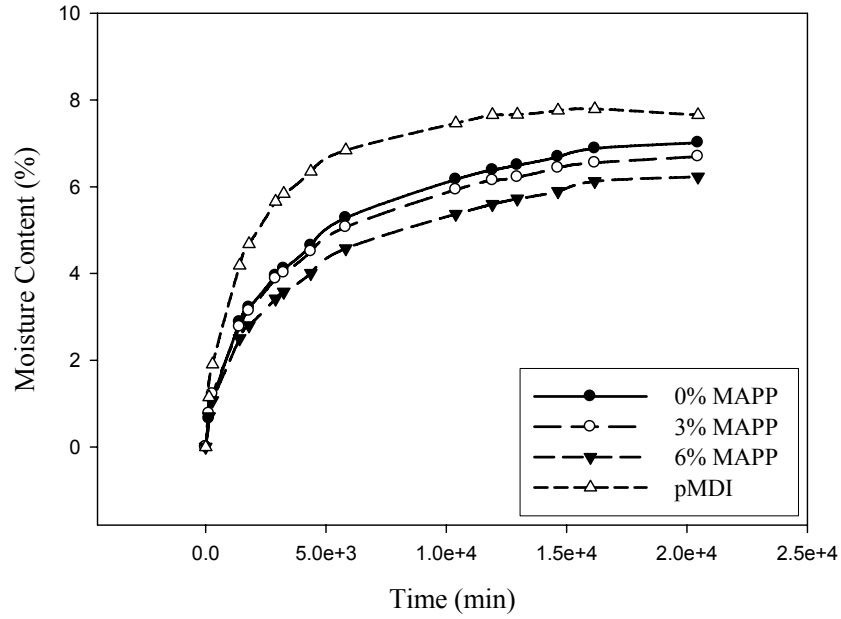


Figure 3.28 Moisture weight gain as a function of time for panels bonded with 25% PF content with varying MAPP levels and pMDI resin panel at 50% RH.

Increase in PF content while holding MAPP level constant did not significantly reduce rate of moisture uptake and EMC (Figure 3.29). With increase of PF content from 6 to 25% at 3% MAPP content the equilibrium moisture content decreased from 6.99%% to 6.41%.

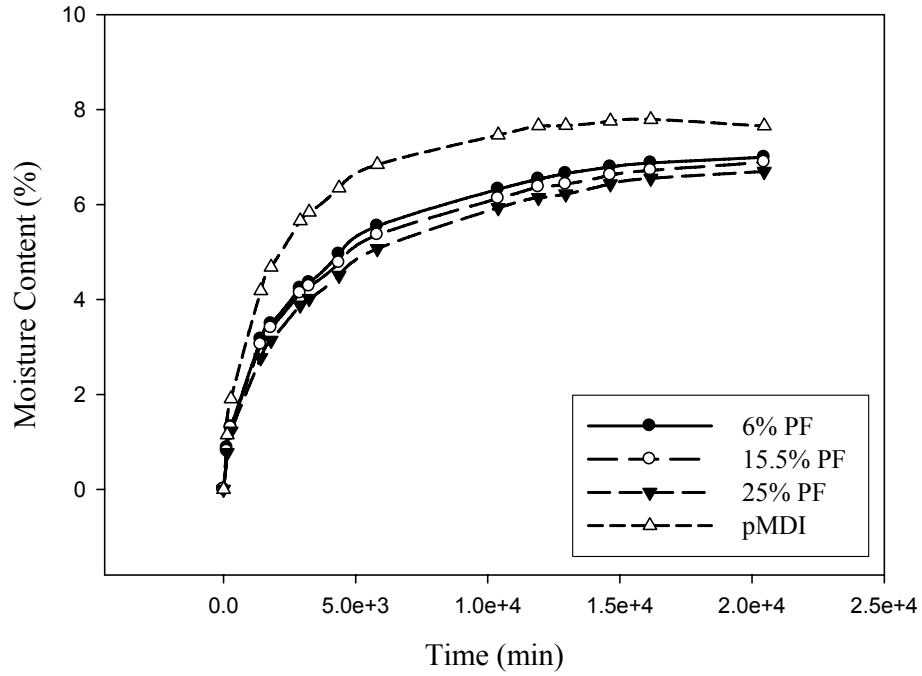


Figure 3.29. Moisture weight gain of test panels with 3% MAPP at varying PF content. Also included are results of pMDI bonded panels.

Diffusion constant for test specimens were calculated. Typical plot for moisture gain vs. square root of time is shown in Figure 3.30.

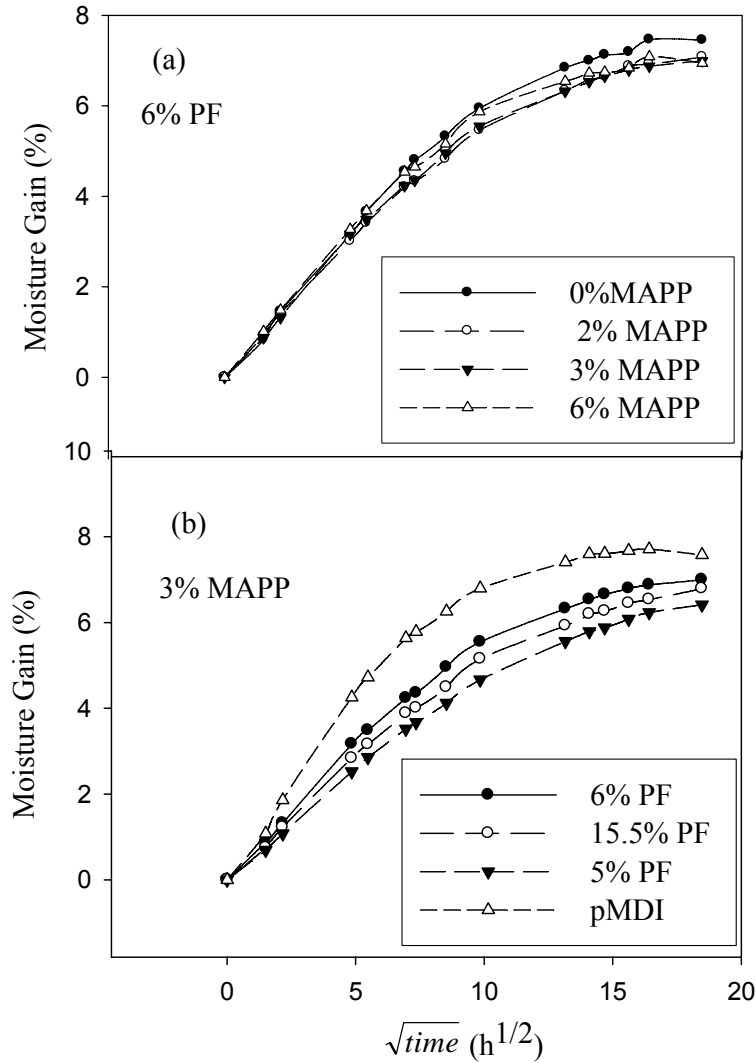


Figure 3.30 Typical plots of moisture gain vs. \sqrt{t} for determination of diffusion constant. (a) Moisture gain vs. \sqrt{t} for specimens with 6% PF content at different MAPP levels. (b) Moisture gain vs. \sqrt{t} for specimens with 3% MAPP at varying PF levels, also compared with pMDI specimen.

Plots showed that the specimens initially gain moisture linearly and then gradually starts to equilibrate. Fick's law of diffusion was applied at the linear region to determine the diffusion constants for each specimen using equations 3.1 to 3.4. Table 3.4 summarizes diffusion coefficient values for different formulations.

Table 3.4 List of diffusion constant for specimens subjected to 50% RH.

PF MAPP	6	10	12	15	15.5	18	20	22	25	pMDI
0	8.50E-05		6.07E-05	*	*	*	*	*	7.16E-05	1.14E-04
0.5	*	*	*	*	*	4.99E-05	*	*	*	
1.5	*	6.78E-05	*	*	*	*	*	5.10E-05	*	
2	6.48E-05	*	*	*	*	*	*	*	*	
3	8.79E-05	*	*	*	7.66E-05	*	*	*	6.41E-05	
4	7.39E-05	6.53E-05	*	*	*	*	*	*	*	
4.5	*	*	*	*	*	*	5.58E-05	*	*	
6	7.79E-05	*	*	5.31E-05	*	*	*	*	5.69E-05	

* Blend with this composition was not tested

Figure 3.31 compares diffusion constant of 6% and 25% PF content panels at different MAPP levels. pMDI panels were found to have higher diffusion constant values than panels made with PF. Diffusion constants of 6% and 25% PF panels were lower than that of pMDI panels by 25% and 37% respectively. For 25% PF content panels with the increase of MAPP content from 0 to 6% resulted in a decrease of diffusion constant by 20%.

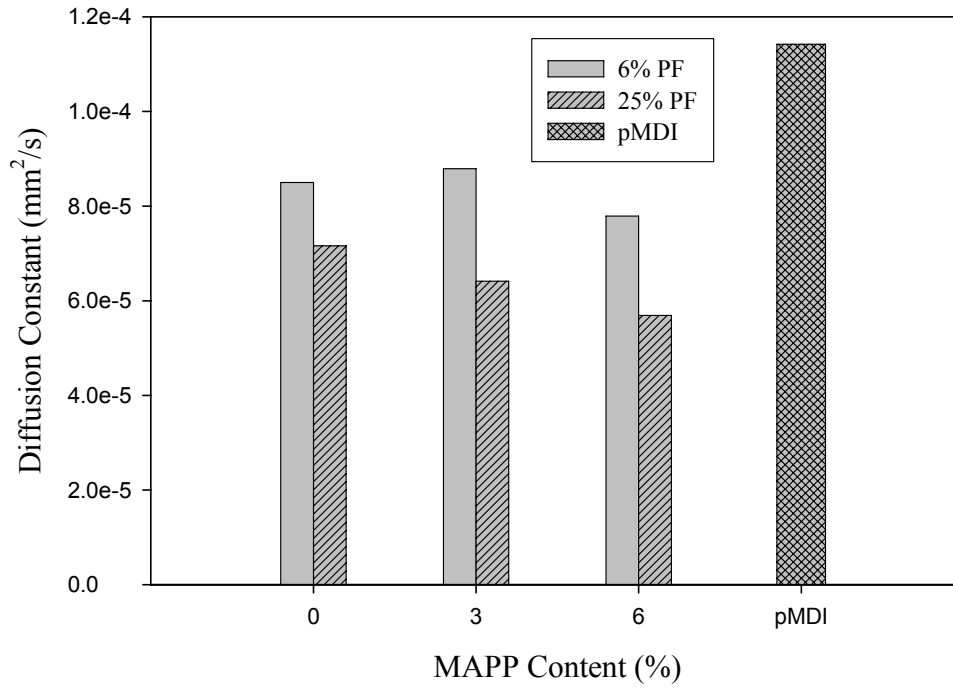


Figure 3.31 Comparison of diffusion constant for 6 and 25% PF content panels at varying MAPP levels after subjecting to 50% RH. Diffusion constant values for pMDI panels are also included

Specimens subjected to 80% RH and 30°C

Figure 3.32 compares the trend of moisture weight gain over time for 6% PF test panels with varying MAPP content and for pMDI bonded test panels.

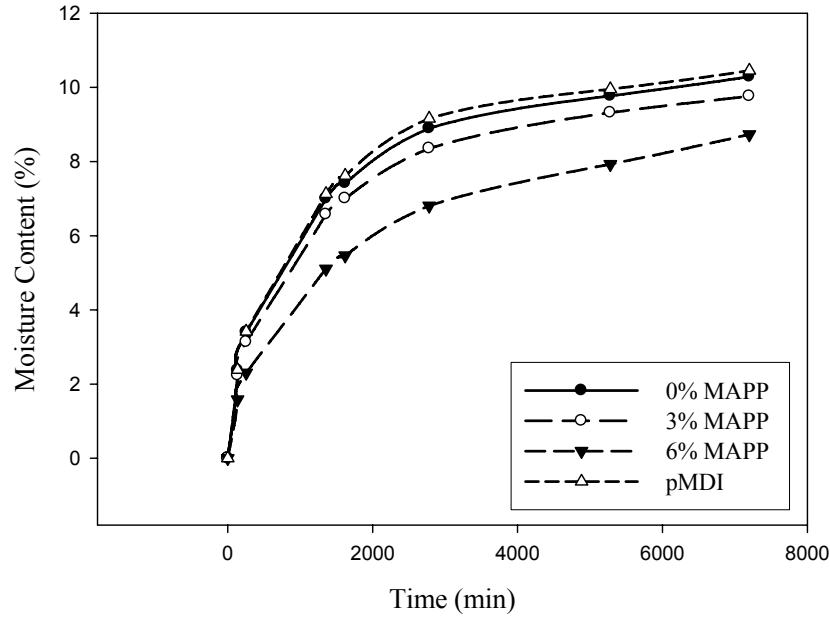


Figure 3.32. Moisture weight gain over time for test panels bonded with 6% PF resin at varying MAPP levels at 80% RH. Moisture weight gain of pMDI test panels is also shown.

Rate of moisture weight gain was significantly different for panels with higher MAPP content.

At 6% PF content, with increase in MAPP level from 0 to 6%, EMC of test panels decreased from 10% to 8%. Results also indicate slower rates of moisture gain with increasing levels of MAPP. Panels with 0% MAPP content had similar trend of moisture gain as that of pMDI panels, whereas with the increase in MAPP content the rates of moisture gain were lowered and the panels equilibrated at lower moisture content.

Moisture weight gain over time for panels with 3% MAPP and varying PF contents is shown in Figure 3.33. The effect of increasing PF content is not as significant as in the case of varying MAPP content, especially at higher PF levels. With an increase of PF content from 6% to 25%, a decrease in equilibrium moisture content of 5% was observed. When compared with pMDI panels, all the formulations were found to have lower EMC than pMDI panels.

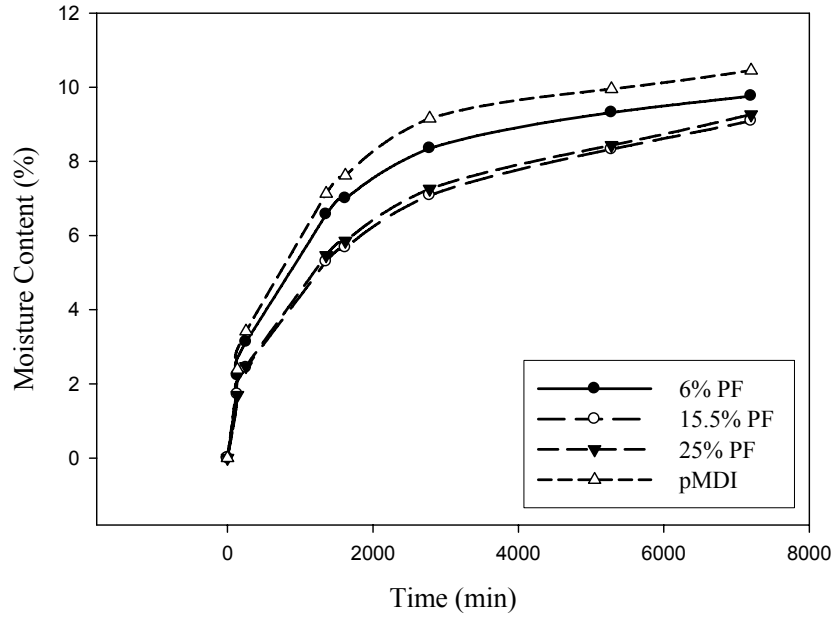


Figure 3.33. Moisture content gain of 3% MAPP content panels with varying PF content, compared with moisture content gain of pMDI panel at 80% RH.

Diffusion constant for specimens at 80% RH was calculated. Typical plots of moisture gain vs. square root of time are shown in Figure 3.34. It was found that specimens initially gained moisture linearly and then gradually starts to equilibrate. This trend was typical for materials that follow Fickian behavior. Fick's law of diffusion was applied at that linear region to determine the diffusion constant.

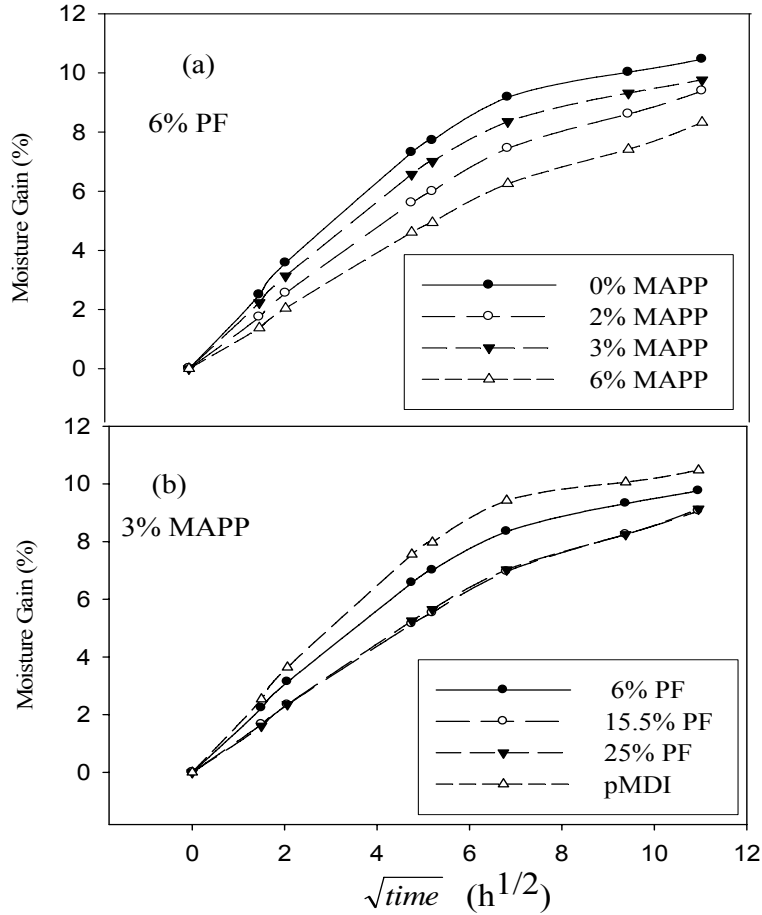


Figure 3.34 Typical plots of moisture gain vs. \sqrt{t} for determination of diffusion constant of specimens subjected to 80% RH. (a) Moisture gain vs. \sqrt{t} for specimens with 6% PF content at different MAPP levels. (b) Moisture gain vs. \sqrt{t} for specimens with 3% MAPP at varying PF levels, also compared with pMDI specimen.

Table 3.5 List of diffusion constant for specimens subjected at 80% RH.

PF \ MAPP	6	10	12	15	15.5	18	20	22	25	pMDI
0	1.52E-04		1.04E-04	*	*	*	*	*	1.00E-04	1.43E-04
0.5	*	*	*	*	*	1.22E-04	*	*	*	
1.5	*	1.13E-04	*	*	*	*	*	9.72E-05	*	
2	1.38E-04	*	*	*	*	*	*	*	*	
3	1.61E-04	*	*	*	1.06E-04	*	*	*	1.04E-04	

4	1.25E-04	1.21E-04	*	*	*	*	*	*	*
4.5	*	*	*	*	*	*	1.01E-04	*	*
6	1.20E-04	*	*	1.03E-04	*	*	*	*	9.59E-05

* Blend with this composition was not tested

Figure 3.35 compares the diffusion constants for 6 and 25% PF content panels at varying MAPP levels. pMDI panels showed higher diffusion constant than specimens bonded with 25% PF. However 6% PF content panels had comparable diffusion constants as that of pMDI panels. For 6% PF content panels with the increase in MAPP content from 0 to 6% resulted in a decrease in diffusion constant by 21%.

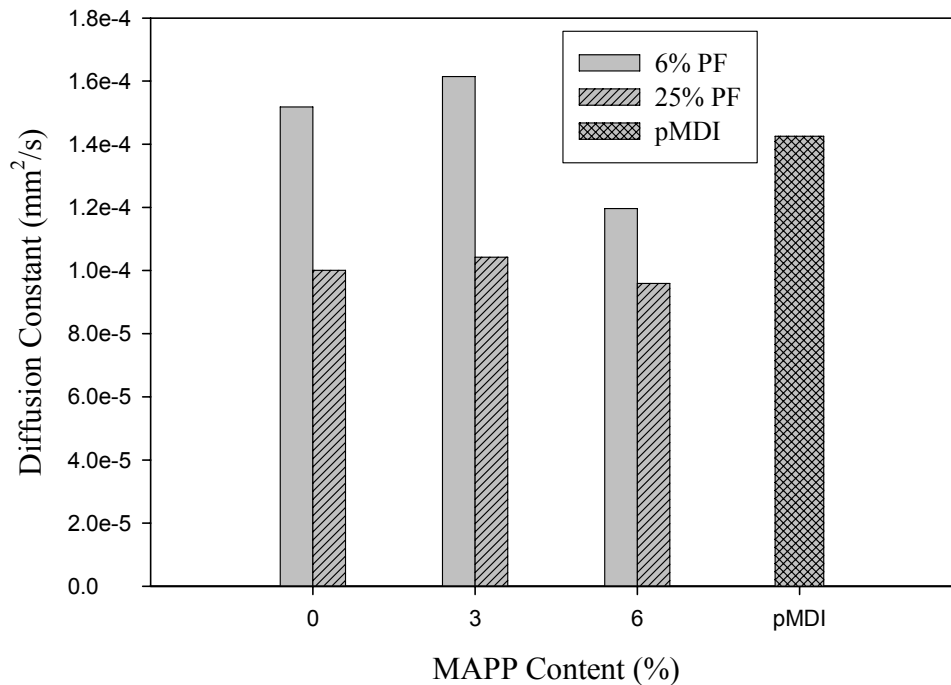


Figure 3.35 Comparison of diffusion constant for 6 and 25% PF content panels at varying MAPP levels after subjecting to 80% RH. Diffusion constant values for pMDI panels are also included

Results indicate that MAPP content had a prominent effect on lowering the EMC of OSC panels besides lowering the rate of moisture gain over time. Diffusion constant was also decreased with the addition of MAPP and higher PF content also showed similar effect. Infiltration of moisture takes place through the voids and micro pores (Wong et al 1999). Addition of thermoplastic MAPP could cause in bulking these pores. This could result in lowering the diffusion constants of the OSC.

Results of tests conducted to evaluate the physical properties were found to follow the hypotheses made at the start of this study. It was hypothesized that addition of MAPP and higher PF content would increase moisture resistance of the panels. Permeance and diffusion constant values showed that addition of MAPP had significant influence in increasing moisture resistance of the panels.

To evaluate the efficacy of varying levels of PF and proportion of MAPP on properties of OSC panels, measured mechanical and physical properties for different resin blends were compared using radar plots. For every formulation property values were ranked. An index was generated for each value where maximum preferred value for each property (i.e., highest values for mechanical properties and lowest values for physical properties) had value of 1 and least preferred value had a value of 0. These indices were then plotted in the form of a radar plot.

Figure 3.36 represents the comparison of properties at 6% PF content with increasing MAPP levels. The plot indicates that addition of MAPP reduced permeance and water absorption properties of the test panels. However addition of MAPP found to increase thickness swelling.

Addition of MAPP also showed detrimental effects on mechanical properties, especially MOR and IB.

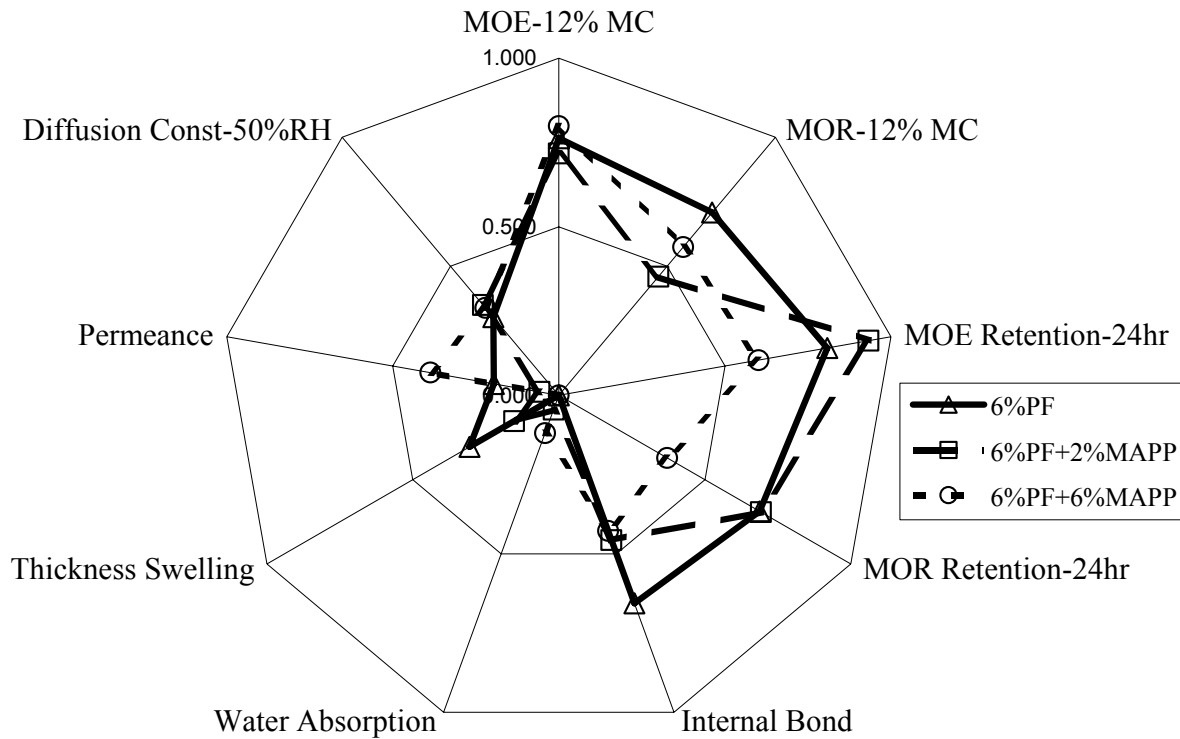


Figure 3.36 Comparison of properties of test panels with 6% PF content and varying levels of MAPP

Effects of varying levels of PF at a constant MAPP level (6%) were monitored in Figure 3.37.

The plot indicates that higher PF content panels (25% PF) performed best both in terms of mechanical and physical properties. Increasing PF content is found to have more significant effect on MOE and MOR retentions after 24 hour water soak, water absorption and thickness swelling, permeance and diffusion constant. Increasing PF content from 6 to 15.5% improved 12% MOE, MOR and internal bond (IB) values, but further addition seemed to have no effect on these properties due to the inclusion of MAPP.

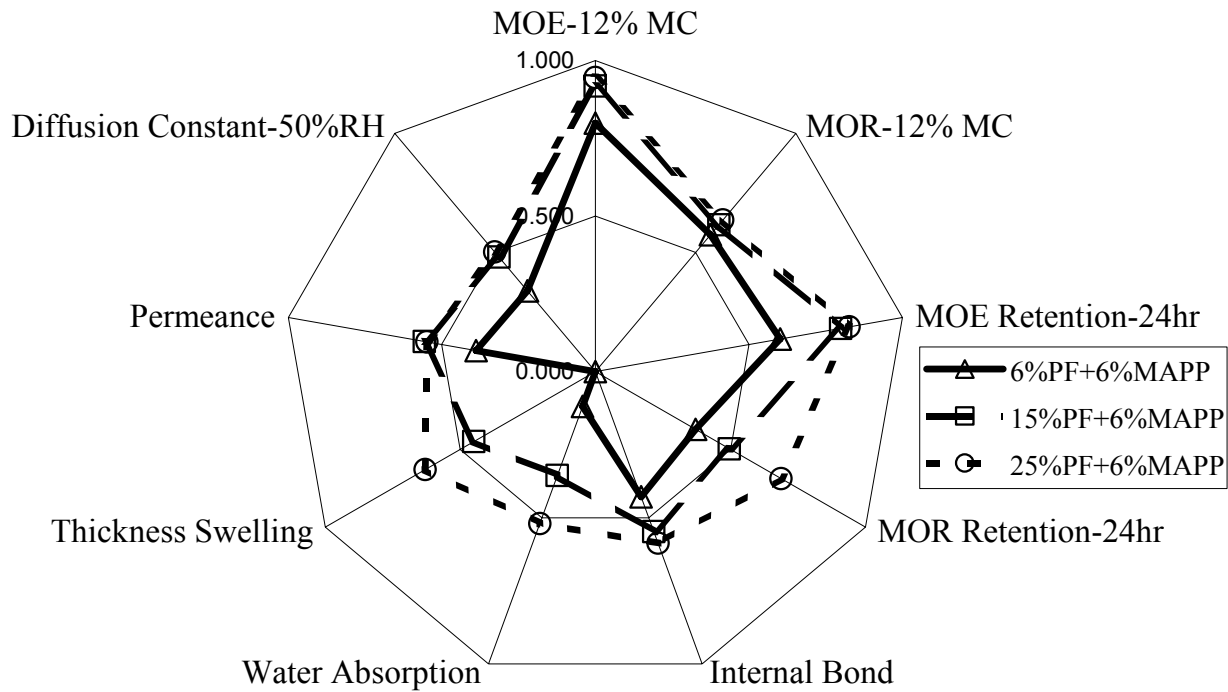


Figure 3.37 Comparison of properties of test panels at 6% MAPP level with varying PF contents

Figure 3.38 compares the properties of two different PF content panels (6 and 25%) with and without 6% MAPP. The plot indicates that 25% PF content panels performed best in terms of improving mechanical properties. At 25% PF content, addition of 6% MAPP reduced mechanical properties and performed similar to neat 6% PF content panels. Thickness swelling was also increased with the addition of MAPP. However, addition of MAPP seemed to improve moisture resistance properties by reducing permeance, diffusion constant and water absorption. Panels showed lowest permeance, diffusion constant and water absorption for panels with 25% PF and 6% MAPP.

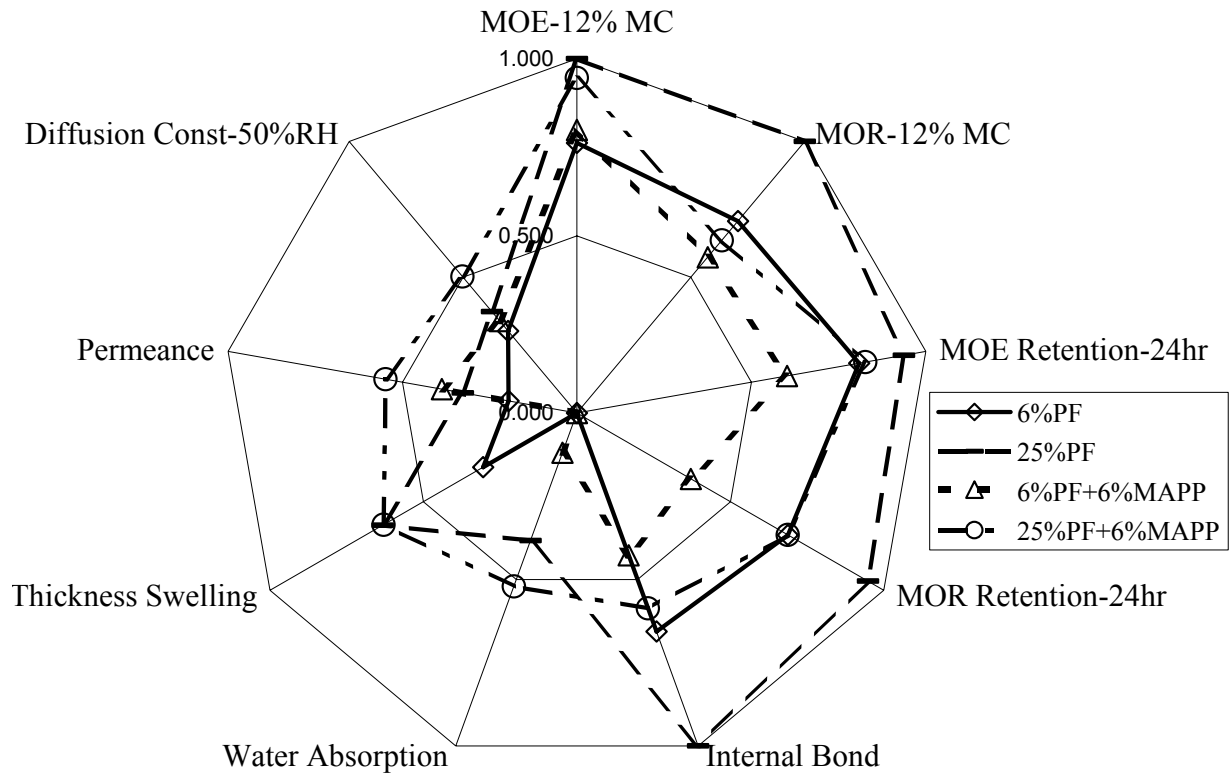


Figure 3.38 Comparison of properties for OSC test panels with neat 6% and 25% PF content and OSC panels with similar PF content at 6% MAPP level.

Conclusions

This study was undertaken to investigate a proof of concept that higher levels of PF resin with inclusion of thermoplastic copolymer coupling agent in producing oriented strand composite will improve its moisture resistance properties without compromising its mechanical properties significantly. Following are some general conclusions of this study:

- Use of higher PF levels was most effective in improving both physical and mechanical properties of OSC panels.
- MAPP level in OSC test panels has a significant influence on their water vapor transmission and permeance. At 6% PF content, increase in MAPP content from 0 to 6% resulted in a reduction of permeance by 23%.
- Equilibrium moisture content (EMC) measurement at 50% and 80% RH conditions indicated that with increasing MAPP content OSC panels equilibrate at lower moisture content. Additionally, increasing MAPP reduces the rate of moisture gain. Specimens found to follow Fick's law of diffusion. Diffusion constants were found to reduce with the addition of MAPP. Panels bonded with PF and MAPP formulations were found to have lower diffusion constants than pMDI panels.
- Results indicated that MAPP content reduced water absorption in long term and short term water soaking tests. For 6% PF content panels, the increase of MAPP content from 0 to 6% resulted in a drop of 28% and 12% respectively in short term and long term water absorption. Increasing PF content also significantly reduced water

absorption in both short and long term water soak tests. At 3% MAPP level, the increase in PF content from 6 to 25% resulted in a decrease in water absorption by 49% in short term soaking and 38% in long term soaking.

- Two hour water soak thickness swelling reduced with the addition of MAPP; however, contrary was true for 24-hour water soak tests. PF content reduced thickness swelling for both short and long term water soak tests. For short and long term soaking cases, a considerable reduction in thickness swelling (over 60%) was observed as PF content was increased from 6 to 25% percent at 3% MAPP level.
- Static bending test for specimens at 12% moisture content indicated that MAPP content had a two fold affect on panel MOE; higher MAPP content at lower levels of PF improved MOE, but at higher levels of PF (over 15%), the trend reversed. OSC test panels showed a significant improvement in MOE with increasing levels of PF resin. For specimens after 24 hours water soak addition of MAPP had adverse effect on MOE. Fraction of MOE retained was reduced with the increase in MAPP content.
- MOR of specimens at 12% moisture content was significantly reduced as MAPP content of the test panels was increased. A drop of 19% in MOR was observed as MAPP content was increased from 0 to 6% at a constant PF level. Increasing PF content had significant positive impact on MOR. For 24 hour water soak specimens addition of MAPP had different effects for lower and higher PF content panels. At 6% PF level addition of MAPP caused lowering in MOR retention. However, at 25%

PF content addition of 3% MAPP showed an improvement in MOR retention by 20% but further increase in MAPP did not show any significant difference.

- Internal bond strength was significantly reduced with the increase in MAPP content, especially at higher PF levels. Increasing PF content considerably improved IB strength of the panels. At 3% MAPP content, the increase of PF content from 6 to 25% resulted in the increase of IB strength by 65%. Large variations in strand geometry used in this study could have also affected internal bond quality of test panels.

From this study, it can be concluded that higher PF content improved mechanical and physical properties of OSC test panels. It was also inferred that addition of thermoplastic co-polymer coupling agent, such as MAPP, at low levels could significantly improve moisture resistance properties of OSC panels; however, addition of MAPP could have detrimental effects on their mechanical properties, especially MOR and IB.

Reference

1. American Society for Testing and Materials. (ASTM) 1994. Standard test methods for water vapor transmission of materials. ASTM E 96-94.
2. American Society for Testing and Materials. (ASTM) 1999a. Standard test methods for evaluating properties of wood-base fiber and particle panel materials. ASTM D 1037-99.
3. American Society for Testing and Materials. (ASTM) 1999b. Standard guide for moisture conditioning of wood and wood-based materials. ASTM D 4933-99.
4. Arora, M.; Rajawat, M. and Gupta, R. 1981. Effect of acetylation on properties of particle boards prepared from acetylated and normal particles of wood. *Holzforschung und Holzverwertung*. 33(1): 8–10.
5. Beech, J. 1975. The thickness swelling of particleboard. *Holzforschung*. 29(1): 11–18.
6. Carll, C.G. 1997. Review of thickness swell in hardboard siding. Effect of processing variables. United States Department of Agriculture. Forest Service. Forest Products Laboratory. General Technical Report FPL–GTR–96.
7. Chateauminos, A., Vincent, L, Chabert, B. and Soulier, J.P. 1994. Study of interfacial degradation of a glass-epoxy composite during hygrothermal ageing using water diffusion measurements and dynamic mechanical thermal analysis. *Polymer*. 35(22):4766-4774.
8. Chow, P.; Bao, Z. and Youngquist, J. 1996. Properties of hardboards made from acetylated aspen and southern pine. *Wood and Fiber Science*. 28(2): 252–258.
9. Clemons, C.; Young, R. and Rowell, R.M. 1992. Moisture sorption properties of composite boards from esterified aspen fiber. *Wood and Fiber Science*, 24(3): 353-363
10. Dai, C. and Steiner, P.R. 1997. On horizontal density variation in randomly-formed short-fiber wood composite boards. *Composites Part A*. 28(A): 57-64.
11. Felix, J.M. and Gatenholm, P. 1991. The nature of adhesion in composites of modified cellulose fibers and polypropylene. *Journal of Applied Polymer Science*. 42: 609-620
12. Felix, J.M. and Gatenholm, P. 1991. The nature of adhesion in composites of modified cellulose fibers and polypropylene. *Journal of Applied Polymer Science*. 42: 609-620
13. Garcia, R.A., Cloutier, A. and Reidl, B. 2005. Dimensional stability of MDF panels produced from fibers treated with maleated polypropylene wax. *Wood Science and Technology*
14. Gu, H., Wang, S., Neimsuwan, T. and Wang, S. 2005. Comparison study of thickness swell performance of commercial oriented strand board flooring products. *Forest Products Journal*. 55(12): 239-245.
15. Hartley, I.D. and Schneider, M.H. 1993. Water vapor diffusion and adsorption characteristics of sugar maple (*Acer saccharum*, Marsh.) wood polymer composites. *Wood Science and Technology*. 27: 421-427

16. Haygreen, G. and Gertjeasen, R.O. 1972. Influence of the amount and type of phenolic resin on the properties of a wafer-type particleboard. *Forest Products Journal*. 22(12): 30-34
17. Hukka, A. 1999. The effective diffusion coefficient and mass transfer coefficient of Nordic softwood as calculated from direct drying experiments. *Holzforschung*. 53(5): 534-540.
18. Lee, W.C. and Biblis, E.J. 1976. Hygroscopic properties and shrinkage of southern yellow pine plywood. *Wood and Fiber*. 8(3): 152-158.
19. Lu, J.Z., Wu, Q. and Negulescu, I.I. 2002. The influence of maleation on polymer adsorption and fixation, wood surface wettability and interfacial bonding strength in wood-PVC composites. *Wood and Fiber Science*. 34(3): 434-459
20. Mahlberg, R., Paajanen, L., Nurmi, A., Kivisto, A., Koskela, K. and Rowell, R.M. 2001. Effect of chemical modification of wood on mechanical properties of wood fiber/ polypropylene fiber and polypropylene/ veneer composites. *Holz als Roh – und Werkstoff*. 59: 319-326
21. Maldas, D and Kokta, B.V. 1991. Surface modification of wood fibers using maleic anhydride and Isocyanate as coating components and their performance in polystyrene composites. *J. Adhesion Sci. Technol*. 5 (9): 727-740
22. Maldas, D. and Kokta, B.V. 1989. Improving adhesion of wood fibers with polystyrene by the chemical treatment of fiber with a coupling agent and the influence on the mechanical properties of composites. *Journal of Adhesion Science and Technology*. 3(7): 529-539
23. Maloney, T.M. 1997. *Modern particleboard and dry-process fiberboard manufacturing*. Miller Freeman Inc. San Francisco, CA. pp. 167-168
24. Marcovich, N.E., Reboredo, M.M. and Aranguren, M.I. 1999. Moisture diffusion on polyester-woodflour composites. *Polymer*. 40: 7313-7320.
25. Patil, Y.P., Gajre, B., Dusane, D., Chavan, S. and Mishra, S. 2000. Effect of maleic anhydride treatment on steam and water absorption of wood polymer composites prepared from wheat straw, cane bagasse and Teak wood sawdust using Novolac as matrix. *Journal of Applied Polymer Science*. 77: 2963-2967
26. Rangaraj, S.V. and Smith, L.V. 2000. Effect of moisture on the durability of a wood/thermoplastic composite. *Journal of Thermoplastic Composite Materials*. 13: 140-161.
27. Simonsen, J., Jacobson, R. and Rowell, R. 1998. Wood fiber reinforcement of styrene maleic anhydride co-polymers. *Journal of Applied polymer Science*. 68 (10): 1567-1573
28. Snijder, M.H.B., Wissing, E. and Modder, J.F. 1997. Polyolefins and engineering plastics reinforced with annual plant fibers. *In Proc. 4th International conference on woodfiber-plastic composites*, Forest Products Society, Madison, WI. : 181-191
29. Stark, N.M., 1999. Wood fiber derived from scrap pallets used in polypropylene composites. *Forest Products Journal*. 49(6): 39-46
30. Suchsland, O. and Enlow, R. 1968. Heat treatment of exterior particle board. *Forest Products Journal*. 18(12):19-23

31. Sun, Bernard C.H, Hawke, Robert N, Gale and Margaret R. 1994. Effect of polyisocyanate level of strength properties of wood fiber composite materials. *Forest Products Journal*. 44(3): 34-40.
32. Sun, Bernard C.H, Hawke, Robert N, Gale and Margaret R. 1994. Effect of polyisocyanate level of physical properties of wood fiber composite materials. *Forest Products Journal*. 44(4): 53-58.
33. Wolcott, M. 2003. Formulation and process development of flat-pressed wood-polyethylene composites. *Forest Products Journal*. 53(9): 25-32.
34. Wong, E.h., Chan, K.C., Lim, T.B. and Lam, T.F. 1999. Non-Fickian moisture properties characterization and diffusion modeling for electronic packages. *Electronic components and technology conference*. 302-306
35. Wu, Q. and Lee, J.N. 2002. Thickness swelling of oriented strand board under long-term cyclic humidity exposure condition. *Wood and Fiber Science*. 34(1): 125-139.
36. Wu, Q. and Suchsland, O. 1996. Prediction of moisture content and moisture gradient of an overlaid particle board. *Wood and Fiber Science*. 28(2): 227-239.
37. Youngquist, J.; Krzysik, A. and Rowell, R. 1986. Dimensional stability of acetylated aspen flakeboard. *Wood and Fiber Science*. 18(1): 90-98.
38. Zheng, J., S. C. Fox, and C. E. Frazier. 2004. Rheological, wood penetration, and fracture performance studies of PF/pMDI hybrid resins. *Forest Product Journal*. 54(10):74-81.

CHAPTER 4

Project Conclusions

The aim of this study was to develop a mechanism to improve moisture durability of oriented strand composite (OSC) without compromising its mechanical properties. In the first part of the study (Chapter 2), effects of adding maleated co-polymers of polypropylene (PP) and polyethylene (PE), namely maleic anhydride polypropylene (MAPP) and maleic anhydride polyethylene (MAPE), on dynamic and toughness properties of phenol formaldehyde (PF) resin was evaluated. Following points summarize the findings of the first part of the study (Chapter 2):

1. MAPO in emulsion form than in powder form results in a uniform distribution within a cured PF resin system yielding a better phase separation with resin matrix. Uniformity and quality of distribution improves as particle size of the co-polymer is decreased; and particle size of MAPO did not have any effect on the dynamic stiffness property of cured PF and MAPO blends.
2. DSC analysis indicated that adhesive blends with PF and MAPP or MAPE have similar curing temperatures and curing time, requiring 2.5 minutes at 145°C to achieve 98% curing of all the tested resin blends.
3. DMA results showed that addition of MAPP at lower proportions improved dynamic stiffness moduli of resin blends; whereas, addition of MAPE at lower proportions improved damping property of cured resin blends.
4. Fracture cleavage test indicated an improvement in fracture energy of resin blend at lower proportions of MAPP (1.5 to 3% of the resin weight) in specimens conditioned to

12% MC; whereas, after 24-hr water soak treatment, resin blends with 3% MAPP yielded higher fracture toughness values.

Based on the results of Phase I of the project, MAPP anionic emulsion was chosen over MAPE anionic emulsion to blend with PF resin in manufacturing oriented strand composite panels.

Second part of this project investigated the effects of higher levels of PF and varying proportions of MAPP in PF on mechanical and physical properties of OSC. Following are some major conclusions of the study:

1. Increasing PF levels was most effective in improving both physical and mechanical properties of the panels.
2. MAPP level in OSC test panels had a significant influence on their permeance, for example reducing permeance by 23% with addition of 6% MAPP to 6% PF.
3. Equilibrium moisture content (EMC) measurement at 50% and 80% RH conditions indicated that with increasing MAPP content OSC panels equilibrate at lower moisture content. Additionally, increasing MAPP reduces the rate of moisture gain. In both the environmental conditions specimens followed Fickian behavior at initial stages of moisture gain. Addition of MAPP caused reduction in diffusion constant of test panels.
4. Results indicated that MAPP content reduced water absorption in long term and short term water soaking tests. An increase of MAPP content from 0 to 6% at 6% PF level

resulted in a drop of 28% and 12% respectively in short term and long term water absorption. Increasing PF content from 6 to 25% while holding MAPP level at 3% resulted in a decrease in water absorption by 49% in short term soaking and 38% in long term soaking.

5. Thickness swelling reduced with addition of MAPP after a 2-hour water soak test, however contrary was true after a 24-hour water soak. For both short and long term soaking, a considerable reduction in thickness swelling (over 60%) was observed as PF content was increased from 6 to 25% percent at 3% MAPP level.
6. Flexure tests of specimens at 12% moisture content indicated an increase in MOE with increasing MAPP content at PF levels under 15%, but the trend reversed above 15% PF level. After 24-hour water soak fraction of MOE retained, in compare to 12% MC specimens, was reduced with the increase in MAPP content. PF content did not have significant effect on MOE retention.
7. Increasing PF content significantly improved MOR of 12% MC specimens. However, MOR values were reduced as MAPP content of the test panels was increased. A drop of 19% in MOR was observed as MAPP content was increased from 0 to 6% at a constant PF level. For 24 hour water soak specimens addition of MAPP had different effects for lower and higher PF content panels. At 6% PF level addition of MAPP caused lowering in MOR retention. However, at 25% PF content addition of 3% MAPP showed an

improvement in MOR retention by 20% but further increase in MAPP did not show any significant difference.

8. Increasing PF content considerably improved the IB strength of the panels. At 3% MAPP content, an increase in PF content from 6 to 25% resulted in an increase of IB strength by 65%. Internal bond strength was significantly reduced with the increase in MAPP content, especially at higher PF levels.

Based on the results of second phase of the study, it can be concluded that higher amounts of PF significantly improved both the mechanical and physical properties of OSC panels. Combining anionic emulsion of MAPP with PF resin would improve moisture resistance properties of OSC; however, addition of MAPP, especially higher proportions, could significantly reduce composite MOR and IB.

This study evoked some issues which should be addressed in future studies. In this study two different ways of resin blend preparation techniques were employed. In the first phase of the study, MAPP and MAPE anionic emulsions were blended with PF and then applied to the wood surface, but for making OSC panels this method was found to be problematic in terms of spraying at the time of blending. Therefore, MAPP and PF were sprayed from two sets of nozzles at the same time. It was assumed that the two liquids would mix in the mist form and would be evenly distributed on the wood flakes. The effect of two different ways of spraying could not be investigated due lack of resources and time.

The pressing schedule of the OSC panel fabrication involved a 20 minutes holding time. This was essential to reach the curing temperature at the core. High amount of moisture was introduced into the system in the form of liquid PF and MAPP emulsion, which demanded this longer pressing cycle. Effect of lower curing cycle could be investigated with the use of powdered PF, where lower amount of moisture would expedite the ramp of temperature.

CHAPTER 5

Appendix

Theory behind the fracture cleavage test

Three fundamental fracture modes are possible: Mode I, Mode II and Mode III.

Mode I fracture can be defined as a fracture where the walls moved perpendicularly away from the fracture plane when the fracture formed.

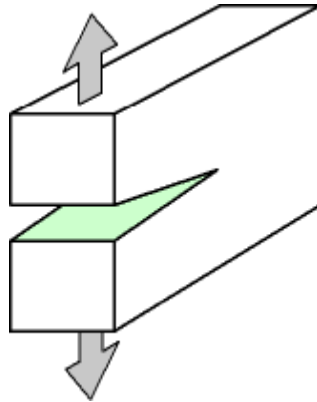


Figure 5.1 Mode I fracture

Mode II fracture can be defined as a fracture when the crack surfaces slide over one another.

This mode is also called sliding mode or in plane fracture mode.

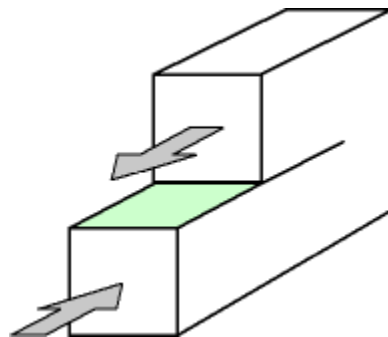


Figure 5.2 Mode II Fracture

Mode III fracture occurs when the crack surfaces move parallel to the leading edge of the crack and relative to each other, causing the crack surface to tear apart. For this reason this mode is also called tearing mode or out of plane mode.

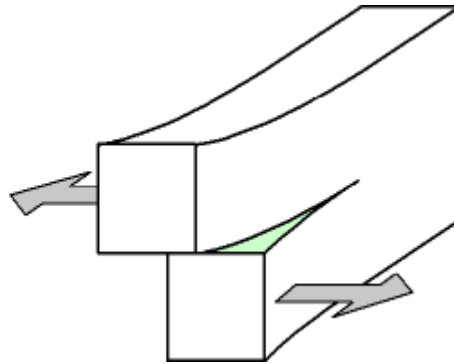


Figure 5.3 Mode III fracture

Derivation of shear corrected compliance method equation

The crack extension energy is often referred to as the mode I fracture energy, G_I (fracture energy at crack initiation, G_{Ic} , and at crack arrest, G_{Ia}), as shown in Equation 2.1 (Blackman et al. 1991, Scoville 2001).

$$G_I = \frac{P_c^2}{2B} \frac{dC}{da} \quad \text{Equation 5.1}$$

Where,

P_c = Critical load when crack extension is initiated or arrested (N)

B = Width of the DCB (mm)

$\left(\frac{dC}{da}\right)$ = Change in compliance (C) with the change in the crack length, a , $\left(\frac{N}{mm}\right)$

A linear relationship exists between the cubic root of compliance and the crack length and a plot can be constructed using the relation:

$$\sqrt[3]{C} = ma + b$$

Equation 5.2

where,

m = slope of the line

b = y –intercept of the line

The correction factor χ is the distance from the origin to the x – intercept of the line and can be found using slope and y –intercept:

$$\chi = \frac{b}{m}$$

Equation 5.3

From equation 5.2 and 5.3 we get the expression for C,

$$C = m^3(a + \chi)^3$$

Equation 5.4

Solving equation 5.4 for $\left(\frac{dC}{da}\right)$ we get,

$$\frac{dC}{da} = 3m^3(a + \chi)^2$$

Equation 5.5

Substituting $\left(\frac{dC}{da}\right)$ in equation 5.1 we get,

$$G_I = \frac{P_C^2}{2B} 3m^3(a + \chi)^2$$

Equation 5.6

Now, from beam theory (Blackman et al. 1991, Gagliano et al. 2001),

$$C = \frac{\delta}{P} = \frac{2a^3}{3EI} \quad \text{Equation 5.7}$$

Where, C = compliance of the beam
 δ = displacement resulting from load P
a = crack length
E = Flexural modulus of the DCB arms and
I = cross sectional moment of inertia of one of these arms

Now from the plot of $C^{\frac{1}{3}}$ vs. a, assuming the best fit trend-line passing through origin (i.e., intercept (b) equals to zero) we have, from equation 5.2,

$$\sqrt[3]{C} = ma,$$

i.e., $C = m^3 a^3,$

Now, putting the value of C in Eqn.5.7 and solving for EI we get,

$$EI = \frac{2}{3m^3}$$

The equation 5.6 is then modified as,

$$G_{Ic} = \frac{P_c^2 (a + \chi)^2}{B EI_{eff}} \quad \text{Equation 5.8}$$

Where, EI_{eff} = effective flexural rigidity of the Double Cantilever Beam specimen.

Table 5.1 Fracture cleavage test specimens and subjected environmental conditions, suggested by one factor response surface model

Run No.	MAPO Content (%)	MAPO Type	Environment
1	0	MAPP	24 hr Soak
2	0	MAPE	24 hr Soak
3	3	MAPE	24 hr Soak
4	0	MAPP	24 hr Soak
5	0	MAPE	24 hr Soak
6	6	MAPE	24 hr Soak
7	0	MAPE	12% MC
8	4.5	MAPP	12% MC
9	3	MAPE	12% MC
10	6	MAPP	24 hr Soak
11	3	MAPP	24 hr Soak
12	3	MAPE	24 hr Soak
13	0	MAPP	12% MC
14	3	MAPP	12% MC
15	0	MAPP	12% MC
16	4.5	MAPE	12% MC
17	6	MAPP	24 hr Soak
18	3	MAPP	24 hr Soak
19	6	MAPE	12% MC
20	1.5	MAPE	24 hr Soak
21	4.5	MAPP	24 hr Soak
22	3	MAPE	12% MC
23	3	MAPP	12% MC
24	4.5	MAPE	24 hr Soak
25	1.5	MAPP	24 hr Soak
26	3	MAPE	24 hr Soak
27	3	MAPE	12% MC
28	1.5	MAPP	12% MC
29	6	MAPE	12% MC
30	0	MAPE	12% MC
31	6	MAPP	12% MC
32	3	MAPP	24 hr Soak
33	3	MAPP	12% MC
34	6	MAPP	12% MC
35	1.5	MAPE	12% MC
36	6	MAPE	24 hr Soak

Experimental Graph for DMA

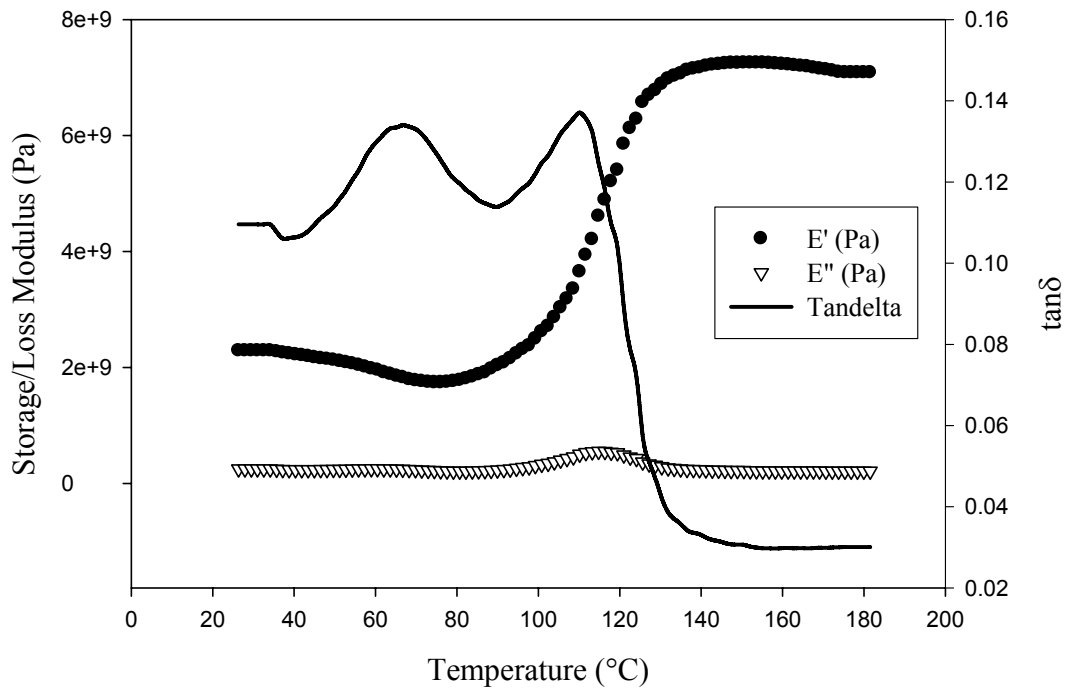


Figure 5.4 Typical plot for storage modulus, loss modulus and $\tan\delta$ during cure of resin blends in DMA

Physical and Mechanical Properties of OSC Test panels

Table 5.2 Summary table of factor coefficients and p-values for mechanical and physical properties of OSC test panels.

Factor Coefficient & p-values	Response Variables											
	12% MC		24h water soak								50% RH	80% RH
	MOE	MOR	MOE- Retention	MOR- Retention	IB	TS-2	TS-24	WA-2	WA-24	Permeance	Diffusion Constant	Diffusion Constant
	MPa	KPa			KPa	%	%	%	%	$\frac{\text{g}}{\text{Pa}\cdot\text{m}^2\cdot\text{s}}\times 10^{-9}$	mm^2/s	mm^2/s
Intercept	-3301.97	-15006.8	-0.15526	-0.43506	-2857.2	29.1	30.42	108.5	109.3	795	3.58	9.6
PF	44.35	394.9	-3.80	-3.19	36.72	-2.14	-2.14	-5.18	-3.94	-44.5	2.11	-1.8
p-value	0.0061	0.0128	0.4322	<0.5258	<0.0001	<0.0001	<0.0001	<0.0001	<0.0001	0.6157	0.5754	0.0003
MAPP	-40.15	-1631.3	-0.025	-0.037	-56.22	0.98	2.51	0.023	0.57	-205	6.02	-2.55
p-value	0.1114	0.001	0.0048	0.0001	<0.0001	0.3434	<0.0001	0.0003	0.0049	0.0152	0.0455	0.0759
Density	207.9	1092.3	1.477	1.909	8.71	0.05	0.07	-0.24	-0.14	-14	-1.31	8.03
p-value	0.0003	0.0009	0.0516	0.0169	<0.0001	0.4176	0.2744	0.39	0.5347	0.1953	0.0542	0.5217
PF*MAPP	-	-	-	-	-1.17	-4.57	-0.077	0.07	-0.027	0.47	-1.14	-
MAPP*Density	-	-	-	-	-0.07	-	-	-	-	4.9	-8.81	-
Density*PF	-	-	-	-	-1.74	-	-	-	-	0.79	-8.87	-
PF ²	-	-	-	-	-0.71	0.05	0.05	0.098	0.072	0.26	1.21	-
MAPP ²	-	-	-	-	12.18	-0.17	-0.09	-0.51	-0.26	-3.1	-4.7	-
Density ²	-	-	-	-	-5.76	-	-	-	-	-0.65	1.37	-
Model R-square	0.58	0.36	0.22	0.36	0.50	0.92	0.92	0.84	0.83	0.83	0.53	0.55